

Dissertation
submitted to the
Combined Faculties for the Natural Sciences and for Mathematics
of the Ruperto-Carola University of Heidelberg, Germany
for the degree of
Doctor of Natural Sciences

presented by

M.Sc. Claudia Guida

born in: Vico Equense, Italy

Oral-examination: 24.10.2014

**An RNAi screen identifies TLR2/6
as mediators of a novel inflammatory pathway
for rapid hepcidin-independent hypoferremia**

Referees: Dr. Lars Steinmetz

Prof. Dr. Ralf Bartenschlager

Table of contents

SUMMARY 1

ZUSAMMENFASSUNG 3

LIST OF TABLES 5

LIST OF FIGURES 6

ABBREVIATIONS 9

1 INTRODUCTION 11

 1.1 Iron 11

 1.2 Iron homeostatic control 11

 1.3 Cellular iron control 11

 1.3.1 The journey of iron through the cell 12

 1.3.2 IRE/IRP regulatory network 13

 1.4 Systemic iron regulation 15

 1.4.1 The hepcidin/ferroportin axis 17

 1.5 Regulation of hepcidin expression 18

 1.5.1 Hepcidin regulation by iron 18

 1.5.2 Hepcidin regulation by hypoxia 20

 1.5.3 Hepcidin regulation by erythroid factors 21

 1.5.4 Hepcidin regulation by inflammation 22

 1.6 Regulation of ferroportin expression 23

 1.6.1 Ferroportin transcriptional regulation 24

 1.6.2 Ferroportin post transcriptional regulation 25

 1.6.3 Ferroportin post translational regulation 26

 1.7 Ferroportin and hepcidin regulation by miRNAs 27

1.8 Iron related disorders	28
1.8.1 Iron overload diseases.....	28
1.8.2 Iron deficiency diseases.....	30
1.9 Aim of the study	33
2 EXPERIMENTAL PROCEDURES	34
2.1 Materials	34
2.1.1 Frequently used reagents and chemicals	34
2.1.2 Transfection reagents	34
2.1.3 Enzymes, recombinant protein and antibodies	35
2.1.4 Buffer and solutions	36
2.1.5 Kits.....	37
2.1.6 Plasmids used for the stable and inducible HeLa cell line generation....	37
2.1.7 Oligonucleotides	38
2.1.8 siRNAs.....	41
2.1.9 Bacterial strain	43
2.2 Cell culture methodologies.....	44
2.2.1 Cell lines and primary cells	44
2.2.2 SiRNA screening.....	44
2.2.3 Validation of the screening results	45
2.2.4 Treatment of BMDMs with TLRs ligands, cytokines and inhibitors	46
2.3 Molecular biology methodologies.....	47
2.3.1 Total RNA extraction and reverse transcription	47
2.3.2 Quantitative PCR	47
2.3.3 Transformation of bacteria	48

2.3.4 Bacterial culture and isolation of plasmid DNA	48
2.3.5 DNA agarose gels.....	49
2.3.6 Western blot analysis.....	49
2.3.7 Plasma biochemistry and tissue iron quantification.....	50
2.3.8 Splenic macrophage isolation	50
2.3.9 DAB-enhanced Perls' staining	50
2.4 Mice	50
2.5 Statistical analysis.....	51
3 RESULTS.....	52
3.1 Establishment of a fluorescent cell-based assay to assess hepcidin-mediated ferroportin regulation	52
3.2 Establishment of hFPN-Rluc reporter assay as alternative siRNA screening system.....	56
3.2.1 Optimization of the screening protocol.....	57
3.3 RNAi screen for kinases and related signaling proteins	60
3.4 Validation of the screening results	67
3.5 The RNAi screen identifies TLR6 as a novel regulator of ferroportin expression.....	77
3.6 TLR2/6 stimulation reduces ferroportin expression in BMDMs	78
3.7 TLR2/6 and TLR4 ligand-specific stimulations similarly reduce ferroportin expression but differentially regulate hepcidin expression	81
3.8 FSL1 and LPS injection induce hypoferremia in mice.....	86
3.9 Hepcidin induction is not required to set acute hypoferremia in mice.....	86
3.10 Investigating the TLR2/6 mediated ferroportin transcriptional regulation ...	94
3.10.1 Testing cytokine stimulation.....	95

3.10.2 Testing specific inhibitors of TLRs pathway	97
4. DISCUSSION AND PERSPECTIVES	101
4.1 Unresolved and controversial aspects of ferroportin regulation	101
4.2 Rationale of the study	103
4.3 A focused RNAi screen identifies hepcidin-independent ferroportin regulators	103
4.3.1 TLR6 is a novel regulator of ferroportin protein expression	106
4.4 Battle for iron.....	106
4.5 Ferroportin mRNA down regulation is a conserved response to pathogen infection.....	109
4.5.1 TLR2/6 heterodimers and/or TLR2 homodimers mediate ferroportin response to FSL1	109
4.6 The importance of hepcidin induction in macrophages	111
4.7 Cytokine contribution to the inflammation-mediated regulation of ferroportin and hepcidin.....	112
4.7.1 The controversial role of TNF α in ferroportin down regulation	112
4.7.2 The importance of IL6 and other cytokines for hepcidin induction and hypoferremia.....	113
4.8 The “critical” role of hepcidin in inducing hypoferremia during acute inflammation.....	114
4.9 Dissecting the TLR-mediated ferroportin regulation: an “inhibitor approach”	118
4.10 Concluding remarks	120
REFERENCES.....	121
ACKNOWLEDGEMENTS.....	131

SUMMARY

Systemic iron homeostasis is essential for human health. Its maintenance critically depends on the interaction between the hepatic hormone hepcidin and the sole known iron exporter ferroportin (FPN) predominantly expressed in hepatocytes, duodenal enterocytes and macrophages. Hepcidin binding leads to FPN internalization and degradation resulting in cellular iron retention.

Iron is an essential nutrient also for pathogens and plays a central role in host-pathogen interactions. The innate immune system fights infections by sequestration of iron in macrophages of the reticuloendothelial system. The resulting hypoferremia represents a major host defence strategy. A current model posits that hepcidin is the crucial effector of this response, as its release from macrophages and hepatocytes provokes FPN protein decrease and, consequently, tissue iron retention.

The aim of my PhD project was to identify novel cellular regulators of hepcidin-mediated ferroportin (FPN) degradation, a fundamental process that controls systemic iron homeostasis. To reach this aim I generated a HeLa cell line expressing a hFPN-renilla fusion protein, which was used for a focused high-throughput RNAi screen targeting kinases and related proteins. Out of 779 genes tested, the screen identified 71 putative regulators of FPN protein stability. Validation experiments confirmed the phenotype of 24 genes. Interestingly, most validated regulators of FPN expression conferred hepcidin-independent FPN regulation. From these I selected 14 genes associated with immune processes for further characterization in murine bone marrow-derived macrophages (BMDMs). Finally, my studies focused on Toll-like receptor 6 (TLR6) as an effective regulator of FPN expression in BMDMs and I investigated how the TLR6 activation pathway modulates iron regulation in the inflammatory context. TLR2/6 ligation by the synthetic lipoprotein derived from *Mycoplasma*: FSL1 triggered a profound decrease in FPN mRNA and protein expression in BMDMs as well as in the liver and the spleen of mice. Unexpectedly hepcidin expression remained unchanged. Hepcidin-independent FPN down regulation was a conserved response to different microbial lipopeptides and elicited a fast, hepcidin-independent hypoferremia pathway. These findings were further confirmed in C326S FPN knock-in mice with a disrupted

hepcidin/FPN regulatory circuitry. This work challenges the prevailing role of hepcidin in inflammatory hypoferremia and suggests that rapid hepcidin-independent FPN down regulation may represent the first line response to restrict iron access to pathogens.

ZUSAMMENFASSUNG

Systemische Eisenhomeoestase ist essentiell für die Gesundheit des Menschen. Ihre Aufrechterhaltung hängt entscheidend von dem Zusammenspiel zwischen dem hepatischen Hormon Heparin und dem einzigen bekannten Eisen-Exporter, Ferroportin (FPN), der überwiegend in Hepatozyten, duodenalen Enterozyten und Makrophagen exprimiert wird, ab. Die Bindung von Heparin an FPN führt zu Internalisierung und Abbau von FPN, was somit die Freisetzung von Eisen verhindert.

Auch für Pathogene ist Eisen ein essentieller Nährstoff und spielt eine zentrale Rolle in der Interaktion von Wirt und Pathogen. Das angeborene Immunsystem nutzt die Zurückhaltung von Eisen in retikuloendothelialen Makrophagen zur Bekämpfung von Infektionen. Der daraus resultierende Eisenmangel ist eine der Hauptverteidigungsstrategien des Wirts. Ein aktuelles Modell postuliert, dass Heparin der entscheidende Effektor dieser Antwort ist, da dessen Freisetzung durch Makrophagen und Hepatozyten den Abbau von FPN bewirkt und somit zur Zurückhaltung des Eisens in Geweben führt.

Das Ziel meines PhD Projektes war es neue zelluläre Regulatoren des heparin-vermittelten Ferroportinabbaus, ein fundamentaler Prozess in der Aufrechterhaltung systemische Eisenhomeoestase, zu identifizieren. Dafür etablierte ich eine HeLa Zelllinie, die ein hFPN-Renilla Fusionsprotein exprimiert. Diese Zelllinie wurde für einen Hochdurchsatz RNAi Screen, der auf Kinasen und verwandte Proteine abzielt verwendet. Der Screen identifizierte 71 von 779 getesteten Genen als mögliche Regulatoren FPN Proteinstabilität. 24 dieser Gene konnten in Validierungsexperimenten bestätigt werden. Interessanterweise, war der Effekt der meisten dieser validierten Kandidaten heparin-unabhängig. Von den validierten Genen habe ich 14 Stück, die mit Immunprozessen assoziiert sind, für die weitere Charakterisierung in Knochenmarksmakrophagen von Mäusen (BMDMs) ausgewählt und fokussierte meine Analysen daraufhin auf den Toll-like Rezeptor 6 (TLR6). Ich untersuchte wie der TLR6 Aktivierungssignalweg die Eisenregulierung im inflammatorischen Kontext moduliert. TLR2/6 Ligation durch das synthetische Lipoprotein, FSL1, von Mycoplasma löst eine starke Abnahme von FPN mRNA- und Proteinexpression sowohl in BMDMs als auch

in der Leber und Milz von Mäusen aus. Interessanterweise Weise änderte sich die Hepcidinexpression nicht. Die Hepcidin unabhängige FPN Herunterregulierung war eine konservierte Antwort auf verschiedene microbielle Lipopeptide und deckte einen schnellen, Hepcidin unabhängigen Mechanismus zur Eisenrestriktion auf. Diese Resultate wurden durch C326S FPN Knock-in Mäuse, deren FPN resistent gegen Hepcidin ist, bestätigt. Diese Arbeit stellt die allgemein geltende Rolle von Hepcidin bei inflammatorischem Eisenmangel in Frage und legt nahe, dass die Hepcidin unabhängige FPN Herunterregulierung der erste, sehr schnelle Schritt in der Zurückhaltung von Eisen vor Pathogenen darstellen könnte.

LIST OF TABLES

Table 2.1 Transfection reagents

Table 2.2 List of buffers and solutions

Table 2.3 List of kits

Table 2.4 Table of primers

Table 2.5 Table of siRNAs

Table 3.1 Inhibitors of TLR signaling pathway tested on BMDMs

LIST OF FIGURES

Figure 1.1 Cellular iron regulation via IRP1/2 system.

Figure 1.2 Systemic iron regulation.

Figure 1.3 The hepcidin/FPN axis.

Figure 1.4 Hepcidin expression regulations by iron and inflammation.

Figure 1.5 First proposed model of hepcidin-mediated ferroportin internalization and degradation.

Figure 3.1 Stable and inducible hFPN-EGFP HeLa cell line generation.

Figure 3.2 Hepcidin effect on HeLa stably expressing human FPN-EGFP fusion protein.

Figure 3.3 pcDNA5-hFPN-Rluc vector map.

Figure 3.4 FPN degradation is a slow process, which is induced by low hepcidin amounts.

Figure 3.5 Pilot screen.

Figure 3.6 Screening strategy.

Figure 3.7 Evaluation of the screening quality.

Figure 3.8 Hit list of hepcidin-independent FPN regulators.

Figure 3.9 Z-score correlation between samples incubated in absence or presence of hepcidin.

Figure 3.10 Distribution of z-score ratios between sample plus and minus hepcidin.

Figure 3.11 List of putative regulators of hepcidin-dependent FPN internalization and degradation.

Figure 3.12 MTT assay identifies cytotoxic effects.

Figure 3.13 Validation of FPN putative regulators by applying pool of 4 siRNA sequences or single siRNA sequences per gene.

Figure 3.14 Validation of FPN putative regulators by comparing siRNA effects in HeLa-FPN-Rluc and HeLa-Rluc cell lines.

Figure 3.15 Validation of hepcidin-dependent FPN putative regulators.

Figure 3.16 Identification of functional links between candidates by STRING analysis.

Figure 3.17 Selection process of FPN candidate regulators.

Figure 3.18 Validation of putative FPN regulators in BMDMs.

Figure 3.19 Identification of TLR6 as novel regulator of ferroportin protein expression.

Figure 3.20 TLR2/6 stimulation by FSL1 reduces ferroportin expression in BMDMs.

Figure 3.21 TLR1-deficient BMDMs retain responsiveness to FSL1.

Figure 3.22 FSL1-mediated TLR2/6 ligation reduces FPN expression in BMDMs without activating hepcidin mRNA expression.

Figure 3.23 FSL1 and LPS stimulation induce cytokines response.

Figure 3.24 Ferroportin and hepcidin regulation by TLR2 and TLR4-specific ligands in BMDMs.

Figure 3.25 FSL1 and LPS injection induce hypoferremia in mice.

Figure 3.26 Hepatic hepcidin induction is not required to set acute hypoferremia in mice.

Figure 3.27 Splenic ferroportin down regulation in the hypoferremic response does not require hepcidin contribution.

Figure 3.28 TNF α , IL6, TFR1 mRNA expression in the spleen of mice injected with FSL1 and LPS.

Figure 3.29 Iron absorption is not altered upon FSL1 and LPS injection.

Figure 3.30 HFE mRNA regulation in liver and spleen of mice injected with FSL1 and LPS.

Figure 3.31 BMDMs derived from FPN^{C326S} knock-in mice down regulate FPN in response to FSL1 and LPS.

Figure 3.32 FSL1 injection in FPN^{C326S} knock-in mice induces hypoferrremia.

Figure 3.33 TNF α stimulation induces FPN mRNA reduction in BMDMs.

Figure 3.34 Inhibition of key components of the TLR2 signaling.

Figure 3.35 PI3K and Src kinase inhibitors increase FPN expression in BMDMs.

Figure 3.36 PI3K inhibitors reduce the FPN decrease induced by FSL1.

Figure 4.1 Pathogen iron uptake strategies.

Figure 4.2 Working model.

ABBREVIATIONS

General abbreviations

% per cent
°C degree Celsius
ACD anemia of chronic disease
AKT v-akt murine thymoma viral oncogene homolog
AP1 activator protein 1
BMDM bone marrow derived macrophage
BMP bone morphogenetic protein
BMP bone morphogenetic proteins
BMPR bone morphogenetic protein receptor
bp base pair
cDNA complementary DNA
CMV cytomegalovirus
Ct Threshold cycles
DcytB duodenal cytochrome b
DMEM Dulbecco's modified Eagle's medium
DMSO dimethyl sulfoxide
DMT1 Divalent metal transporter 1
DNA deoxyribonucleic acid
dNTP deoxynucleotide triphosphate
E. coli Escherichia coli
ECL enhanced chemiluminescence
EDTA ethylenediaminetetraacetic acid
EGFP enhanced green fluorescent protein
EPO erythropoietin
ESA erythropoiesis-stimulating agents
FCS fetal calf serum
FPN ferroportin
FRT flipase recombination target
g gram
GDF15 growth differentiation factor 15
GFP green fluorescent protein
GTP guanosine triphosphate
h hour
H₂O water
HAMP hepcidin antimicrobial peptide
HCl Hydrogen chloride
HFE High Fe, human hemochromatosis protein
HH hereditary hemochromatosis
HIF hypoxia inducible factor
HJV hemojuvelin
HO heme oxygenase
IDA iron deficiency anemia
IgG immunoglobulin G
IL interleukin
IRE iron responsive elements
IRIDA iron-refractory iron-deficiency anaemia
IRP iron-regulatory protein
JAK Janus kinase
kb kilo base pair (1000 bp)

kDa kilo Dalton
l liter
LB Luria-Bertani
LIP labile iron pool
LPS lipopolysaccharide
m milli
M molar
MAP mitogen-activated protein
MEK1 MAPK/ERK kinase 1
min minute
mol mole
mRNA messenger RNA
MVB multivesicular bodies
n nano
NaCl Sodium chloride
NFkB nuclear factor of kappa light polypeptide gene enhancer in B-cells
NRAMP1 natural resistance-associated macrophage protein 1
PAGE polyacrylamide gel electrophoresis
PBS phosphate-buffered saline
PCR polymerase chain reaction
Pen/Strep Penicillin/Streptomycin
PI3K phosphoinositide 3-kinases
PVDF polyvinylidene fluoride
Rluc renilla luciferase
RNA ribonucleic acid
RNAi RNA interference
rpm rotations per minute
RPMI-1640 Roswell Park Memorial Institute-1640
RT reverse transcription
SD standard deviation
SDS sodium dodecyl sulphate
sec seconds
SEM standard error of measurements
siRNA small interfering RNA
SLC40A1 solute carrier family 40 (iron-regulated transporter), member 1
SMAD mothers against decapentaplegic homolog
STAT3 signal transducer and activator of transcription 3
STEAP six transmembrane epithelial antigen of the prostate
TBE tris/borate/EDTA
TBS tris-buffered saline
Tf transferrin
TfR1 transferrin receptor 1
TfR2 transferrin receptor 2
TGFβ transforming growth factor-β
TLR toll like receptor
TMPRSS6 transmembrane protease, serine 6
TNF tumor necrosis factor
Tris tris(hydroxymethyl)aminoethane
TWG1 twisted gastrulation homolog 1
U units
UTR untranslated region
V Volts
WT wild type
μ micro

1 INTRODUCTION

1.1 Iron

Iron (Fe) is the fourth most abundant element in the Earth's crust and one of the essential elements for human life (1). It exists in a wide range of oxidation states, -2 to +6, whereby the ferrous (Fe^{2+}) and the ferric (Fe^{3+}) states are the most common ones and for its ability to fluctuate between these two oxidation states it is indispensable for many biological reactions and life. Iron-containing enzymes and proteins are utilized from primitive archea to humans and are involved in processes, such as oxygen transport (e.g. hemoglobin), metabolic reactions (e.g. cytochromes) or iron transport (e.g. transferrin). Proteins can contain iron in prosthetic groups as iron—sulfur cluster, like several enzymes of the mitochondrial respiratory chain or as heme (2, 3), like myoglobin, the muscle oxygen storage protein. In addition elementary iron can also function as cofactor for enzymes such as ribonucleotide reductase which is essential for DNA synthesis. Although vital, its chemical reactivity as transition metal, renders free iron potentially dangerous by generating highly reactive free radicals that can mediate cell damage (4). Free Fe^{2+} ions in solution are known to trigger Fenton's reaction $\text{Fe}^{2+} + \text{H}_2\text{O}_2 \rightarrow \text{Fe}^{3+} + \text{OH}^\cdot + \text{OH}^-$ which causes the production of highly reactive hydroxyl radicals able to mediate peroxidation of lipids and oxidation of protein and nucleic acids (5).

1.2 Iron homeostatic control

The association of iron with proteins neutralizes its potentially harmful effects and drives its crucial biological functions in the cells. However additional and tight cellular and systemic regulations have evolved to maintain a plasma iron concentration that ensures adequate supplies while preventing detrimental organ iron overload or deficiency.

1.3 Cellular iron control

1.3.1 The journey of iron through the cell

In the plasma iron circulates bound to transferrin (Tf), each molecule containing two specific high-affinity Fe^{3+} binding sites. Diferric transferrin binds to transferrin receptor 1 (TfR1) at the plasma membrane and triggers the invagination of clathrin-coated endosomes (6). In acidified endosomes conformational changes in both Tf and TfR1 promote the release of Fe^{3+} from transferrin. As ferric iron is not bioavailable, the ferrireductase activity of the STEAP (Six Transmembrane Epithelial Antigen of the Prostate) family of metalloproteinases mediates the reduction of Fe^{3+} to Fe^{2+} (7, 8). Fe^{2+} is then transferred to the cytoplasm by divalent metal transporter 1 (DMT1) and apo-Tf and TfR1 are recycled to the cell surface. In addition to TfR1, a homologous protein, transferrin receptor-2 (TfR2) whose expression is restricted to hepatocytes, erythroid cells and duodenal crypt cells, can bind Tf, even though with lower affinity. Although predominant, Tf-dependent iron uptake is not the only mechanism mediating iron entry into cells. Several pathways for non-Tf bound iron have been described. For instance, in intestinal absorptive cells DMT1 mediates iron uptake after Fe^{3+} from the diet is reduced to Fe^{2+} by the cytochrome b-like ferrireductase (Dcytb) (9). Iron may also enter the cell via other iron-bound protein such as hemoglobin which is released by erythrocytes, especially during intravascular hemolysis. Hemoglobin binds to the acute phase protein haptoglobin forming a complex which is then removed from the plasma via the scavenger receptor CD163 mainly expressed on monocytes and macrophages (10). Iron in heme can also move into cytoplasm via heme transporters, such as heme carrier protein 1 (HCP1) identified in brush-border membrane of duodenal enterocytes (11) and the mammalian homolog heme responsive gene 1 (HRG-1), a transmembrane heme permease in *C. elegans*, which is mainly expressed in macrophages and transports heme from the phagolysosome to the cytoplasm during erythrophagocytosis (12). The activity of these transporters is coupled to the activity of the cytoplasmic heme oxygenase (HO) that extracts iron from heme.

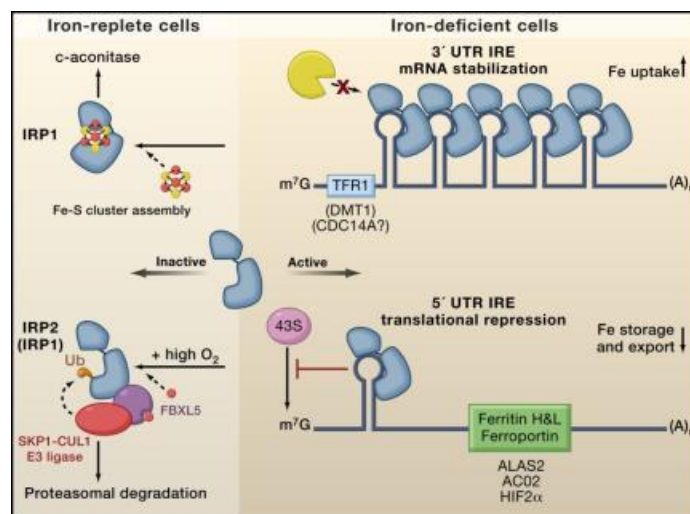
Once in the cell, most of the iron is directed towards mitochondria where is used for Fe-s cluster biogenesis and heme synthesis in erythroblasts. Approximately only 5% of cellular iron is maintained as redox-active iron source for immediate metabolic needs producing the so called labile iron pool (LIP). The portion that is not required is sequestered and stored by ferritin, a multimeric protein consisting of 24 light and heavy chain subunits. For its enzymatic properties ferritin can convert Fe^{2+} in Fe^{3+} and store up to 4500 iron atoms (13) achieving both iron detoxification and storage.

Unlike iron uptake, which can be mediated by several mechanisms, only one iron export protein is known at present: ferroportin (FPN) which is the only iron exporter in vertebrates (14-16) mediating iron release mainly from duodenal enterocytes, macrophages, hepatocytes, placental syncytiotrophoblasts and cells of the central nervous system. Iron exit requires its oxidation to Fe^{3+} which is performed by the multicopper oxidases ceruloplasmin (17) and its intestinal homolog hephaestin which work in concert with FPN to load iron onto Tf for transport in the bloodstream. The function of multicopper oxidases prevents the generation of oxygen radicals that are otherwise produced by spontaneous oxidation of iron. Furthermore thanks to their high affinity for oxygen they effectively increase the rate of oxidation which is particularly important, for example, under low oxygen tension conditions.

1.3.2 IRE/IRP regulatory network

The coordination between iron uptake, utilization, storage and export is maintained through the regulation of iron-related genes at several levels, from transcription to translation. In particular, posttranscriptional regulation has been well characterized and plays a key role in modulating cell response to iron levels. It relies on the trans-acting iron regulatory proteins (IRPs) and their interaction with iron-responsive elements (IREs) (18), conserved motifs in the mRNA of iron-related genes. Single IRE is located in the 5' untranslated regions (UTRs) as in FPN and

ferritin transcripts and inhibits the translation process upon IRP binding (19). Conversely, multiple IREs placed in the 3' UTR serve to stabilize the mRNA, as for TfR1 transcript. IRPs exist in two isoforms, IRP1 and IRP2 which bind to IREs in response to the cellular labile iron pool. When iron levels are high IRP1 switches from its active RNA binding form to an Fe-s cluster containing cytoplasmic aconitase that interconverts citrate in isocitrate, at the same time IPR2 is targeted for proteosomal degradation (20). On the other hand, in iron-depleted cells IRP1 is activated as RNA binding protein and IRP2 is stabilized, becoming both fully active to inhibit, for example, the translation of FPN, reducing iron exit and stabilize TfR1 mRNA, increasing iron uptake, both effects counteracting iron deficiency (Figure 1.1). The importance of appropriate IRP regulation has been highlighted by several mouse models. The lack of both proteins determines early death of mouse embryos (21, 22). IRP1^{-/-} mice misregulate iron metabolism only in the kidney and brown fat, whereas IRP2^{-/-} mice show altered expression of target proteins in all tissues (22) and develop microcytosis (23), suggesting that the activity of these two proteins is only partially redundant. Furthermore, conditional expression of a constitutively active IRP1 was reported to cause abnormal body iron distribution and impaired erythropoiesis (24), confirming the essential role of the IRP/IRE regulatory network even in the systemic iron homeostasis. Importantly, the IRP/IRE system seems also to extend beyond the well-studied iron metabolism targets, as suggested by the identification of novel IRP targets involved, for example, in the cell cycle regulation and oxygen metabolism (25).



Hentze et al., *Cell*, 2010

Figure 1.1 Cellular iron regulation via IRP1/2 system. In iron-replete cells IRP1 is inactivated by conversion into the Fe-S cluster containing aconitase, while IRP2 is targeted for proteasomal degradation. Low cellular iron levels activate IRP1 and stabilize IRP2 allowing the binding to the IREs located in the 5' UTRs which causes translation inhibition and in the 3' UTRs which causes mRNA stabilization. Translation repression applies, for example, to ferroportin and ferritin transcripts, ultimately reducing iron storage and export, while mRNA stabilization rises the expression of Tfr1, increasing iron uptake. Both effects counterbalance the cellular iron deficiency.

1.4 Systemic iron regulation

The human body approximately contains 3-4 grams iron, mostly (around 65%) present in haemoglobin of erythrocytes. The cells of all tissues contain iron in iron-containing proteins required for the energy metabolism and cellular proliferation, however the liver and the spleen are the major reserve organs for iron which is stored in macrophages and hepatocytes.

The distribution and the mobilization of iron between distinct body compartments involve several organs and tissues (Figure 1.2). Under normal circumstances only 1-2 mg dietary iron per day is absorbed in the proximal duodenum and released into the blood bound to the iron-transporter protein Tf. Most of this iron is taken up by erythrocyte precursors in the bone marrow and utilized for haemoglobin synthesis. About 70% of circulating body iron is in red blood cells and is recycled

by the macrophages of the reticuloendothelial system that remove old or damaged erythrocytes from the bloodstream.

Iron absorption normally balances small iron losses which mainly derive from desquamation of epithelium or minor bleeding, thus the recycling system is mainly responsible for the plasma iron turnover and its homeostatic control.

The coordination of iron flows from tissues to circulation needs to be tightly maintained to prevent iron accumulation or deprivation which ultimately result in diseases.

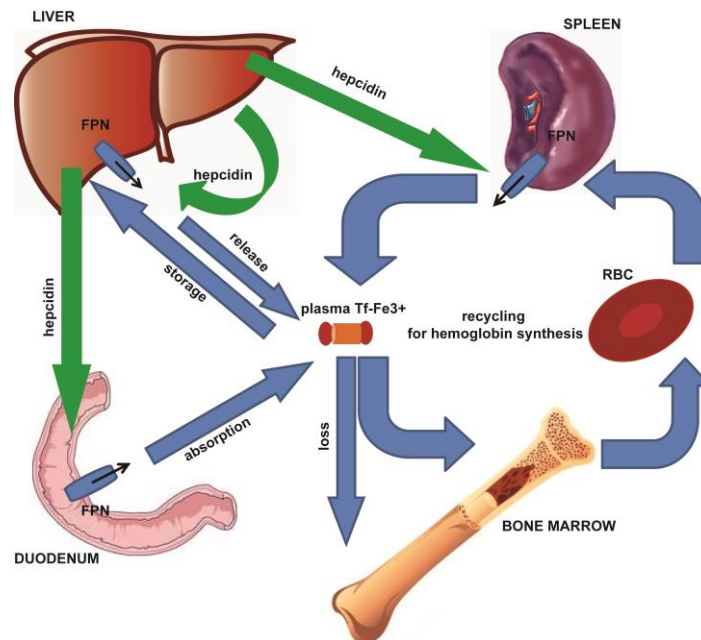


Figure 1.2 Systemic iron regulation. Different cell types and tissues coordinate iron homeostasis. Dietary iron enters the body through intestinal mucosal cells and is then bound to plasma transferrin to be delivered to cells. Only 1-2 mg of iron are normally absorbed and are sufficient to balance physiological minor iron losses. Most of the iron that enters the plasma comes from macrophages that recycle iron from senescent or damaged erythrocytes. In turn, the majority of this iron is used for hemoglobin synthesis by erythrocyte precursors in the bone marrow to sustain the erythrocyte turnover. When iron accumulates, it is deposited in parenchymal tissues such as the liver which is the main storage compartment. The release and the distribution of iron in the body are controlled

via the binding of the liver hormone hepcidin to the iron exporter FPN (mainly expressed in enterocytes, macrophages and hepatocytes) which cause FPN endocytosis and proteolysis.

1.4.1 The hepcidin/ferroportin axis

The maintenance of iron homeostasis critically depends on the interaction between the liver peptide hormone hepcidin and the cell surface iron exporter FPN (26, 27). Hepcidin expression in the liver is regulated by different stimuli, such as iron availability, inflammation and hypoxia (26). It binds to FPN at the plasma membrane of enterocytes, macrophages and hepatocytes inducing its internalization and degradation, resulting in decreasing iron export and cellular iron retention (28). Thus the hepcidin/FPN circuitry controls dietary iron absorption, iron release from macrophages, mobilization of iron from hepatic stores and iron transfer across the placenta (Figure 1.3).

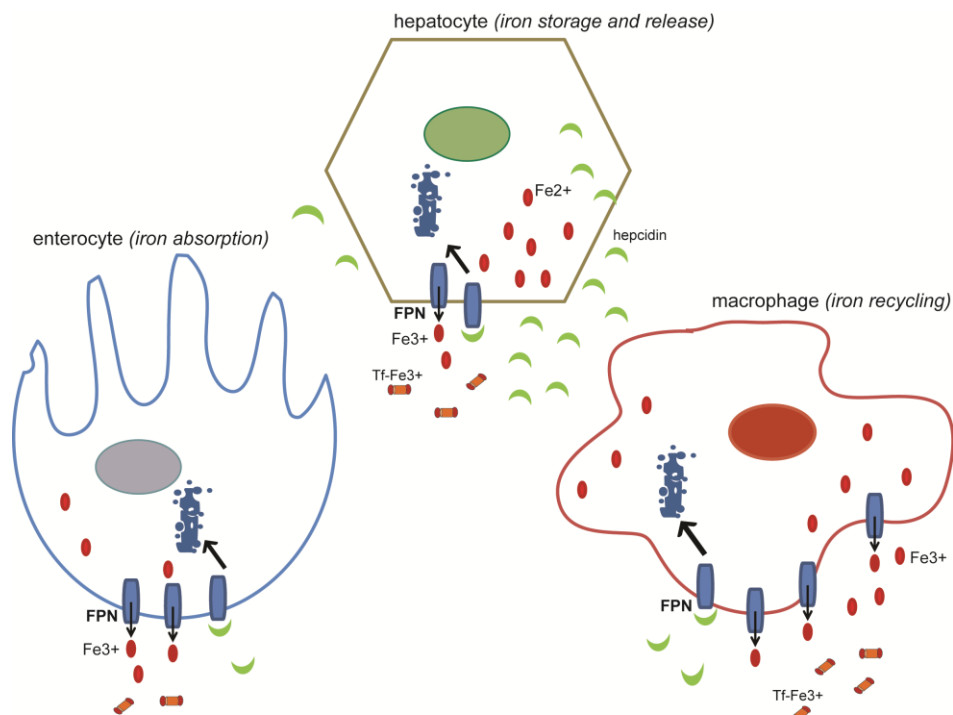


Figure 1.3 The hepcidin/FPN axis. Hepcidin is a 25 amino acids peptide produced by the liver. FPN is a transmembrane protein mainly expressed in hepatocytes, macrophages and enterocytes

and it is the only known iron exporter. Hepcidin binds to FPN at the plasma membrane and induces its internalization and degradation. When hepcidin concentration is low, FPN is fully active and iron enters plasma where it is loaded onto transferrin for transport (Tf-Fe³⁺), on the other hand when hepcidin concentration is high, FPN is internalized and iron is trapped in enterocytes, macrophages and hepatocytes.

1.5 Regulation of hepcidin expression

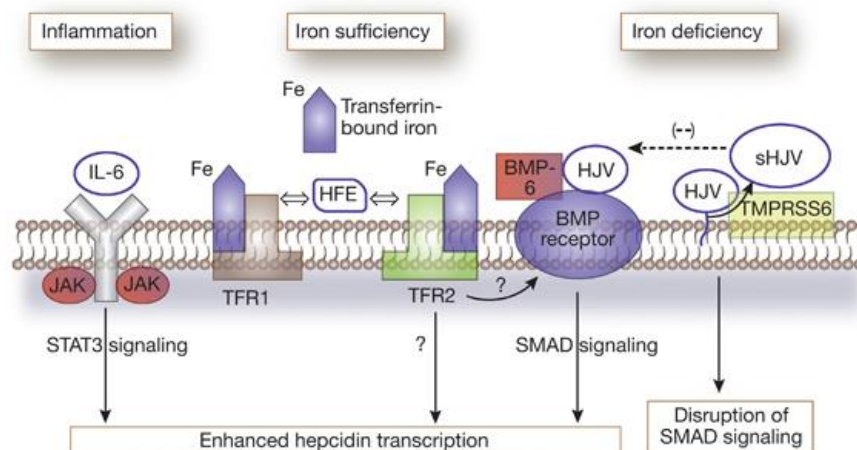
Hepcidin discovery dates from 2000 and was made in human blood ultrafiltrate and in urine (29, 30). It was identified as cysteine-rich antimicrobial peptide even though it shows only modest antimicrobial activity *in vitro* at very high concentration. Although the relevance of its antimicrobial function *in vivo* remains unclear, its role in iron homeostasis is very well established. Hepcidin levels are rapidly modulated in consequence of several stimuli and dysregulation of its synthesis has severe implications in a large spectrum of iron disorders.

1.5.1 Hepcidin regulation by iron

Hepcidin appears to be a principal regulator of systemic iron homeostasis. In turn its synthesis is regulated by plasma iron concentration and iron stores, primarily at transcriptional level. Iron supplementation in the diet induces hepcidin mRNA increase in mice (31) while low iron diet leads to the opposite outcome. The core components of this regulatory mechanism are the bone morphogenetic protein receptor (BMPR) and the SMAD signalling proteins. Hepatic iron level are sensed through increased production of bone morphogenetic proteins (BMP) which belong to the transforming growth factor- β (TGF- β) superfamily and bind to BMP Type I and Type II serine threonine kinase receptors. Several BMP ligands can induce hepcidin expression in cultured cells, however BMP6 appears to be the key endogenous regulator of hepcidin *in vivo* (32, 33). Its production increases when hepatic iron levels are high, suggesting that this may represent the signal reflecting iron store amounts. The activation of BMPR upon BMP binding causes the phosphorylation of intracellular receptor associated SMAD proteins (R-SMADs)

which together with the common mediator SMAD4 translocate to the hepatocyte nucleus to induce hepcidin transcription. Consistently, it has been shown that phosphorylation of R-SMADs in the liver increases with iron enrichment in the diet and mildly decreases with iron restriction (34). Hepatic BMP signalling is augmented by the iron-specific BMPR coreceptor hemojuvelin (HJV) to induce hepcidin (35). HJV in turn is regulated by the liver-specific protease matriptase2 (also called TMPRSS6) which, stabilized by iron deficiency, cleaves and inactivates HJV (36) negatively regulating hepcidin expression (Figure 1.4). Attenuation of hepcidin activation also comes from iron-stimulated expression of other SMAD proteins, such as SMAD6 and SMAD7 that have been described to mediate a negative feedback regulation (37, 38).

Extracellular iron concentration is sensed by the interaction of transferrin bound iron (Tf-Fe) and the “the iron sensing complex” composed of TfR1, TfR2, the human hemochromatosis protein (HFE) and HJV (39) which physically interact on the cell surface of hepatocytes. The interaction of HFE with TfR1 or TfR2 shifts according to Tf-Fe concentration (40). Under iron-rich conditions HFE is released from TfR1 (which has higher affinity to transferrin-bound iron) and becomes available for interaction with TfR2 enhancing SMAD signalling and promoting hepcidin up regulation (Figure 1.4). Consistent with this model, mice lacking HFE or TfR2 were shown to have an attenuated BMP signalling (39) while mice expressing a mutated form of TfR1 which constitutively binds HFE exhibited low hepcidin levels and developed hemochromatosis (41). Although the importance of these proteins for hepcidin regulation is supported by study of patients who carry mutations in the related genes, the exact regulatory mechanisms of their interaction is not yet understood.



Coyne, *Kidney International*, 2011

Figure 1.4 Hepcidin expression regulations by iron and inflammation. The activation of BMP receptor after BMP binding (e.g. BMP6) induces hepcidin transcription via the SMAD signalling pathway. Under iron sufficiency conditions, transferrin-bound iron binds to TFR1 and displaces HFE which becomes available for interaction with TFR2. HFE-TFR2 interaction enhances hepcidin transcription either directly or in concert with the BMP/SMAD signalling pathway. Under iron deficiency conditions hepcidin transcription is impaired via the protease TMPRSS6 which cleaves the BMPR coreceptor HJV, releasing soluble HJV (sHJV) which negatively regulates BMP/SMAD signalling. Inflammation induces IL6 production by macrophages. IL6 binds to its receptor and triggers Janus kinase (JAK) to activate STAT3 signalling which ultimately leads to hepcidin transcription induction.

1.5.2 Hepcidin regulation by hypoxia

Hepcidin is inhibited by hypoxia by several proposed mechanisms. In particular oxygen deficiency stimulates erythropoiesis via erythropoietin (EPO) production and consequently increases iron requirements, leading to hepcidin reduction. Consistently, in humans hypoxia caused by high altitude results in lower hepcidin levels (42, 43). The hypoxia-responsive system involves hypoxia inducible factors (HIF-1 and HIF-2), which are stabilized under hypoxic condition and regulate the transcription of several iron-related genes. It was reported that HIF complexes may directly repress hepcidin promoter activity both in cells and in murine livers (44, 45). However experiments with transgenic mice lacking or constitutively expressing HIF2 α indicate that hepcidin regulation occurs through EPO-mediated increased erythropoiesis rather than via direct effects on hepcidin promoter (46). Hypoxic

responsive elements were also found in the TMPRSS6 promoter, suggesting that the increased transcription of this protein represents an additional mechanism to inhibit hepcidin (47) in such conditions.

1.5.3 Hepcidin regulation by erythroid factors

The synthesis of new red blood cells requires about 20 mg of iron every day. Increased demand of iron for erythropoiesis (in consequence of hemolysis or phlebotomy) suppresses hepcidin (48) to rise iron availability. The EPO produced by the kidney to stimulate erythropoiesis, for example under hypoxic conditions, was reported to directly mediate hepcidin inhibition in hepatic cells (49). However in bone marrow-depleted mice neither EPO treatment nor hemolysis was demonstrated to alter hepcidin levels, suggesting that this compartment is actually essential for hepcidin modulation (50). Subsequent studies have identified two soluble factors, members of TGF- β superfamily, growth and differentiation factor 15 (GDF15) and twisted gastrulation homolog 1 (TWSG1) as “erythroid regulators” (51, 52) accounting for hepcidin suppression. Although TWSG1 was shown to inhibit hepcidin *in vitro* by altering the BMP signalling, the mode of action for GDF15 remains as unclear as the cross-talk between erythroid signals and the BMPs. Very recent is the identification of an erythroid factor made by erythroblasts named “erythroferrone” (Erfe) whose expression was proven to increase in the bone marrow and the spleen of mice after phlebotomy or EPO stimulation(53). This response preceded the expected hepcidin reduction which was prevented in Erfe knock-out mice. Furthermore injection of recombinant Erfe were demonstrated to reduce hepcidin expression in wild type mice while the addition of the supernatant of HEK293T cells overexpressing Erfe significantly decreased hepcidin expression in murine hepatocytes. These lines of evidence and the observation that Erfe mRNA levels are increased in mouse model of β -thalassemia, suggest that this is the long-sought erythroid factor responsible for hepcidin suppression which may contribute to the pathogenesis of iron-loading anemia.

1.5.4 Hepcidin regulation by inflammation

Iron is a growth factor for invading pathogens. As defence strategy circulating iron levels are reduced during infection leading to hypoferrremia commonly associated to infections and inflammatory conditions. Numerous studies have demonstrated that inflammation modifies the expression of several iron-related genes, including hepcidin. Hepcidin induction by inflammatory stimuli was reported by several publications, all corroborating its crucial role in setting the inflammation-mediated hypoferrremia (54-56). One of the most common mouse models for acute inflammation utilizes lipopolysaccharide (LPS) injection. This Gram negative bacterial membrane constituent is recognized by a member of Toll like receptor family, TLR4 mainly expressed in macrophages and dendritic cells where it initiates the inflammatory response. Intraperitoneal injection of LPS results in hepatic hepcidin induction which mediates the reduction of circulating iron by causing the degradation of ferroportin (57). Murine primary hepatocytes were shown to increase hepcidin expression upon TLRs ligand stimulation (58), however the expression of TLRs, and in particular of TLR4, in this cell type is subjected to controversy (59) (60) and it is possible that such response is rather mediated by macrophage contamination of the cell preparation. Hepcidin up regulation was demonstrated also in macrophages and neutrophils exposed to LPS, Gram negative and Gram positive bacteria suggesting that hepcidin release from myeloid cells contributes to restrict iron access to pathogens in infection microenvironment (57, 61). Among inflammatory cytokines, interleukin-6 (IL-6) seems to be a critical component of hepcidin activation in hepatocytes as reported by *in vivo* and *in vitro* data (55, 58). IL-6 binding to its receptors (gp80 and gp130) triggers Janus kinase 2 (JAK2) to phosphorylate the signal transducer and activator of transcription (STAT)3 transcription factor which in turn activates the hepcidin promoter through its STAT3 binding motif (62-64) (Figure 1.4). However distinct reports have indicated that other cytokines, like IL-1 and IL-22 (65, 66) might be involved in hepcidin stimulation under inflammatory conditions. Interestingly, there appears to

be crosstalk between JAK/STAT3 pathway and the BMP pathway to mediate hepcidin activation as suggested by liver specific SMAD4 knockout mice which fail to induce hepcidin and develop hypoferrremia upon IL-6 injection (67). Moreover BMP inhibitors were reported to block IL6-mediated hepcidin transcription *in vitro* (68) and injection of LPS in wild type mice has revealed a role of activinB (a member of TGF- β superfamily) in inducing hepcidin through SMAD1/5/8 signalling pathway (69). The involvement of the iron-related BMP signalling has been additionally supported by evidence in HFE and TFR2 knock-out mice which failed to mount a normal hepcidin response following LPS injection (70, 71) and by the identification of BMP-responsive elements in the hepcidin promoter important for IL-6 mediated response (72).

1.6 Regulation of ferroportin expression

Ferroportin (FPN), also known as SLC40A1, Ireg1, MTP1 and HFE4 was firstly identified as an iron exporter in enterocytes by three independent groups in 2000 (14-16) . It appears to be the sole member of the SLC40 transporter family and is highly conserved among mammals with 90-95% homology among human, mouse and rat orthologs. FPN-deficient mice were demonstrated to accumulate iron in enterocytes, macrophages and hepatocytes shortly after birth, consistent with the essential role of FPN in the iron export of these tissues (73). The human *SLC40A1* gene encodes for a 570 amino acids protein which was proposed to assemble in 12 putative transmembrane domains (74, 75). Controversial data were reported about its quaternary structure and it remains unclear whether it is a monomer (75-77) or a dimer (78, 79). FPN is highly expressed in cells and tissues playing a critical role in systemic iron homeostasis, such as placenta and intestine responsible for iron absorption and transfer, and macrophages and hepatocytes, major sites of iron recycling. Expression of FPN also protects cells from manganese (80) and zinc (81) toxicity, suggesting that it can mediate the export of

other transition metals. While hepcidin expression is only known to be regulated at transcriptional level, several levels of control characterize FPN regulation.

1.6.1 Ferroportin transcriptional regulation

Transcriptional regulation of FPN was first shown following erythrophagocytosis in the J774 macrophage cell line (82) and bone marrow derived macrophages (83, 84). The degradation product of hemoglobin, heme, transcriptionally co-regulates heme oxygenase 1(HO1) (the enzyme that catalyzes heme degradation) and FPN, accelerating iron extraction from heme and the recycle of iron into the plasma. It has been proposed that while the protoporphyrin ring of heme is sufficient to increase FPN transcription in an iron-independent manner (85), the iron release from the heme moiety controls FPN post transcriptionally (84). Molecular insights were obtained with the identification of the transcriptional repressor Btb And Cnc Homology 1 (Bach1) as sensor of cellular heme levels. It antagonizes the activity of small Maf proteins (sMAF) that bind Maf recognition element (MAREs) in HO1 and FPN promoters to promote transcription. Heme binding induces Bach1 dissociation from sMAF and also stabilizes the Nuclear Factor Erythroid 2-like (NRF2) which binds to sMAF to enhance gene transcription utilizing specific forms of MAREs called Antioxidant Response Elements (ARE). MARE/ARE enhancer elements were identified at position -7007/-7016 of FPN promoter. Mutations of these elements were shown to abrogate transcription in reporter constructs (85).

Increased erythropoiesis in hypoxic conditions while reduces hepcidin, also induces FPN mRNA levels. The stabilization of HIFs factors and in particular of HIF2 α seems to directly activate FPN expression as suggested by the FPN transcription reduction following the intestine specific deletion of HIF2 α (86) and by chromatin immunoprecipitation studies showing HIF2 α binding to FPN promoter region in murine duodenum. Furthermore HIF-responsive elements (HREs) were identified in the FPN promoter whose mutations prevented FPN up regulation in response to low oxygen (87).

Direct induction of FPN transcription in macrophages is additionally caused by iron and other transition metals such as copper, zinc and cadmium (81, 88, 89). However in case of iron-induction, the relevant transcription factor has not been yet identified. For zinc and cadmium the molecular mechanism is clearer and involves the binding of the Metal Transcription Factor 1 (MTF-1) on two Metal Responsive Elements (MREs) sequences in the FPN promoter (81).

Reduction in FPN transcription occurs during inflammation. LPS stimulation triggers FPN expression down regulation (57, 61, 90) in the spleen and in the liver to rapidly reduce iron availability for pathogens. It has been proposed that this effect is independent of specific cytokines, as mice lacking IL-6, TNF α or IL-1 were shown to retain the hypoferremic response and reduce FPN mRNA level upon LPS injection (57). However the cytokine contribution remains controversial, as it was also reported that TNF α mediated hypoferremia during the early inflammatory response by regulating the expression of FPN in macrophages (91). The importance of FPN function during infection is also supported by the finding that macrophages isolated from mice carrying a heterozygous loss-of-function mutation in FPN, exhibit increased susceptibility to intracellular bacterial growth (92). Nevertheless, little is still known about the molecular players responsible for FPN transcription in the inflammatory context and more work is needed to clarify its role in the immune response.

1.6.2 Ferroportin post transcriptional regulation

At the post-transcriptional level FPN is regulated via the IRE/IRP system. Similar to other iron-related genes, FPN mRNA contains an iron responsive element (IRE) in its 5' untranslated region (UTR). As described in paragraph 1.3.2 in low iron conditions, the iron regulatory protein IRP binds the IRE element blocking the mRNA translation. On the other hand, when iron levels are restored, the inactivation of the IRPs allows the FPN mRNA translation. This mechanism

protects cells both from excessive iron depletion in case of low intracellular iron and from the toxicity that can derive from an excessive iron accumulation (93).

Erythroid cells and duodenal enterocytes additionally express a FPN transcript variant which lacks the 5'-IRE, termed FPNB. This transcript is insensitive to iron regulation but keeps unaltered the open reading frame producing a protein that is functional but remains responsive to hepcidin. FPNB is produced from an alternate promoter located upstream of the canonical one, and is subjected alternative splicing of the 5'-UTR sequence (94). This form accounts for 25% of total FPN mRNA in the duodenum where it supports iron export even under conditions of iron deficiency. Much higher levels are present in erythroblasts which keep responsiveness to systemic iron deficiency via hepcidin regulation (95).

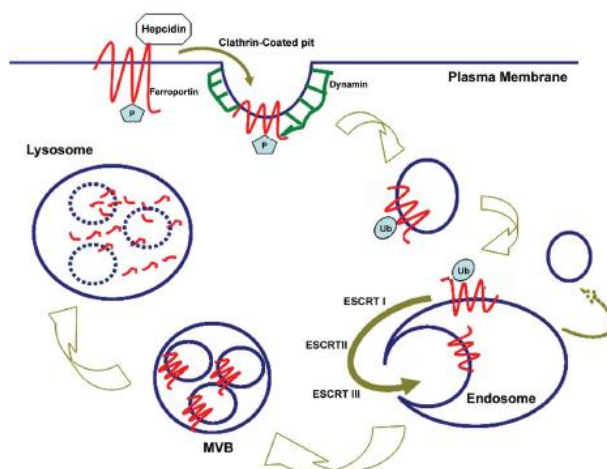
1.6.3 Ferroportin post translational regulation

FPN post translational regulation mainly is mediated by hepcidin activity. As described above (paragraph 1.4.1) hepcidin binding to FPN induces its internalization and degradation modulating the amount of iron exported. This explains both recessive iron overload disorders resulting from decreased hepcidin production and iron deficiency disorders resulting from increased hepcidin levels. Hepcidin was shown to induce FPN loss in cultured macrophages and hepatocytes (96) while *In vivo* lines of evidence came from hepcidin knockout mice which were reported to exhibit increased level of FPN in duodenum, spleen and liver.

The mechanism underlying the ferroportin internalization and degradation has been deeply investigated since its identification. Several publications have supported a model according to which hepcidin binding to FPN causes phosphorylation of two adjacent tyrosines (302, 303) in a cytoplasmic domain of FPN which triggers its internalization by clathrin-coated pits. Ubiquitination then targets FPN for degradation in lysosomes through the multivesicular bodies (MVB) pathway requiring the participation of the ESCRT complexes (97) (Figure 1.5). The Janus Kinase 2 was then reported to initiate the process (98). However this model has

been lately re-examined by two publications showing that neither JAK2 nor phosphorylation of FPN residues 302 and 303 is indeed required for hepcidin-mediated internalization and that ubiquitination is actually the key molecular signal for FPN endocytosis (99, 100).

Besides, the presence of endogenous FPN in raft domains demonstrated in macrophages (101) has questioned the proposed clathrin-dependent FPN internalization, revealing the existence of new possible cellular pathways involved in hepcidin-mediated FPN endocytosis.



De Domenico et al., Molecular Biology of the Cell, 2007

Figure 1.5 First proposed model of hepcidin-mediated ferroportin internalization and degradation.

1.7 Ferroportin and hepcidin regulation by miRNAs

Over the last years several lines of evidence implicating small non-coding RNAs in iron metabolism have been accumulated and reviewed (102) adding a further regulatory mechanism to the post transcriptional regulation of FPN and other iron-related genes. MicroRNAs are a class of small non-coding RNA which regulate gene expression via base-pairing with complementary sequences within mRNA molecules (103). At the cellular level iron homeostasis seem to be

regulated by miRNAs at multiple steps from iron acquisition to export. Modulation of cellular iron export by FPN was recently shown in association with miR-485-3 whose overexpression led to increased cellular ferritin levels by repressing FPN expression. Conversely, both inhibition of miR-485-3p activity and mutation of the miR-485-3p target sites on the FPN 3'UTR mediated opposite effects (104). Together, these findings support a model that includes both IRPs and microRNAs as iron-responsive post-transcriptional regulators of FPN.

Liver-specific miR-122 provides an example of miRNAs-mediated iron regulation at systemic level (105). Depletion of miR-122 in mice was shown to lead to systemic iron deficiency and mildly impaired hematopoiesis associated with increased mRNA level of HFE, HJV, hepcidin and BMPR1A. In particular it was proven that HFE and HJV are directly targeted by miR-122 which affects hepcidin expression in the liver and causes iron reduction in the plasma.

1.8 Iron related disorders

The study of molecular mechanisms underlying genetic iron disorders has been very helpful in deciphering the molecular mechanisms controlling systemic and cellular iron homeostasis. Major iron disorders can be classified in iron overload and iron deficiency diseases due to iron excess and iron scarcity, respectively. The key factor in many of these conditions is hepcidin misregulation and the resulting imbalance of the hepcidin/FPN regulatory system.

1.8.1 Iron overload diseases

Hereditary Hemochromatosis (HH) is a primary iron overload disease. In HH patients, dietary iron absorption exceeds iron loss by approximately 3mg per day, resulting in excessive iron accumulation in several organs, in particular liver and pancreas. Iron overload generates oxidative stress damaging tissues. The most common consequences are hepatomegaly, liver cirrhosis, hepatocellular

carcinoma, diabetes mellitus, hypogonadism, cardiomyopathies and arthritis. If untreated, massive iron accumulation can be lethal (106, 107).

HH is a genetically heterogeneous disease but all the mutations share the common effect of disrupting the hepcidin/FPN regulation, due to the lack of hepcidin synthesis or FPN functionality or to the lack of the hepcidin/FPN interaction. According to the gene involved in the pathogenesis, the clinical severity and the onset of the disease, HH has been divided in subtypes. HH type 1-3 is characterized by mutations in the iron-sensing machinery that result in an inappropriately low or absent hepcidin production in response to the increased systemic iron level. HH type I is caused by mutations in HFE (108-110) and is the most common form of the disease accounting for around 85% of cases. At least 32 mutations of the HFE gene have been described, however the vast majority of patients with HH type 1 are homozygous for the C282Y mutation which leads to a misfolded, non-functional protein. Despite the high frequency of this missense mutation in the Caucasian population, this kind of HH shows low and variable penetrance. HH type II is a juvenile and more severe disorder characterized by early onset in childhood and caused by rare mutation in HJV (HFE2) (111-113) or hepcidin itself (114). The HH type III is another late-onset form of disease produced by mutations in TfR2 (115). These are all recessive forms of HH. The only genetically autosomal-dominant form derives from missense mutations in the FPN gene (116) causing two distinct alteration of its functions.

Classical ferroportin disease is caused by loss of function mutations that lead incorrect targeting of the protein to the plasma membrane or to the production of an inactive iron transporter. Clinically, this disease is hallmarked by hyperferritinemia in presence of a normal to low transferrin saturation and by iron overload in specialized iron-exporting cells, such as the Kupffer cells of the liver and the splenic macrophages. Affected patients often do not tolerate phlebotomy since it rapidly results in very low transferrin saturation and anemia. (117) The

flatiron (ffe) mouse model carrying the SLC40A1-H32D mutation which causes an impaired ferroportin localization and activity fully recapitulates this disorder (118).

A HH-like phenotype is caused by “gain of function” mutations that render FPN insensitive to hepcidin-mediated degradation. The clinical phenotype is hallmarked by hyperferritinemia and high transferrin saturation. The continuous and unregulated iron uptake provokes iron accumulation in hepatic cells while macrophages are iron depleted. This so called *non classical ferroportin disease* is rare and only a few mutations have been reported. Among these, the C326S/Y mutation has been well characterized in cell-based assays (76, 119) and a mouse model was generated (190). The cysteine 326 is located in the third extracellular loops of FPN and its free thiol group is necessary for the hepcidin binding. Mutations of this amino acid residue prevent the hepcidin/FPN interaction causing hemochromatosis (120). The non-classical ferroportin disease is the only member of the HH family which is associated with increased hepcidin levels (121) thanks to the responsiveness of HFE/TfR2/HJV iron sensing machinery that is critical to maintain hepcidin synthesis.

1.8.2 Iron deficiency diseases

Iron deficiency is not always associated with anemia which occurs, by definition, when hemoglobin levels are below 13 g/dl in men and 12 g/dl in women. Decreased iron stores without anemia determine *latent iron deficiency* conditions characterized by decreased ferritin level in an early phase and soluble high transferrin receptor levels (released from erythroid cells) in a later phase. However more common are the subtypes of iron deficiency linked to anemia.

1.8.2.1 Iron deficiency anemia

Iron deficiency anemia (IDA) represents half of all anemia cases worldwide and is characterized by low hemoglobin levels as a result of depleted iron stores. It is caused by insufficient dietary intake and absorption or it is consequent of increased

iron needs, for example in pregnancy or in case of blood loss. Oral iron supplementation or, in worse cases, intravenous iron administration are usually sufficient to revert the clinical phenotype. More severe are subtypes of anemia linked to ineffective erythropoiesis and genetic alterations.

1.8.2.2 Iron-loading anemias

Iron-loading anemias are usually associated with red blood cell disorders, such as thalassemia. In this disorder it was observed (122-124) that hepcidin levels did not correlate with liver or systemic iron load but with altered erythropoietic parameters. Increased and ineffective erythropoiesis (or hemolysis) augments iron demand and leads to hepcidin suppression despite progressive iron overload in the body. Low hepcidin allows iron hyperabsorption and maldistribution, exacerbating systemic iron overload and iron accumulation in the organs. This finding also suggests that erythropoietic factors have a dominant effect over iron on hepcidin regulation, as additionally confirmed in sickle cell anemia (125) and myelodysplastic syndrome (126).

1.8.2.3 Iron refractory-iron deficiency anemia

Loss-of-function mutations in hepatic protease TMPRSS6 are known to cause iron –refractory iron deficiency anemia (IRIDA) (127). In this genetic disorder the negative regulation of HJV, mediated by TMPRSS6 under iron deficiency conditions (Figure 1.4), is lost, leading to accumulation of HJV, dysregulated BMP/SMAD signalling, and consequently, inappropriately high levels of hepcidin. This ultimately causes uncontrolled FPN degradation due to high hepcidin loads and, therefore, to iron deficiency anemia which is unresponsive to oral iron therapy and parental iron treatment, as iron absorption and release from store are irreversibly impaired by inappropriate hepcidin expression.

1.8.2.4 Anemia of inflammation

Anemia of chronic disease (ACD), also known as anemia of inflammation is the most prevalent anemia subtype. It is associated with inflammatory conditions, such as cancer, infections, rheumatoid arthritis and chronic kidney disease. It is characterized by a multifactorial etiology, involving immune cell activation and massive inflammatory cytokine production. ACD is a normocytic anemia with blunted erythropoiesis (128). Despite decreased circulating iron (low serum iron) and iron binding capacity (low transferrin saturation), macrophages retain and accumulate iron impairing mobilization of iron from stores (129). The main cause for iron deficiency is attributed to excess levels of hepcidin, whose synthesis is induced by inflammatory cytokines, as indicated by several reports (130-132) and as described in 1.5.4. The treatment options for ACD include blood transfusion, iron administration and erythropoiesis-stimulating agents (ESAs). However different adverse effects are related to all of these treatments. For example, tumor progression seems to be accelerated by ESAs treatment in cancer and myelosuppressive therapy (133, 134). Toxic effects are expected also from long-term intravenous iron therapy. For instance excess iron may increase the risk of infection, as iron represents a growth factor for pathogens. Thus, many studies are now focused on identifying alternative treatments targeting the main cause of this pathophysiology: hepcidin excess and FPN activity reduction. Novel strategies to decrease hepcidin levels include hepcidin antagonists (anti-hepcidin antibody, short interference RNA against hepcidin, engineered lipocalins as hepcidin binding proteins) and hepcidin inhibitors which target the signaling pathways mediating hepcidin synthesis (BMP6-HJV-SMAD and IL6-STAT3) (68, 135). In addition several screening approaches aim at identifying new molecules which may work as ferroportin agonists and stabilizers to correct iron deficiency (136). However the safety and the efficacy of all these treatments for humans remain to be proven. Finally, understanding the hepcidin-independent FPN transcription response during inflammation, whose molecular mechanisms are still poorly understood, will help to design and develop novel and more therapeutic approaches for this widespread condition.

1.9 Aim of the study

Hepcidin-mediated FPN regulation plays a pivotal role in controlling and maintaining iron homeostasis. At the beginning of this project few molecular details of this process had been. Thus, the specific aim of this study was to identify genes and cellular processes that control hepcidin-induced FPN internalization to better understand this pathway and find novel regulators suitable for pharmacological manipulation. I expected that this would establish the basis for novel treatment options of iron-related disorders in which the hepcidin/ferroportin circuitry is altered.

To reach this aim a large-scale RNAi screening approach was chosen to investigate the function of kinases and other related signalling molecules in FPN regulation.

2 EXPERIMENTAL PROCEDURES

2.1 Materials

2.1.1 Frequently used reagents and chemicals

Glycine, Tris-(hydroxymethyl)-methylamine (Tris), sodium chloride (NaCl), methanol, ethanol, isopropanol and sodium dodecyl sulphate (SDS), deoxyribonucleotide triphosphates (dNTPs) were from Carl Roth GMBH (Karlsruhe, Germany). Triton X100 was obtained from Fluka Analytical (Munich, Germany). Lysis Buffer and substrates for renilla luciferase assay were from Promega (Madison, WI, US). Dulbecco's Modified Eagle Medium (DMEM), Roswell Park Memorial Institute-1640 (RPMI-1640), Opti-MEM®, fetal calf serum (FCS), sodium pyruvate and penicillin/streptomycin (Pen/Strep) were all from Gibco BRL div. of Invitrogen (Karlsruhe, Germany), Dulbecco's phosphate buffered saline (PBS) from PAA laboratories (Pasching, Austria). Hyclone fetal Bovine serum defined for bone marrow derived macrophages was from Thermo Scientific and macrophage colony-stimulating factor from mouse was obtained from Sigma-Aldrich. Random primers were purchased from Invitrogen (Karlsruhe, Germany). Cell culture multi-well plates, dishes, flasks, tubes and falcons were obtained from Sarstedt (Nümbrecht, Germany) or Greiner Bio-One (Frickenhausen, Germany). PVDF membranes were from GE Healthcare (Little Chalfont, UK).

2.1.2 Transfection reagents

Listed below in Table 2.1 are the transfection reagents that were used in this work. Unless stated otherwise, the manufacturer's recommendations were followed.

Application	Name	Supplier
Plasmid DNA transfection (generation of cell lines)	<i>TransIT</i> ®-LT1 Transfection Reagent	Mirus Bio
Reverse siRNA transfection (Hela)	Dharmafect1 Transfection Reagent	Dharmacon
Direct siRNA transfection (BMDMs)	Lipofectamine RNAiMAX	Life Technologies

Table 2.1 **Transfection reagents.**

2.1.3 Enzymes, recombinant protein and antibodies

The restriction enzymes, T4 DNA Ligase, Calf Intestinal Alkaline Phosphatase (CIAP), DNA polymerase I were obtained from New England Biolabs (NEB) (Ipswich, MA, USA) and were used according to the NEB guidelines. The reverse transcriptase, RevertAid™ H Minus M-MuLV, was from MBI Fermentas (Burlington, Ontario, Canada).

Recombinant human hepcidin/LEAP-1 was obtained from Peptides International, Inc. (US). Recombinant murine IL6 and IL1 β were purchased from R&D Systems (Wiesbaden, Germany), recombinant mouse Tumor Necrosis Factor- α was from Life Technologies.

Primary monoclonal anti-GFP was obtained from Roche (Mannheim, Germany). Primary rabbit anti-mouse MTP11 IgG and anti-rat HFE IgG were purchased from Alpha Diagnostic (San Antonio, US). Primary rabbit anti-Tet Repressor was from Sigma-Aldrich as well as all the secondary anti-mouse and anti-rabbit IgG peroxidase conjugate antibodies. Primary anti-phospho-Src Family(Tyr416) antibody and anti-phospho-Akt(Ser473) antibody were purchased from Cell Signaling Technology.

2.1.4 Buffer and solutions

All buffers and solutions used in this study are listed in Table 2.2.

Buffers and Solutions	Preparation
Antibiotic solutions (1000x)	100 mg/ml ampicillin in H ₂ O
DNA loading buffer (6x)	0.9% (w/v) bromophenol blue 60% (v/v) glycerol 60 mM EDTA pH 8.0
Luria-Bertani (LB) agar (autoclaved)	15 g/l Bacto™ Agar in LB broth
LB broth (autoclaved)	10 g/l Bacto™ Tryptone 5 g/l Bacto™ Yeast extract 5 g/l NaCl pH 7.6 (adjusted with 5 N NaOH)
TBE (10x)	0.89 M Tris base, pH 8.3 0.89 M boric acid
Running buffer for SDS-PAGE electrophoresis	25 mM Tris 192 mM Glycine 0.1% (w/v) SDS
Transfer Buffer for Western blot	25 mM Tris 192 mM glycine 10% methanol
RIPA buffer	10 mM Tris-HCl pH8 150 mM NaCl 1 mM EDTA 1% NP-40 0,1% SDS
NET buffer	1% (v/v) Triton X-100 50 mM Tris-HCl pH 7.4 5 mM EDTA 150 mM NaCl 20 mM NaF 1 mM Na ₃ VO ₄
4x Laemmli Sample Buffer	250 mM Tris-HCl pH 6.8 8% (w/v) SDS 40% (v/v) glycerol 10% b-mercaptoethanol 0.06% (w/v) bromophenol blue

TBST(10X)	100mM Tris.HCl pH 7.6 150mM NaCl, 0.5% Tween® 20
-----------	--

Table 2.2 **List of buffers and solutions.**

2.1.5 Kits

Listed below in Table 2.3 are the kits that were used in this work. Unless stated otherwise, the manufacturer’s recommendations were followed.

Application	Name	Supplier
Plasmid DNA extraction from E. Coli bacteria cultures	NucleoBond Xtra Midi® , NucleoSpin Plasmid®	Macherey-Nagel, Düren, Germany
Plasmid DNA extraction from agarose gels	NucleoSpin Extract II®	Macherey-Nagel, Düren, Germany
RNA extraction	RNAeasy Plus®	Qiagen, Hilden, Germany
Renilla luciferase reporter assay (or Dual luciferase reporter assay)	Renilla-Luciferase-Reporter assay system (or Dual Luciferase-Reporter assay system)	Promega, Madison, WI, US
Quantitative PCR (qPCR)	SYBR Green PCR Master Mix	Applied Biosystems (ABI), Warrington, UK
Senescence associated β -gal activity	Cellular Senescence Assay Kit(SA- β -gal Staining)	Cell Biolabs, Inc.

Table 2.3 **List of kits.**

2.1.6 Plasmids used for the stable and inducible HeLa cell line generation

To generate the stable and inducible HeLa cell lines the Flp-In™-T-Rex™ Mammalian Expression System (Invitrogen) was applied according to the

manufacturer's instructions. All the required plasmids were obtained from Invitrogen. Three different constructs were used to generate three different stable and inducible HeLa cell lines:

pcDNA5toFRT-hFPN-EGFP

pcDNA5toFRT-hFPN-Rluc

pcDNA5toFRT-Rluc

The coding sequence of human ferroportin fused to the coding sequence of enhanced green fluorescent protein was subcloned in pcDNA5toFRT expression vector (Invitrogen) by using AflIII and NotI restriction sites. To generate the hFPN-Rluc construct, EGFP was cut and renilla coding sequence was subcloned in the same vector by using KpnI and NotI restriction sites. pcDNA5toFRT-Rluc construct was obtained by subcloning Rluc in pcDNA5toFRT by using HindIII and NotI. The correct sequences of DNA constructs employed in the experimental studies were verified by DNA sequencing (GATC biotech AG, Konstanz, Germany).

The selective antibiotics: BlastidicinS, ZeocinTM and HygromycinB were purchased by InvivoGen and were used at concentration 5 µg/ml, 200µg/ml and 200µg/ml respectively.

2.1.7 Oligonucleotides

All primers were purchased from Sigma-Aldrich (Taufkirchen, Germany) or biomers.net (Ulm, Germany). PCR primers were obtained in desalted, lyophilized form, and were diluted in H₂O.

2.1.7.1 Primers used for sequencing of DNA constructs

The following primers were used for DNA constructs used for the HeLa cell line generation:

FW 5'-3' CMV-F: CGCAAATGGGCGGTAGGCGTG

RV 5'-3' BHG-REV: TAGAAGGCACAGTCGAGG

2.1.7.2 Primers used for quantitative PCR analysis

All the primers used for quantitative PCR are listed in table 2.4.

<i>Gene (human)</i>	<i>FW 5'-3'</i>	<i>RV 5'-3'</i>
AZU1	tgagcggagaatggctacga	gtatcgtcacgctgctggt
	aacctgaacgacctgatgctg	atcgtcacgctgctggga
MAP4K3	attacccccacacaaacctg	aatgagccatctcgttcacc
EVI1	aatgcgactaaagtgattcagtg	cctaagggtgggtaaacctgga
MAP3K1	caccaccactgcattgcaaa	gatctacaaggggacatattaagg
TSSK2	gcaaaaagtcaaatctgcctactc	gttttctgcggctgatgat
TEX14	ccgcaccagaagtgatcttac	ccctccagggtatgcatc
TGFBR1	aaattgctcgacgatgtcc	cataataaggcagttgtaacttca
NRBP1	agataaattcctgaagatgacag	tgtcacctcctcctgctgt
TGFBR2	tccatctgtgagaagccaca	gggcatggcaaacgtctc
BCKDK	gagaagtgggtggacttgc	catagggatgaaggggaacc
CKMT1B	ggtaacatgaagagaggtttgaaag	cagccagttcttgataagt
OXSR1	agcccatcattacctgtgaact	aacccagcccaattctatt
TTBK1	gccaaactacgtggtcaagg	cctggtcagcaggtccat
	ggcagacgatcagaaggagt	agagacaagcaccagcgttt
	cattctacccccagcttcac	caagggcagactgggttt
ITPKB	tgaggggaccctaccagat	ccaggctggtgcttccta
	tgtgaccaagccacggtacat	ccctcgttttggtctcttga
ACVR1	catgaattggctttggaga	ctttggcagtgtagcctta
	tggcagagttatgaggcact	atgggagtgagcaggtctct
TLR6	tgaaacagctcttttgagtaaatgc	tccattgggaaagcagagt
PHKA1	caacttactgattcacctcatcc	tcccagactggtctctagg
EPHB6	ccccggactggagaagac	gggtggactataatcccttatttc
	ccaggaacctgccagcgggtg	ggcaggggtgaaggagtggttcctctg
IPMK	cacatgtacgggaaggacaa	catattatagaattccagctctctgg
EPHB3	tgccaaggagtcccagtg	agggtgtacggctgttg
PIP4K2A	atggaattaagtccatgaaaac	gcatcataatgagtaaggatgtcaat
ALDH18A1	tgacctgcaggggttatta	ttttcattccacagccagtc
BLNK	tcaaccaagccaaattcctc	ccccactgttcgacctg

EIF2AK1	ccactcgttcaagacaggtg	gctaaactcgtcactacaagtgaaa
PIP5KA1	ttgctcttctcatctttccaac	cccctcttaccttagctcca
HK3	atcgtggactgcatcgtg	ttgtccagttcaggagga
BMPR1B	tttcatgccttggtgataaaggt	gcttgtttaactttttgttcctctc
EPHA4	aagaggacagggacggagag	agttatcctataccgggtccattt
RET	catcaggggtagcgaggtt	gggaaaggatgtgaaaacagc
	gctccactcaacgtgtc	gcagcttgactggacgtt
RBKS	aggcagtggaagaggag	cagttttggcaaacgagaag
EPHA8	acctcagctactaccgtgacg	actggagatcaggtcactgg
ADAM9	catgacagtgcacagctagtctaa	cacactgttcccacaaatgc
MAP2K7	ccccgacagacactgtga	ggctgaatgaacagcgactc
EPHB1	ttcgtaacagatgcaacaagaa	tattccagcccctttggatt
AP2M1	agggcatcaagagtcagca	gctcattccgacgatactga
CLTC	ccagattctgccaattcgtt	tggttgatacccaggttct
ACTIN	ttccgctccctgaggcactct	tctgctggaagggtggacagcga
FERROPORTIN	tgctgtttgcaggcgtcatt	ttgcagcaactgtgcacagtt
CAV1	acagcccagggaaacctc	ggatgggaacgggttagaga
MON1A	ctggaggcagacaagaac	ggcgcacgaataactacctg
JAK2	ggtgaaagtccatattctgtt	aggccacagaaaacttgctc
NEDD4	accacaacaaccggacca	gtccgactccgaggacac

GENE (MOUSE)	FW 5'-3'	RV 5'-3'
MECOM (EVI1)	aggaagattgaaataggcgaaa	ctgcacatcacctgttctcc
BCKDK	tgctcaagaatgccatgaga	tgagatcctgatgatgagatcaat
ADAM9	tgcaaggatgaccgaagg	tagtcgcagagaggaagg
BLNK	cgaagttacacaacgcacag	ggcatgtgatccaggaggt
ITPKB	ggcgggaaacctcagtt	cttcctcttgatgcctcg
PHKA1	tccatgtggagtctgcctg	caaccagaagttggcggtat
IPMK	gccaagagagctggaattt	ttgggcagggttttcg
BMP2K	ccgtcccttcatttctcac	ttggagaatgtccgtcgtt
EPHB6	cagttccagcaccccaata	tgacaggccgactcttagtg
TEX14	cagtgctcctcatgaacgaag	tgaggatatcaaggcatca
TLR2	ctgcactggtgtctggagtc	gggcacctacgagcaagat
TLR4	ggactctgatcatggcactg	ctgatccatgcattggtaggt
MAP3K1	gcagtttaaccttactcattttgg	agttccattccaacacctga
MAP2K7	attgggggttgactgct	ggagcctggcctctccta
PIP4K2A	caacagctcaccaccctg	ggcattaattgcataaacatcaa
36B4	gcgacctggaagtccaacta	atctgctgatctgcttgg
TLR6	gggtttctgtctggctca	ggtaccgtcagtgctggaa

FPN	tgtcagcctgctgttgcaaga	tcttcagcaactgtgtcaccg
HAMP	ataccaatgcagaagagaagg	aacagataccacactgggaa
IL6	gctacaaactggatataatcagga	ccaggtagctatggactccagaa
TNFA	tgctatgtctcagcctctc	gaggccatttgggaactct
TFR1	cccatgacgttgaattgaacct	gtagtctccacgagcgggaata
DMT1A	gggaagaagcagccaagg	gggggtctgtgctctagaat
IL1B	gcaactgtcctgaactcaact	atctttgggggtccgtaact
HFE	tcttgatcctccacgttc	tcatccacatagcccctagc

2.4 Table of primers

2.1.8 siRNAs

All siRNAs used to validate the screening are listed in Table 2.5. SiRNAs for human genes were purchased from Dharmacon as pool of 4 siRNAa sequences per gene (Lafayette, CO, US) (list on the left side), while others (on the right side) and siRNAs for murine genes were purchase from Ambion (Life Technologies) as single sequences. Three negative controls targeting no gene were used as scrambles. The first two in the list were obtained from Ambion, the last one from Dharmacon. All siRNAs were obtained in desalted, lyophilized form, and were diluted in H2O.

siRNA ID (human)	Gene symbol	Gene accession	siRNA ID (human)	Gene symbol	siRNA sequence
MU-006759-00	PANK4	NM_018216	117501	SLC40A1	CCAUGUACCAUGGAUGGGUtt
MU-009859-01	PRKAG3	NM_017431	15673	DNM2	GGAGCUAAUCAAUACAGUUtt
MU-008914-00	AZU1	NM_001700	147117	AP2B1	GGAUCCCUAUGUUCGAAAtt
MU-004884-01	DCLK1	NM_004734	125716	MON1A	GCUCUACAUGUGUUACAGCtt
MU-003588-02	MAP4K3	NM_003618	134054	EPN1	CGUGCGUGAGAAAGCUAAGtt
MU-005025-02	PIK3R4	NM_014602	136860	NEDD4L	CCCAUCUAAUCACAGACUCtt
MU-006530-02	EV11	NM_005241	607	JAK2	GGUGUAUCUUUACCAUUCtt
MU-003930-02	TGFBR2	NM_003242			
MU-003575-02	MAP3K1	NM_005921			
MU-004932-01	BCKDK	NM_005881			
MU-005379-01	TSSK2	NM_053006			
MU-004016-01	MAP2K7	NM_145185			
MU-008885-00	CDK5R2	NM_003936			
MU-006748-00	MVD	NM_002461			
			siRNA ID (mouse)	Gene symbol	Gene accession
			s69749	MECOM	NM_021442
			s77071	MAP3K1	NM_011945
			s62904	BCKDK	NM_009739
			s77070	MAP2K7	NM_001042557
			s232234	ADAM9	NM_001270996
			s69395	BLNK	NM_008528

Experimental procedures

MU-005386-02	TEX14	NM_031272
MU-006708-01	CKMT1B	NM_020990
MU-003929-02	TGFBR1	NM_004612
MU-004870-02	OXSRI	NM_005109
MU-005356-02	NRBP1	NM_013392
MU-004680-02	TTBK1	NM_032538
MU-004671-01	RPS6KB2	NM_003952
MU-019425-02	PDK4	NM_002612
MU-006743-02	ITPKB	NM_002221
MU-005389-02	TLK2	NM_006852
MU-005385-03	TAF1L	NM_153809
MU-004172-03	SPHK1	NM_021972
MU-005041-01	TAF1	NM_004606
MU-005326-00	MLKL	NM_152649
MU-004030-02	PINK1	NM_032409
MU-015901-01	EVI5L	NM_145245
MU-004924-02	ACVR1	NM_001105
MU-003110-02	CSK	NM_004383
MU-005156-01	TLR6	NM_006068
MU-004846-03	TAOK1	NM_020791
MU-019682-01	PHKA1	NM_002637
MU-010230-00	SQSTM1	NM_003900
MU-003224-03	CDC2	NM_001786
MU-003166-02	PTK6	NM_005975
MU-003125-02	EPHB6	NM_004445
MU-006740-02	IPMK	NM_152230
MU-003123-02	EPHB3	NM_004443
MU-006786-00	RBKS	NM_022128
MU-004030-02	PINK1	NM_032409
MU-003176-03	SYK	NM_003177
MU-003923-00	PIM1	NM_002648
MU-004838-01	RAGE	NM_014226
MU-003120-03	EPHA8	NM_001006943
MU-005071-01	BMP2K	NM_017593
MU-006785-01	ALDH18A1	NM_001017423
MU-003121-02	EPHB1	NM_004441
MU-006778-01	PIP4K2A	NM_005028

s71633	PIP4K2A	NM_008845
s115701	ITPKB	NM_001081175
s71572	PHKA1	NM_008832
s88141	IPMK	NM_027184
s100528	BMP2K	NM_080708
s65587	EPHB6	NM_001146351
s96393	TEX14	NM_001199293
s76898	TLR2	NM_011905
s75209	TLR6	NM_011604

MU-003560-06	RAC1	NM_006908
MU-020353-01	BLNK	NM_013314
MU-005359-00	PIM2	NM_006875
MU-005007-00	EIF2AK1	NM_014413
MU-004780-02	PIP5K1A	NM_003557
MU-006736-00	HK3	NM_002115
MU-006705-00	CHKB	NM_005198
MU-004934-01	BMPR1B	NM_001203
MU-003118-02	EPHA4	NM_004438
MU-003170-02	RET	NM_020630
MU-005352-02	MYLK2	NM_033118
MU-003524-01	PRKCD	NM_006254
MU-003545-10	AURKA	NM_198437
MU-004504-03	ADAM9	NM_001005845
MU-006760-02	PAPSS2	NM_004670
MU-003758-04	PRKCB	NM_002738
MU-005306-02	STRADB	NM_018571
MU-003146-02	JAK2	NM_004972
MU-005449-01	CCR2	NM_000648
MU-005013-01	TNNI3K	NM_015978
MU-004926-02	ACVR2A	NM_001616
MU-003163-03	PDGFRB	NM_002609
MU-008442-00	AKAP4	NM_003886
MU-006754-00	NME5	NM_003551

scramble ID	name
AM4611	Silencer Negative Control siRNA
AM4635	Silencer Negative Control siRNA
D-001210-03-05	siGENOME non targeting siRNA 3

2.5 Table of siRNAs. Some siRNAs for human genes (on the right side) are no longer available with the indicated ID. However their sequences are reported.

2.1.9 Bacterial strain

For propagation of vectors, the heat shock competent *E.coli* strain, XL1 blue, (La Jolla, CA, USA) was used. The genotype of this strain is the following: hsdR17,

supE44, recA1, endA1, gyrA96, thi, relA1, lac/F['][proAB+ lacl, lacZΔM15:Tn10(TetR)].

2.2 Cell culture methodologies

2.2.1 Cell lines and primary cells

The human HeLa cell line was cultured in Dulbecco's Modified Eagle's Medium (DMEM, high glucose) supplemented with 10% heat-inactivated low-endotoxin FCS and 1% penicillin/streptomycin. Cell cultures were maintained at 37°C under 5% CO₂.

Bone marrow derived macrophages (BMDMs) were flushed from tibia and femur using ice-cold HBSS and filtered through a 70 μm cell strainer. Cells were seeded at a density of 350,000 cells/cm² in RPMI1640-Glutamax medium supplemented with 10% of heat-inactivated FBS, 1% penicillin/streptomycin and 10 ng/ml M-CSF1. After 4 days, non-adherent cells were removed by washing with HBSS and the medium was replaced daily.

2.2.2 SiRNA screening

The stable and inducible HeLa cell line was established by applying the Flp-InTM-T-RexTM system according to manufacturer's instructions. The pcDNA5/FRT/TO plasmid contained the coding sequence of human ferroportin fused to *Renilla* luciferase or only *Renilla* luciferase under the control of a tetracycline-regulated, hybrid human cytomegalovirus (CMV)/TetO2 promoter. For the siRNA screen the cell-based *Renilla* luciferase assay was adapted to the 384-well plate format and high-throughput conditions. The Protein Kinase siRNA library Thermo Fisher siGenome (Dharmacon) targeting protein kinases and other related genes (779 genes) was used. The library was arrayed in 384-well white plates (Greiner Bio-One), each well containing 1.25 pmol of a pool of 4 synthetic siRNA duplexes (final concentration in wells, 25 nM). Viability controls included a siRNA pool directed against PLK1 and COPB2. As a negative control, 3 scrambled siRNAs were used.

Reverse transfection of HeLa cells was performed by dispensing 15 μL of RPMI1640-Glutamax medium together with 0.05 μL of Dharmafect1 reagent (Dharmacon) to the siRNA-containing 384-well plates. After 30 minutes incubation at ambient temperature, HeLa cells (2500 per well) were added to the siRNA transfection mix in a 30- μL volume of Dulbecco modified Eagle medium supplemented with 10% heat-inactivated low-endotoxin fetal bovine serum. Forty-eight hours after siRNA transfection, the medium was replaced with 30 μL fresh medium containing 0,5 $\mu\text{g/ml}$ doxycycline (Sigma-Aldrich). Three hours later doxycycline was removed by extensive washing with PBS and fresh culture medium was added to cells. Two hours later cells were incubated in absence or presence of 1 $\mu\text{g/ml}$ hepcidin (0,4 μM) for 18 hours. After incubation cells were lysed with 20 μL Passive Lysis Buffer 1x (Promega) and plates were frozen. All dispensing steps were performed with the use of MultidropCombi dispensing systems (Thermo Scientific). Renilla Luciferase activity was measured by adding Renilla luciferase assay substrate (Promega) and quantified by Centro LB 960 luminometer (Berthold Technologies).

2.2.3 Validation of the screening results

2.2.3.1 Validation in HeLa cells

To analyze viability and hyperproliferative effects induced by siRNAs, the MTT colorimetric assay (Sigma-Aldrich) that measures the reduction of yellow 3-(4,5-dimethylthiazol-2-yl)-2,5-diphenyl tetrazolium bromide (MTT) by mitochondrial succinate dehydrogenase was applied.

Validation of data from the screen was performed in a 96-well format with single or pooled siRNAs targeting the candidate genes (Table 2.5). 20 μL of 250 nM siRNA was spotted in well-plates. Dharmafect1 (0.2 μL) diluted in 60 μL of RPMI were added to each well and incubated 25 min at room temperature. After incubation 10×10^3 cells in 120 μL volume of complete culture medium (without antibiotics) were seeded on top of the transfection mix and cultured for 48h. After this the medium

was replaced with 200 μ l fresh medium containing 0,5 μ g/ml doxycycline. Three hours later doxycycline was removed by extensive washing with PBS and fresh culture medium was added to cells. Two hours later cells were incubated in absence or presence of 1 μ g/ml hepcidin (0,4 μ M) for 18 hours. After incubation cells were lysed with 100 μ l Passive Lysis Buffer 1x and 30 μ l of lysate was used for Renilla luciferase assay.

2.2.3.2 Validation in BMDMs

Validation of putative regulators of FPN protein stability in BMDMs was performed by applying direct RNA interference and following FPN protein analysis by Western blot. RNAi was mostly performed in a 6-well plate format, using at least 5 wells per a single siRNA candidate testing. BMDMs were processed as previously explained and seeded (700×10^3 per well) onto 6 well plates. After 4 days from seeding the medium was replaced and 1 day after RNAi was applied by using Lipofectamine RNAiMAX reagent (Invitrogen) according to manufacturer's instructions. 7,2 μ l of 10 μ M siRNA and 7,2 μ l lipoRNAiMax were used and the siRNA-reagent mix was added to cells in medium without Pen/Strep and macrophage colony stimulation factor. The day after the medium was replaced with a complete one. Cells were scraped from the culture plate 54h after the siRNA-reagent mix drop. 1/5 of the lysate was used for total RNA extraction, all the rest was used for total protein extraction. In some cases ammonium iron(III)citrate (Sigma-Aldrich) was used at concentration of 50 μ M for 16h.

2.2.4 Treatment of BMDMs with TLRs ligands, cytokines and inhibitors

BMDMs were seeded onto 6 well-plates (700×10^3 per well) or 10-cm dish ($3,5 \times 10^6$) and treated, after 5 days from seeding, with FSL1, PAM3CSK4 (InvivoGEN), PamOct2C-(VPG)4VPGKG (EMC, microcollection) and LPS (*Escherichia coli* serotype O111:B4) at a concentration of 20 ng/ml (FSL1) and 100 ng/ml for 6, 12 and 24h. Cells were then harvested for total RNA and protein extraction.

BMDMs were seeded onto 12 well-plates (350×10^3 per well) and incubated, after 5 days from seeding, in presence of mouse recombinant TNF α (GIBCO), IL6 and IL1 β (R&D Systems) at concentration of 0,5, 0,1, 0,02, 0,005 and 0,001 $\mu\text{g/ml}$ for 6, 12 and 24h. Cells were then harvested for total RNA extraction.

BMDMs seeded onto 12 well-plates (350×10^3 per well) were incubated, after 5 days from seeding, with the following inhibitors at the indicated final concentrations: LY294002(50 μM), Wortmannin(1 μM), PP1(10 μM), Saracatinib(10 μM), Bafetinib(10 μM), SB202190(15 μM), SP600125(15 μM), UO126(10 μM), PDTC(15 μM), SN50(15 μM). After 30 minutes of pre-incubation, FSL1 (100 ng/ml) was added to the medium for 6 hours. Cells were then harvested for total RNA extraction.

2.3 Molecular biology methodologies

2.3.1 Total RNA extraction and reverse transcription

Total RNA extraction from cells was performed with Qiagen RNAeasy Plus kit (Qiagen), while total RNA from tissues was isolated using Trizol (Life Technologies) according to manufacturer's instruction. The concentration and purity of the RNA was determined by Nanodrop2000 (Thermo Scientific). 1 (or 0.5) micrograms of total RNA was used for reverse transcription (RT). The RNA and 1 μl of random primers (0.2 $\mu\text{g}/\mu\text{l}$) were denatured at 70°C for 10 min, and cooled down on ice for 2 min. The reverse transcription reaction mixture contained a total volume of 25 μl consisting of RT buffer (Fermentas), 0.4 mM dNTPs, 100 units of RevertAid H Minus M-MuLV Reverse Transcriptase (Fermentas), 1 μl random primers (0.2 $\mu\text{g}/\mu\text{l}$) and 1 μg of denatured total RNA. The mix was incubated at 42°C for 90 min, then at 70°C for 10 min for stopping the reaction. The cDNA samples were diluted for the subsequent qPCR analysis by adding 175 μl of H₂O to cDNA obtained from cells or 475 μl of H₂O to cDNA from tissues.

2.3.2 Quantitative PCR

For quantitative PCR (qPCR) following the standard RNA extraction/cDNA synthesis protocol (see 2.3.1.) the reaction mix (20 μ l) contained 10 μ l SYBR Green PCR Master Mix, 0.5 μ M of the forward and reverse primers and 5 μ l of cDNA. The qPCR mixture was run on ABI Prism 7500 Applied Biosystems (Applied Biosystems) following amplification conditions: 50°C 2 min, 95°C 10 min, (95°C 15 s, 60°C 15 s) \times 40 cycles. Intron-spanning primers were designed to specifically amplify the human or murine transcripts. Sequences of the primers are shown in Table 2.4. Threshold cycles (C_t) were defined as the fractional cycle number at which the fluorescence passed the fixed threshold. C_t values were extracted by using the 7500 software v2.0.1 (ABI) and calculations for normalisation and analysis were done in Excel (Microsoft Office). The mRNA/cDNA abundance of each gene was calculated relative to the expression of the housekeeping gene 36B4 encoding for an acidic ribosomal phosphoprotein P0 (RPLP0) and data were analyzed by applying the $\Delta\Delta C_t$ method (Livak and Schmittgen, 2001).

2.3.3 Transformation of bacteria

Ligation mixtures (10 μ l) were mixed with 100 μ l of the transformation-competent *E.coli* strain, XL1 blue, incubated on ice for 20 min. The cells were heat-shocked for 90 s at 42°C and then placed on ice for 2 min. 400 μ l of LB medium was added and the mixture was incubated for 1h at 37°C with 1100 rpm shaking. The transformed bacteria were then spread on LB agar plates containing the appropriate antibiotic and incubated overnight at 37°C.

2.3.4 Bacterial culture and isolation of plasmid DNA

Single bacterial clones were incubated in 4 ml or 100 ml LB medium containing the appropriate antibiotic in the shaker, overnight at 37°C. To isolate plasmid DNA, the NucleoSpin Plasmid $\text{\textcircled{R}}$ NucleoBond or NucleoBond Xtra Midi $\text{\textcircled{R}}$ kits were used according to the manufacturer's instructions. DNA concentration was determined

using Nanodrop2000 (Thermo Scientific). Sequencing of DNA constructs was performed to confirm the sequences by GATC Biotech AG (Konstanz, Germany).

2.3.5 DNA agarose gels

DNA samples mixed with DNA loading buffer were loaded on 1% agarose (w/v) gels containing ethidium bromide. 250 ng of 1 kb or 100 bp DNA ladder used as a size marker allowed the estimation of the size of DNA fragments. Agarose gels were usually run at 100V, and visualised using a UV transilluminator (Herolab UVT-28 ME).

2.3.6 Western blot analysis

Cells were harvested by centrifugation at 13000 rpm for 30 second in cold PBS and cell pellets were lysed in ice-cold NET or RIPA buffer supplemented with 1X Complete Mini Protease Inhibitor Mixture (Roche Applied Science) and, in some cases, phosSTOP phosphatase inhibitors cocktail (Roche Applied Science). After incubation on ice for 30 min, lysates were clarified by centrifugation at 10,000 rpm for 10 min in a cooled microcentrifuge and supernatants were collected. Protein concentration was measured using the DC Protein Assay (Biorad). Samples were mixed with 4X Laemmli buffer and denatured by heating at 95 °C for 5 min. For FPN protein analysis samples were not denatured. The samples were subjected to 10% or 12% SDS-PAGE and the proteins were transferred to a PVDF membrane using wet transfer method. The membrane was blocked with 5% nonfat dry milk in TBS containing 0,1% Tween 20 (TBS/T) for 1 h at room temperature. Primary antibodies indicated in 2.1.3 were incubated for 1h at room temperature or overnight. The membranes were then washed with TBS/T and incubated with anti-rabbit IgG secondary antibody (Sigma-Aldrich). After washing, the immune complexes formed on the blot were visualized by ECL-Plus (Amersham Biosciences), quantified with Vilber Lourmat (Eberhardzell, Germany) Fusion-FX Chemiluminescence system and normalized to β -actin.

2.3.7 Plasma biochemistry and tissue iron quantification

Plasma iron concentration and unsaturated iron binding capacity were assessed using the SFBC and UIBC kits (Biolabo, Maizy, France). Transferrin saturation was calculated using the formula $SFBC/(SFBC+UIBC) \times 100$. Tissue non-heme iron content was measured using the bathophenanthroline method and calculated against dry weight tissue (Torrance and Bothwell, 1968).

2.3.8 Splenic macrophage isolation

Mouse macrophages were magnetically separated from splenic cell suspensions by CD11b MicroBeads (MACS) according to manufacturer's instruction.

2.3.9 DAB-enhanced Perls' staining

Tissues were fixed in 10% formalin overnight at room temperature and embedded in paraffin. Microtome sections, 5- μ m thick, were stained with potassium ferrocyanidesolution (Sigma-Aldrich) followed by 3,3-diaminobenzidinetetrahydrochloride (DAB) (Sigma-Aldrich) development.

2.4 Mice

C57BL/6N wild type male mice aged between 10 and 11 weeks were purchased from Charles River Laboratories. C326S-FPN mutant mice on a C57BL/6 background were generated as reported (190). Mice were housed in the EMBL animal facility under constant light-dark cycle and maintained on a standard diet containing 220 ppm iron (Teklad 2018S, Harlan, Rossdorf, Germany) with ad libitum access to water and food. Inflammation was induced by intra-peritoneal injection of FSL1 (InvivoGEN) and LPS (*Escherichia coli* serotype O111:B4) 25 ng/g bodyweight, unless otherwise indicated. Control mice were injected with an equivalent volume of sterile saline solution. Heparinized blood was collected by cardiac puncture from mice euthanized by CO₂ inhalation. All mouse breeding and

animal experiments were approved by and conducted with the guidelines of the EMBL institutional Animal Care and Use Committee.

2.5 Statistical analysis

For analysis of the screening data, the CellHTS2 package (Bioconductor) was used to calculate z-scores as a measure of the generated phenotype. To obtain z-scores this median was subtracted from each logarithmic value and divided by the median absolute deviation of a whole plate. High z-scores were indicative of reduced FPN activity, low z-scores were indicative of increased FPN activity. The threshold value was computed as the mean signal of the distribution plus two times the standard deviation. Mean z-scores for control siRNAs were first calculated within each replicate and then between replicates. For the screening data the mean z-score of 2 replicates was calculated.

All the other results from this study are expressed as a mean. At least 3 independent experiments were represented as mean plus or minus standard deviation (SD) or standard error (SEM). Two tailed, Student's *t* test was used for estimation of statistical significance.

3 RESULTS

3.1 Establishment of a fluorescent cell-based assay to assess hepcidin-mediated ferroportin regulation

The first screening strategy I optimized was based on cell-image analysis. The labs of Jan Ellenberg and Rainer Pepperkok (EMBL) developed a robust protocol for the reverse transfection of cells on small interfering (si)RNA arrays, which, in combination with multi-channel immunofluorescence or time-lapse microscopy, was suitable for genome-wide RNA interference (RNAi) screens in intact human cells (137, 138). This innovative assay was already used for the successful identification of regulatory genes (139).

To establish a fluorescent read-out of FPN expression I generated a stable HeLa cell line that expressed a human FPN/EGFP fusion protein in an inducible manner and adapted this cell-based assay to the high throughput setting of RNAi arrays and automated fluorescence microscopy. In this cellular model hepcidin treatment was expected to shift the fluorescence from the outer membrane to intracellular vesicles. By measuring intensity and localization of the fluorescent signal both before and after hepcidin application, the consequences of specific gene interference could be assessed. For instance, if fluorescence was exclusively detected on the cell surface before and after hepcidin addition, the respective siRNAs inhibited hepcidin-mediated FPN-EGFP internalization, as expected for kinases, which were supposed to be responsible for the hepcidin-mediated FPN phosphorylation. This approach provided in principle several advantages. It allowed visualizing FPN internalization steps and monitoring potential siRNA lethal effects. However it required a robust control phenotype in order to quantify fluorescent read-out changes.

HeLa cells were shown to support hepcidin-mediated FPN internalization (28) and, importantly, were used to set up a robust protocol of reverse transfection of cells on siRNA arrays (137, 139), making the usage of this cell line ideal for my purpose. To establish a stable HeLa cell line I applied the FlipIn T-Rex system (Invitrogen) that allowed me to generate a cell line stably expressing the Tet Repressor gene under the

control of the constitutive human cytomegalovirus promoter and the FPN-EGFP fusion gene under the control of the inducible cytomegalovirus promoter with Tet Repressor binding site, inserted in a single flipase (Flp) Recombination Target (FRT) site. The system provided in principle an isogenic stable cell line, with the same genetic background and the same inducibility level (Figure 3.1).

resistance gene lacks a promoter and the ATG initiation codon. Proper integration of pcDNA5/FRT plasmid places the ATG initiation codon (from pFRT/*lacZeo*) in frame with the hygromycin resistance gene, and inactivates the *lacZ-Zeocin* fusion gene. Thus, stable Flp-In expression cell lines can be finally selected for hygromycin and blasticidin resistance and Zeocin sensitivity.

Stable FlpIn T-Rex clones were selected for antibiotic resistance according to the protocol and tested for inducibility and the hepcidin response by Western blotting and by epifluorescence microscopy. Two problems arose over time: instability of the construct integration and lack of isogenicity among the cell population. To overcome these problems I generated a second, independent inducible stable cell line using a different type of HeLa cell and applying the same protocol (Figure 3.1). In this second attempt I tried to single out an isogenic population by additionally picking single clones even after the FPN-EGFP integration, when the cell population was already supposed to be isogenic according to the principle of the system. All clones were screened for β -galactosidase activity (that must be lost after FPN-EGFP integration) and for FPN-EGFP expression after induction with wide field microscopy. The most responsive clones to hepcidin addition were selected. Nevertheless neither of the two cell lines guaranteed the feasibility of the screening. Cell image-based screening required a cell-based assay with a robust read-out under control conditions: 1) Fluorescence signal indicative of FPN expression should be localized on the cell surface after induction by doxycycline and 2) should be undetectable after hepcidin treatment. Unfortunately the phenotype obtained with the stable lines did not seem to satisfy these requirements. In the first stable line (HeLa FPN-EGFP-clone C8) only few positive cells expressed the EGFP signal on the plasma membrane which was weak and required a long induction time. On the other hand, the second stable line (HeLa FPN-EGFP-clone C10) showed a very strong fluorescence signal even after a very short induction with a low doxycycline concentration, but the cells clustered together precluding single cell analysis. Although in both cases hepcidin treatment caused a fluorescence shift from the outer membrane to intracellular vesicles, these vesicles were preserved for long time after incubation with hepcidin (Figure 3.2). The intracellular fluorescence persistence of the vesicles prevented to establish a robust reference control and to perform the quantification of the fluorescent signal.

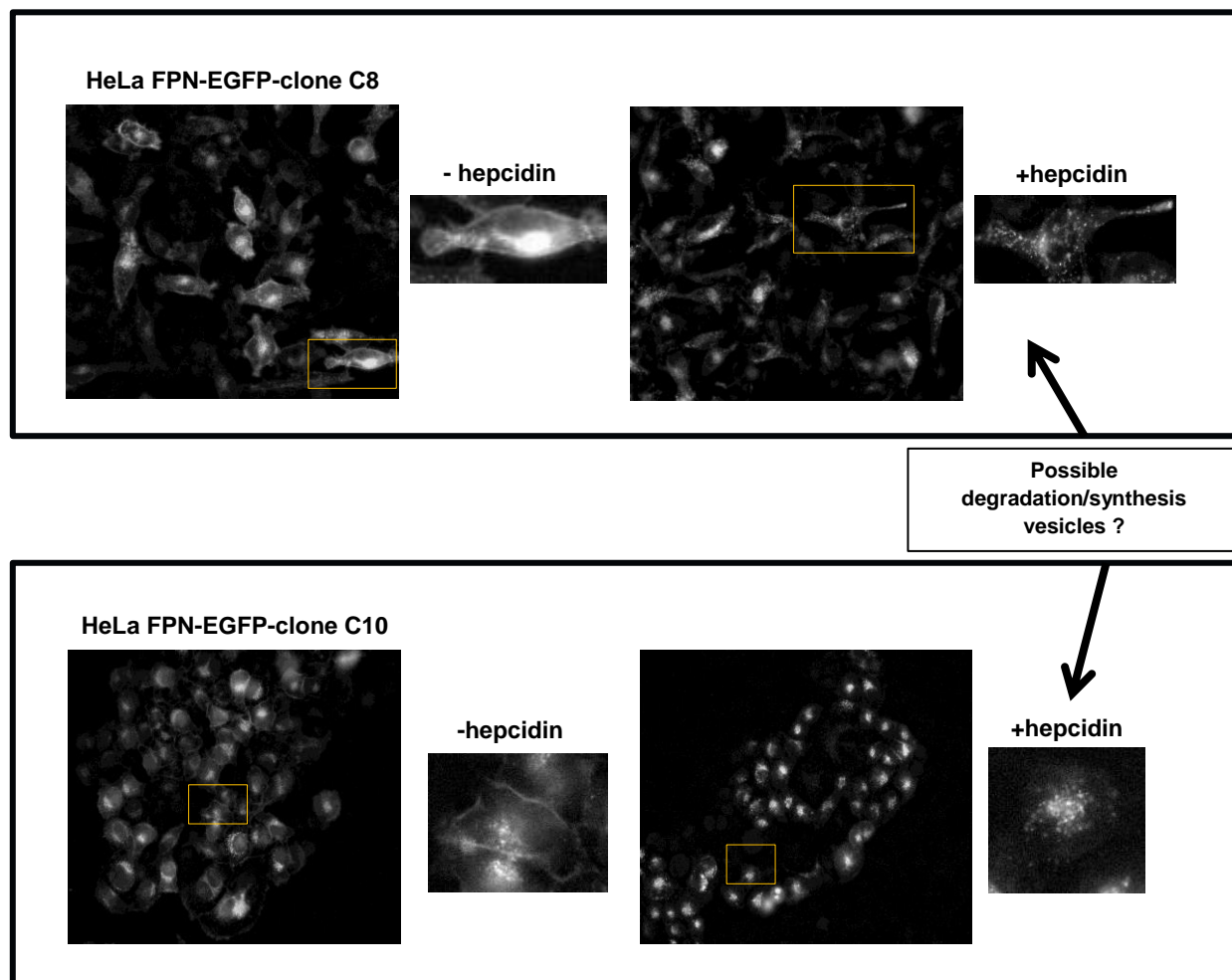


Figure 3.2 Hepcidin effect on HeLa stably expressing human FPN-EGFP fusion protein. Stable HeLa cells originated from two different clones were treated with doxycycline (2 ng/ μ l for 12 hours for the clone C8 and 0.05 ng/ μ l for 2.5 hours for clone C10) to induce FPN expression. After induction cells were washed out to remove doxycycline and cultured in fresh medium for additional 12 hours. They were then incubated for 4 hours in absence or presence of 0,4 μ M purified human hepcidin. Images were acquired by fluorescence microscopy (Zeiss CellObserver).

3.2 Establishment of hFPN-Rluc reporter assay as alternative siRNA screening system

To circumvent the problems described in paragraph 3.1, I generated a new stable and inducible HeLa cell line expressing the hFPN coding sequence fused to a renilla (Rluc) reporter gene by using the pcDNA5/TO/FRT hFPN-Rluc vector (Figure 3.3) and

applying the protocol previously described (Figure 3.1). In this system RLuc activity was indicative of FPN expression levels and provided a sensitive and fast read-out of its down regulation following hepcidin treatment. Although this approach did not permit monitoring intermediate stages of FPN internalization and lethal siRNA effects, it was technically less complex.

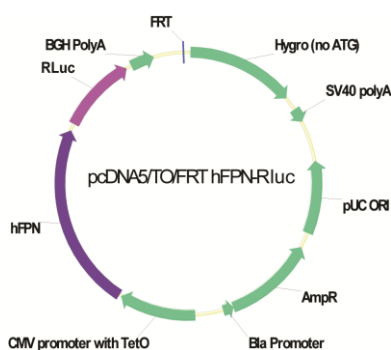


Figure 3.3 pcDNA5-hFPN-RLuc vector map.

3.2.1 Optimization of the screening protocol

Using the HeLa FPN-RLuc cell line, I optimized the screening strategy. One of the most relevant advantages of the stable and inducible cell line system was the presence of the inducible promoter which allowed to “switch on and off” the FPN reporter gene expression by adding and removing doxycycline from the medium. This modulation was an important advantage to prevent the override of the hepcidin response. If FPN-RLuc would be continuously expressed, it would be hard to quantify its reduction, mediated by hepcidin, thus preventing a solid analysis of hepcidin effects. However I observed that doxycycline removal from the medium didn’t immediately stop FPN-RLuc expression which continued to increase at some extent after the inducer was washed out. To optimize the hepcidin-mediated FPN response under my experimental conditions I tested several parameters: time of cells cultured in fresh medium after doxycycline washout, hepcidin concentration and hepcidin incubation time. The incubation time with hepcidin appeared to be the most relevant one. As shown in figure 3.4A the longer hepcidin treatment was prolonged, the greater the reduction in FPN-RLuc activity. Similar results were also obtained with 20x fold lower hepcidin concentration (Figure

3.4B) suggesting that in this experimental system FPN degradation was a slow process which required low amount of hepcidin.

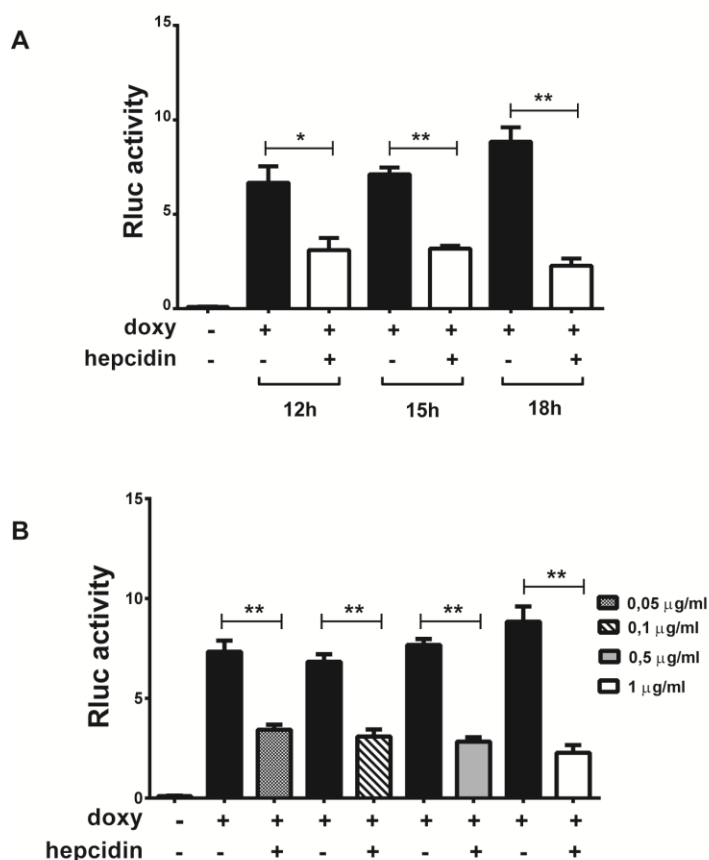


Figure 3.4 FPN degradation is a slow process, which is induced by low hepcidin amounts. (A) FPN-Rluc expressing HeLa cells were induced with doxycycline (0,5 ng/ μ l) for 3h. After induction doxycycline cells were washed and incubated in fresh medium. After 2h they were incubated in the presence or absence of hepcidin (1 μ g/ml) for the indicated times. Rluc activity was measured after cell lysis. **(B)** Cells were induced as in A and then treated with hepcidin at increasing concentration for 18h. All data are reported as means \pm SEM, * $P < 0,05$, ** $P < 0,01$, Student's t test.

Controversial data were published about the hepcidin-mediated FPN internalization, making difficult the identification of positive siRNA controls to add in the screening. However during the optimization phase of the assay I tested some siRNAs targeting mediators of clathrin-dependent endocytosis which was the first proposed mechanism initiating the FPN internalization (97). In particular, members of clathrin adaptor complex, such as AP2M and AP2B as well as dynamin (the GTPase responsible for

endocytosis) were examined. In my pilot screening shown in figure 3.5 I also included FPN siRNA, as knockdown efficiency indicator and some siRNAs known to induce cell death, such as polo-like kinase 1 (PLK1), ubiquitin C (UBC) and Coatamer Protein Complex (COPB) routinely used in the lab of Prof. Boutros as viability controls in kinome and genome-wide screening. In addition, caveolin was tested as component of lipid rafts (the other pathway proposed to mediate FPN endocytosis in macrophages)(101) while MON1a was included as modulator of the FPN trafficking to the surface of iron-recycling macrophages, according to one publication (140). Finally, I also examined the effect of the siRNA targeting NEDD4, the E3 ubiquitin ligase reported to be responsible for the hepcidin-independent FPN internalization induced by low intracellular iron level (141). I expected the RNA interference of some of these transcripts to alter the extent of FPN-Rluc reduction upon hepcidin addition.

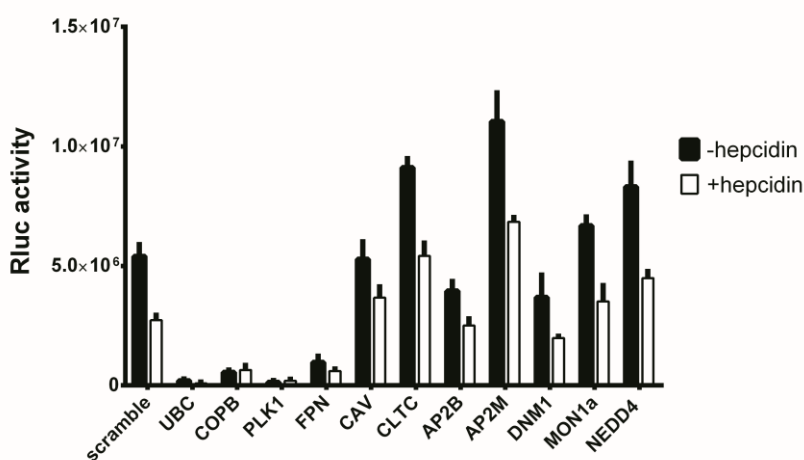


Figure 3.5 Pilot screen. FPN-Rluc HeLa cells were seeded on siRNAs targeting the indicated human transcripts. After 48h cells were induced by doxycycline addition and processed as described in figure 3.3 by using 1 μ g/ml hepcidin for 18h. UBC: ubiquitin C, COPB: coatamer protein complex, PLK1: polo like kinase1, FPN: ferroportin1, CAV: caveolin, CLTC: clathrin, AP2B, AP2M: adaptor protein beta2, mu2, DNM1: dynamin1, MON1a: mon1 secretory trafficking family member A, NEDD4: Neural Precursor Cell Expressed, Developmentally Down-Regulated 4

Unfortunately, despite the good knockdown efficiency (data not shown) achieved with most of the genes tested by measuring their mRNA level reduction, the depletion of the

indicated transcripts only mildly affected the hepcidin-mediated reduction of Rluc activity compared to the one observed with scramble control. Nevertheless I selected AP2M and NEDD4 siRNAs as controls for the screening in addition to siRNAs affecting viability (PLK1 and COPB) and FPN siRNA controls which, on the other hand, consistently reduced Rluc activity levels as expected.

3.3 RNAi screen for kinases and related signaling proteins

In collaboration with Prof. Boutros lab I performed a focused RNAi screen targeting a limited number of genes (779), predominantly encoding kinases and related proteins that, at this stage of the project, were expected to control FPN internalization and degradation. The Protein Kinase siRNA library Thermo Fisher siGenome contained pool of 4 different siRNA sequences per gene. The usage of siRNA pools rather than single sequence in principle ensured a greater phenotypic penetrance, however it also raised the risk of possible off-target effects. The cell-based *Renilla* luciferase assay was adapted to the 384-well plate format and high-throughput conditions and three scrambled-negative silencer-siRNAs were spotted as negative controls per each plate. The stable integration of one copy of FPN-Rluc gene in the genome of the cells overcame in this case the need of controlling the transfection efficiency which was usually required in case of transient transfection of similar reporters. On the other hand it also resulted in much lower gene-reporter expression levels demanding more sensitive detection system. According to the scheme in figure 3.6 HeLa-FPN-Rluc cells were reversed transfected with siRNAs spotted in 384-well plates. Forty-eight hours later, FPN expression was induced by doxycycline. Three hours later doxycycline was removed by extensive washes to stop FPN induction and fresh culture medium was added to the cells. They were then incubated in the presence or absence of hepcidin for additional 18 hours. Cells were finally lysed and plates were frozen. Rluc activity was measured the day after by adding *Renilla* luciferase assay substrate and quantified by luminometer.

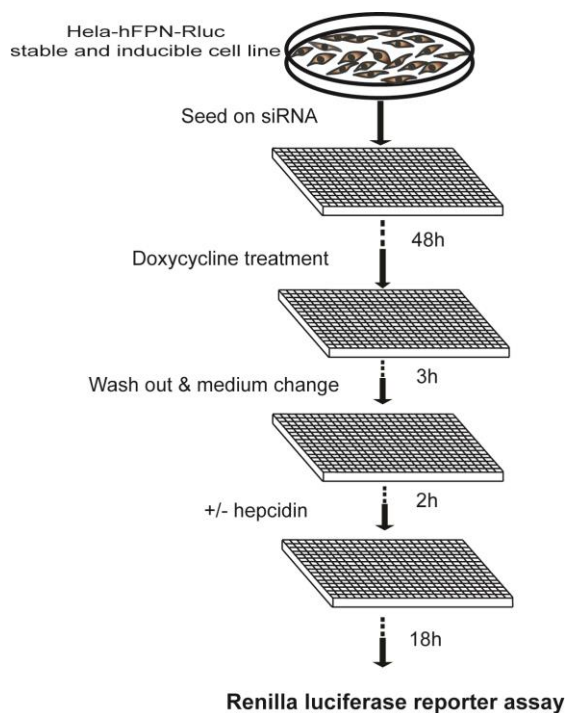


Figure 3.6 Screening strategy.

The screening was performed in duplicate, each replicate with and without hepcidin treatment. Computational data analysis using the Bioconductor package cellHTS2 assessed the quality of the assay (142) (Figure 3.7). On the level of individual plates the scatterplot between replicates (Figure 3.7A) assessed the reproducibility of the assay and the Spearman rank correlation (0.78) quantified the spread of the data. Data were normalized to the plate median. The Z-score represented a measure of the generated phenotype scored for its statistical significance: large positive z-scores were indicative of reduced FPN-Rluc activity, negative z-scores were indicative of increased FPN-Rluc levels. These values were calculated taking into account the mean and the standard deviation of the whole distribution according to this formula: $Z_{kj} = \pm (y_{kj} - M) / S$ where y_{kj} was the normalized value for the k^{th} well in the j^{th} replicate, M was the mean and S the

standard deviation of the y values. The final z-score was calculated as the mean z-scores between replicates. As expected, z-scores of negative control siRNAs (scrambles) distributed around 0 while FPN RNAi and viability controls resulted in high positive z-scores. The threshold value was computed as the mean of the distribution plus two times the standard deviation (Figure 3.7B). NEDD4 and AP2M1 siRNAs did not show significant effects on FPN regulation (Figure 3.7C) confirming the mild phenotype already observed in the pilot screening.

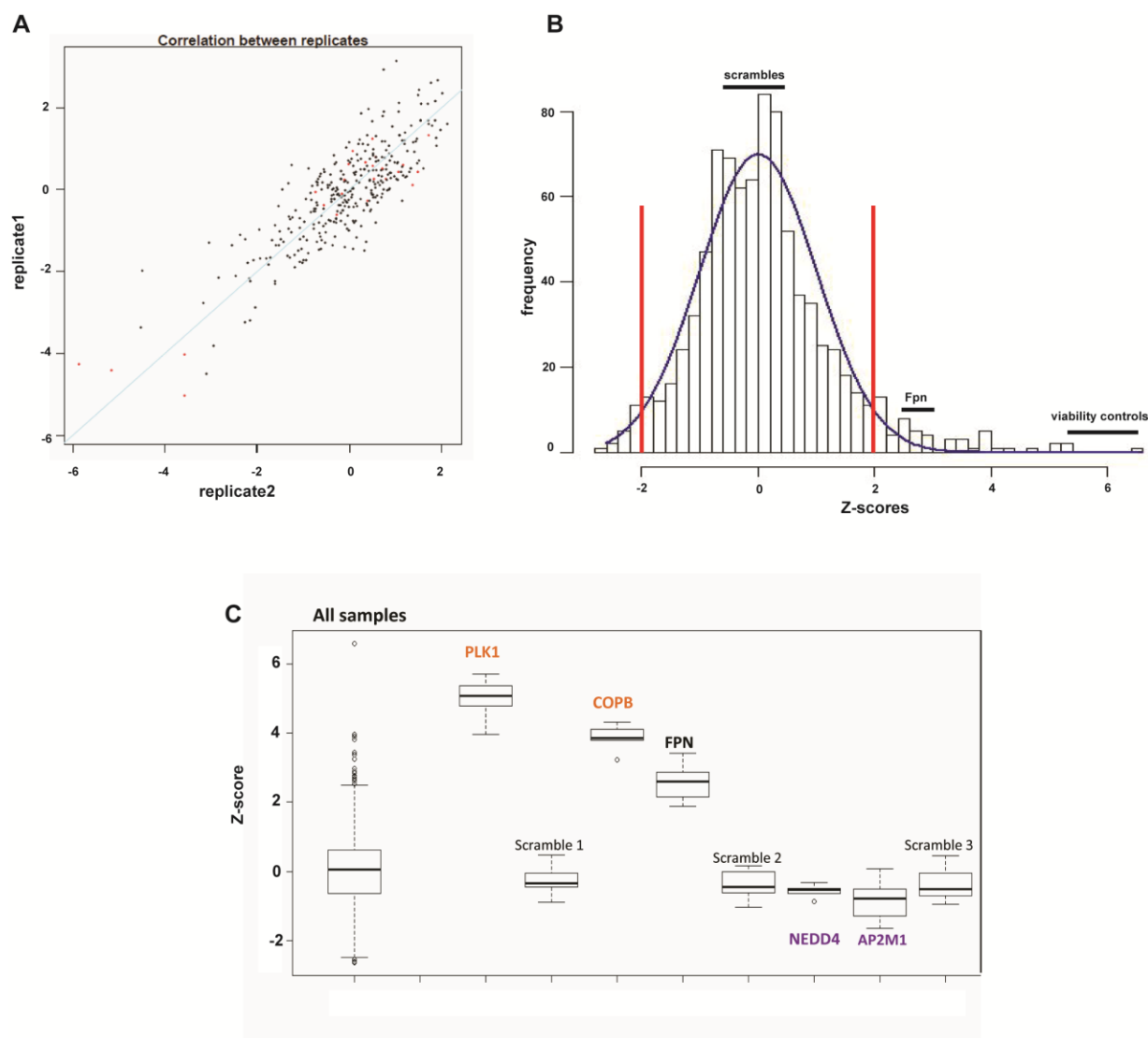


Figure 3.7 Evaluation of the screening quality. (A) Z-score correlation between the two replicates. Spearman rank correlation is 0.78. (B) Z-score distribution of the screening. The red bars represent the threshold values for potential FPN repressors (negative z-score) and potential FPN activators/stabilizers

(positive z-score). Scramble, FPN and viability controls are indicated. **(C)** Box plot distribution of the data. Scrambles, FPN, PLK1, COPB, NEDD4 and AP2M1 are indicated.

The analysis of the screening performed in the absence of hepcidin treatment allowed for the identification of putative FPN activators/stabilizers, whose depletion down regulated FPN-Rluc signal and putative FPN repressors, whose depletion increased FPN-Rluc activity (Figure 3.8). However some siRNAs, causing Rluc activity decrease, were expected to affect cell viability giving false positive read-out of FPN regulation. Previous cell viability screening performed in HeLa cells in Prof. Boutros lab had already identified some of them. These and other genes known to be key component of cell cycle (listed in red) were excluded from the hit list in the validation phase. Interestingly, JAK2 kinase reported to be a key component of FPN internalization mechanism (97) did not cross the threshold (z.score: -1.34), further questioning its role in this molecular process.

Candidate FPN activators/stabilizers

Candidate FPN repressors

gene	z-score
PANK4	3,89
FGFR3	3,81
PRKAG3	3,43
CDC2L2	3,38
AZU1	3,24
DCAMKL1	2,97
MAP4K3	2,89
DCK	2,76
PIK3R4	2,75
EVI1	2,68
NEK11	2,62
TGFBR2	2,55
MAP3K1	2,53
BCKDK	2,5
STK22B	2,5

gene	z-score
PDK4	-2,63
ITPKB	-2,55
TLK2	-2,48
TAF1L	-2,37
SPHK1	-2,36
TAF1	-2,34
FLJ34389	-2,29
PINK1	-2,19
LOC115704	-2,18
ACVR1	-2,18
CSK	-2,17
TLR6	-2,16
KIAA1361	-2,13
PHKA1	-2,1
SQSTM1	-2,08

ERN1	2,46	CDC2	-2,08
MAP2K7	2,34	RAGE	-2,04
CDK5R2	2,29	PTK6	-2,01
MVD	2,29	EPHB6	-1,99
CDC2L1	2,19	IMPK	-1,97
TEX14	2,18	MGC26597	-1,96
CHEK1	2,17		
CKMT1	2,17		
TGFBR1	2,09		
OSR1	2,07		
NRBP	2,06		
PMVK	2,06		
EXOSC10	2,03		
PIK3C2A	2,03		
WEE1	2,01		
CNKSR1	2		
TTBK1	1,82		
RPS6KB2	1,7		

Figure 3.8 Hit list of hepcidin-independent FPN regulators. Genes in red were not included in the validation process.

The hepcidin treatment applied to the cells in the screening aimed at identifying potential modulators of the hepcidin-mediated FPN internalization and degradation. For this purpose z-scores were separately calculated for each siRNA (as previously described) in absence and in presence of hepcidin and the correlation between them was analysed (Figure 3.9). The lack of correlation identified genes that altered the hepcidin-mediated FPN-Rluc reduction, increasing or reducing the ratio between Rluc activity measured in absence and in presence of hepcidin.

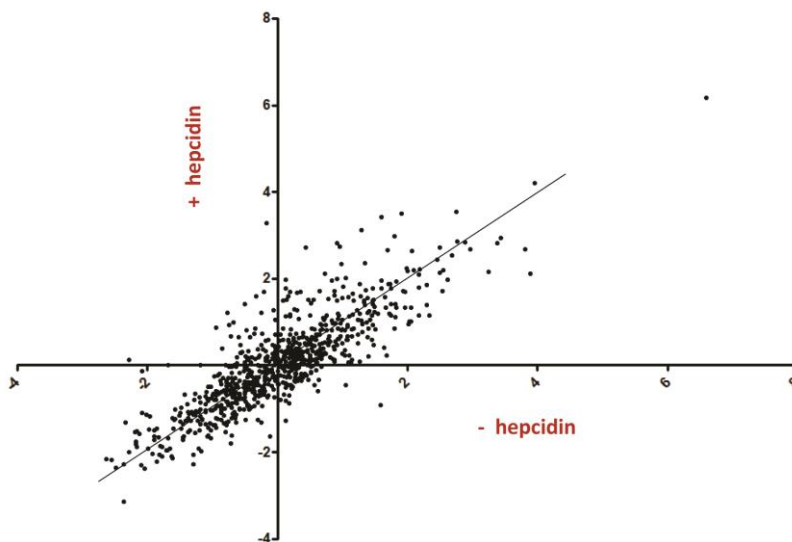


Figure 3.9 Z-score correlation between samples incubated in absence or presence of hepcidin. Z-scores were calculated for each siRNA and normalized to the median of each plate in absence and in presence of hepcidin treatment, separately. The correlation between all samples was plot.

Although for most genes FPN-Rluc regulation showed correlation, some genes were identified as possible hepcidin-dependent FPN regulators. The final z-score assigned to these candidates represented the difference between the z-scores calculated in presence and in absence of hepcidin treatment. Low z-scores were indicative of siRNAs increasing the hepcidin-dependent Fpn-Rluc reduction, high z-scores were indicative of siRNAs impairing this process. High negative z-scores were assigned to many candidates, while only few high positive z-scores were identified. To focus on a reasonable number of candidates for both categories for validation experiments, the threshold of the resulting distribution was set asymmetrically (3x fold the standard deviation for negative z-scores and 1.2x fold the standard deviation for positive z-scores) (Figure 3.10). Therefore, I chose 21 siRNAs which potentially functioned as fine modulators (“repressors”) of the FPN degradation process, which was exacerbated after their depletion. In addition I selected 8 candidates potentially required for the FPN internalization and degradation pathway (activators), as the RNA interference of their transcripts slowed down or prevented the FPN-Rluc decrease after hepcidin addition (Figure 3.11).

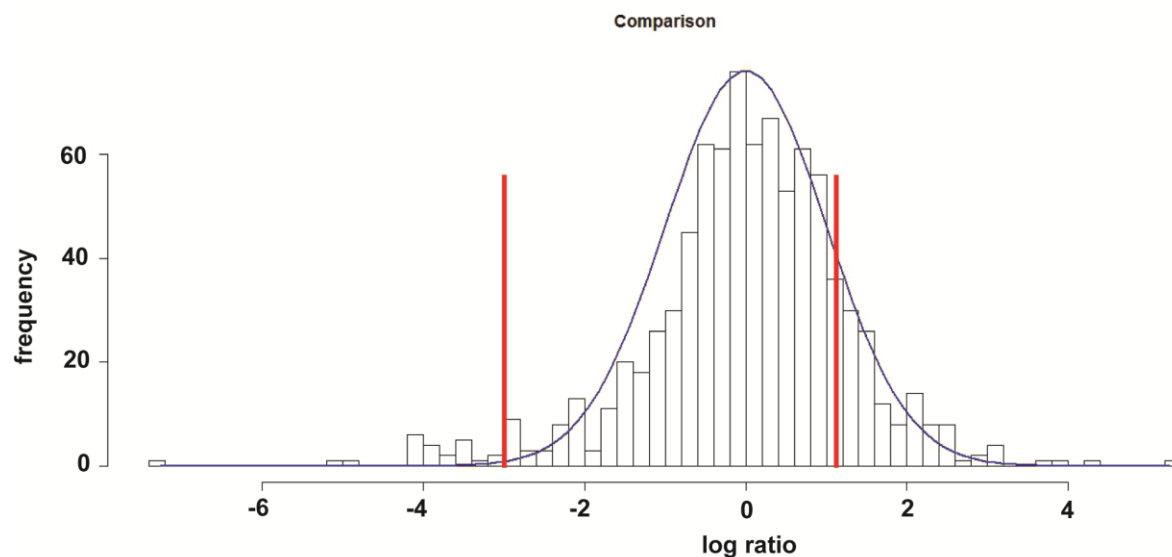


Figure 3.10 Distribution of z-score ratios between sample plus and minus hepcidin. The red bars represent the threshold values.

Candidate “repressors”

gene	diff score
EPHB3	-15,10
RBKS	-7,27
PINK1	-5,08
SYK	-4,83
PIM1	-4,17
RAGE	-4,09
EPHA8	-4,07
BMP2K	-4,03
ALDH18A1	-4,00
EPHB1	-3,98
PIP4K2A	-3,90
RAC1	-3,88
BLNK	-3,84
PIM2	-3,84

Candidate activators

gene	diff score
MYLK2	3,06
PRKCD	3,18
PANK4	3,73
STK6	5,25
ADAM9	1,20
PAPSS2	1,20
PRKCB1	1,21
ALS2CR2	1,40

EIF2AK1	-3,73		
PIP5K1A	-3,54		
HK3	-3,52		
CHKB	-3,48		
BMPR1B	-3,37		
EPHA4	-3,16		
RET	-3,10		

Figure 3.11 List of putative regulators of hepcidin-dependent FPN internalization and degradation.

3.4 Validation of the screening results

Within the 779 screened genes, the high throughput assay identified 21 FPN-Rluc putative activators, 21 putative repressors, 21 putative “repressors” of hepcidin-mediated FPN internalization and degradation and 8 potential activators. One of the limitations of the assay system was the impossibility to monitor cell morphology and viability throughout the screening process. This issue was of particular importance for the group of candidates which caused a reduction in the FPN-Rluc signal. To identify siRNAs inducing viability or hyperproliferation effects I applied a MTT colorimetric assay that measured the reduction of 3-(4,5-dimethylthiazol-2-yl)-2,5-diphenyl tetrazolium bromide (MTT) by mitochondrial succinate dehydrogenase. The reduction of MTT only occurs in metabolically active cells, thus the level of the enzyme activity represented a measure of the cell viability and activity. PLK1 siRNA was used as positive control for toxicity. NNM5, ACVR2A and AKAP4 were not identified as hits in the screening, resulting in z-scores analogous to scramble, however they were included in the initial phase of validation as additional negative controls. The MTT assay did not show hyperproliferation effects in consequence of any gene knockdown, nevertheless in several cases the metabolic activity of the cells was reduced (red bars) suggesting toxicity (Figure 3.12). These candidates were excluded from the following validation approaches.

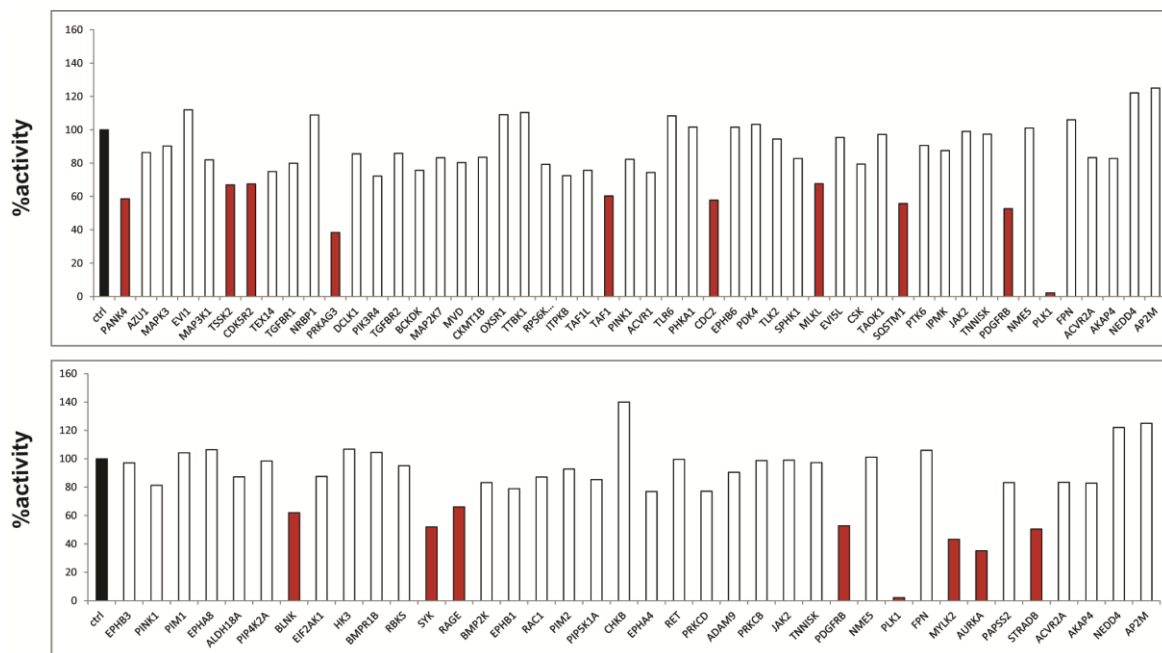


Figure 3.12 MTT assay identifies cytotoxic effects. The mitochondrial succinate dehydrogenase activity was measured after knocking down all the indicated genes. 70% of residual enzymatic activity identified toxicity and correlated with cytotoxic effects assessed through visual inspections of cells. Red bars indicate the siRNAs which induced cytotoxic effects. Data are means from 2 independent experiments \pm SD.

The screening was performed in duplicates by using a pool of 4 siRNA sequences per target gene. To validate the generated hit lists I first tested the corresponding RNAi in several additional independent experiments in the same experimental conditions as performed for the screening. For 14 potential activators/stabilizers and 5 potential repressors of FPN, I confirmed the FPN-Rluc decrease and increase, respectively (Figure 3.13 A, B). To further enhance confidence in these results, I transfected either the siRNA pool directed against the respective candidates or each single siRNA contained within the siRNA pool, separately (Figure 3.13 C, D). For most of the genes the Rluc regulation I observed with the pool was confirmed with more than one single siRNA sequence.

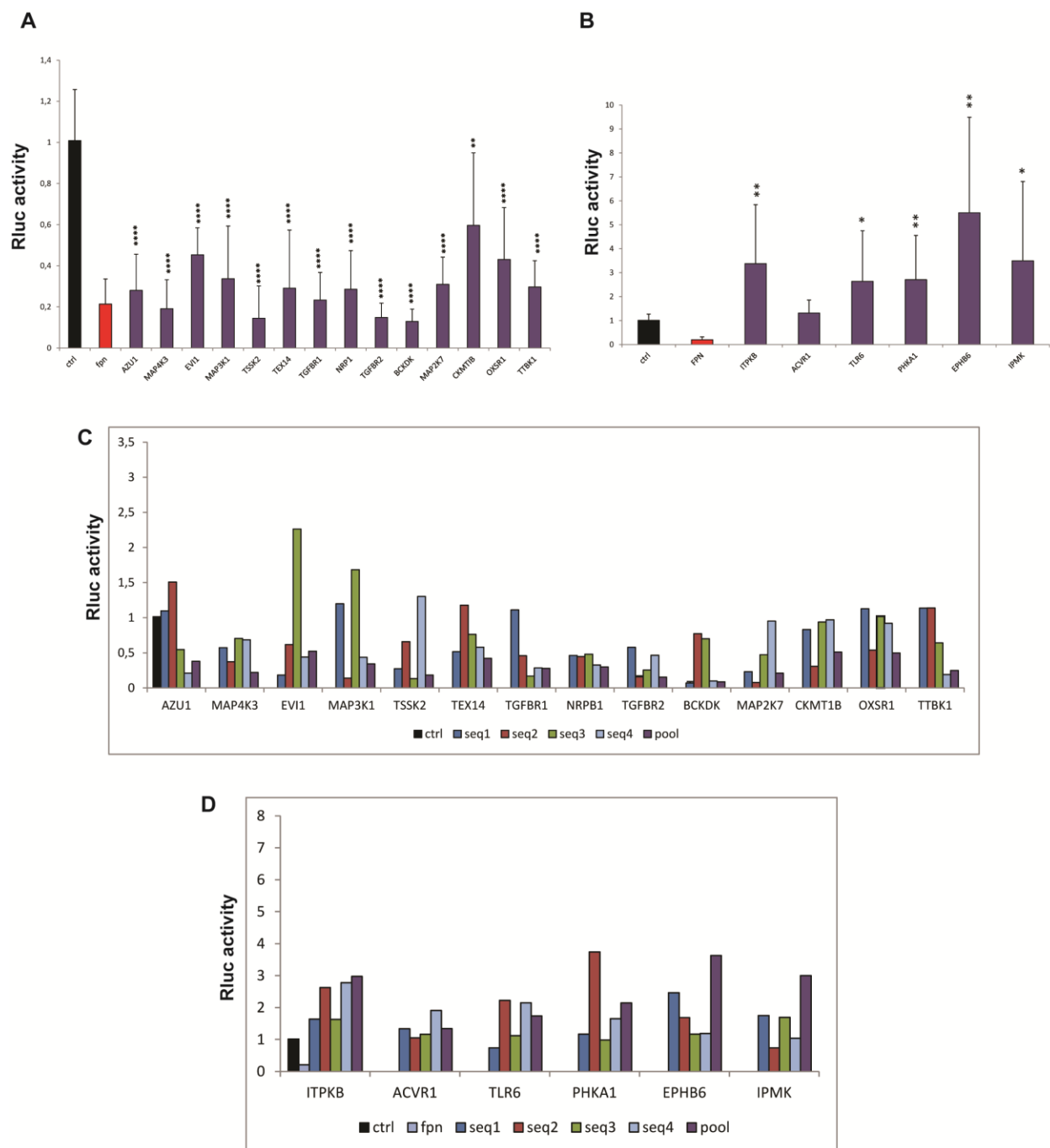


Figure 3.13 Validation of FPN putative regulators by applying pool of 4 siRNA sequences (A, B) or single siRNA sequences (C, D) per gene. Rluc activity was measured following the knock down of the indicated genes. All data are reported as means \pm SD from 5 independent experiments (A, B) and from 2 independent experiments (C, D) * $P < 0,05$, ** $P < 0,01$, *** $P < 0,001$, **** $P < 0,0001$, Student's t test.

High throughput RNA extraction methods did not provide sufficient amounts of RNA to evaluate the knockdown efficiency achieved by all siRNAs by measuring their mRNA level reduction. Because of this technical limitation I decided not to correlate the FPN phenotype with the knockdown efficiency of each siRNA sequence. I therefore chose to assess the specificity of the candidate gene knockdown by applying an alternative strategy.

The flippase recombination target site used, integrates the FPN-Rluc construct into a specific locus which can be also targeted by another gene as control (Figure 3.1). According to this principle, I generated a stable and inducible HeLa cell line which expressed only the Rluc reporter and I tested Rluc regulation in parallel to FPN-Rluc upon the RNA interference of the candidates by applying the same screening strategy in the two cell lines. The pool of 4 siRNA sequences was used for the RNAi of each candidate. siRNAs inducing significant Rluc regulation in the HeLa-Rluc cell line identified unspecific hits (Figure 3.14). According to this, 8 candidates out of 14 were confirmed and included in the final hit list of FPN activators.

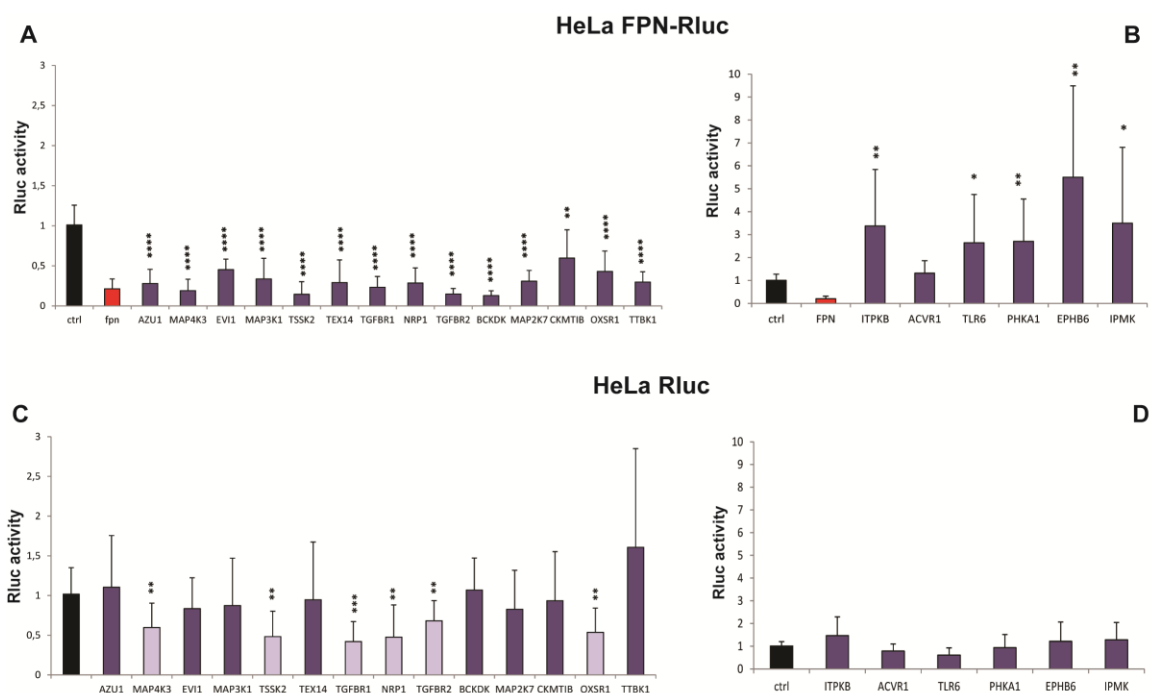


Figure 3.14 Validation of FPN putative regulators by comparing siRNA effects in HeLa-FPN-Rluc and HeLa-Rluc cell lines. Rluc activity was measured upon the candidate knockdown in HeLa cells expressing FPN fused with Rluc (**A, B**) and in HeLa cells expressing only Rluc (**C, D**). Putative FPN activators are indicated in (**A**) and (**C**). Putative FPN repressors are indicated in (**B**) and (**D**). Light violet bars represent unspecific regulators of FPN. Data are means \pm SD from 5 independent experiments, * $P < 0,05$, ** $P < 0,01$, *** $P < 0,001$, **** $P < 0,0001$, Student's *t* test.

The validation of the putative hepcidin-dependent FPN regulators was also performed. For these hits I measured Rluc activity of cells subjected to RNA interference and simultaneously treated with or without hepcidin. The ratio between the resulting values (without and with hepcidin treatment) was calculated and plotted. Because of a high variability of the assay five repetitions of the experiments were performed. From the 16 putative hepcidin-dependent FPN-Rluc regulators tested, 4 showed a consistent hepcidin-dependent phenotype (Figure 3.15 A). Noteworthy by analyzing the Rluc activity only in absence of hepcidin treatment I observed that for 10 candidates FPN-Rluc expression was significantly modulated irrespectively of hepcidin treatment indicating that the lack of these genes affected FPN-Rluc protein level rather than its hepcidin-mediated regulation (Figure 3.15 B). These candidates were then subjected to the same validation strategy applied to hepcidin-independent hits, by testing the effects of their corresponding siRNAs in HeLa cells expressing only the reporter protein. Seventy percent of them showed specific FPN regulation (Figure 3.15 C).

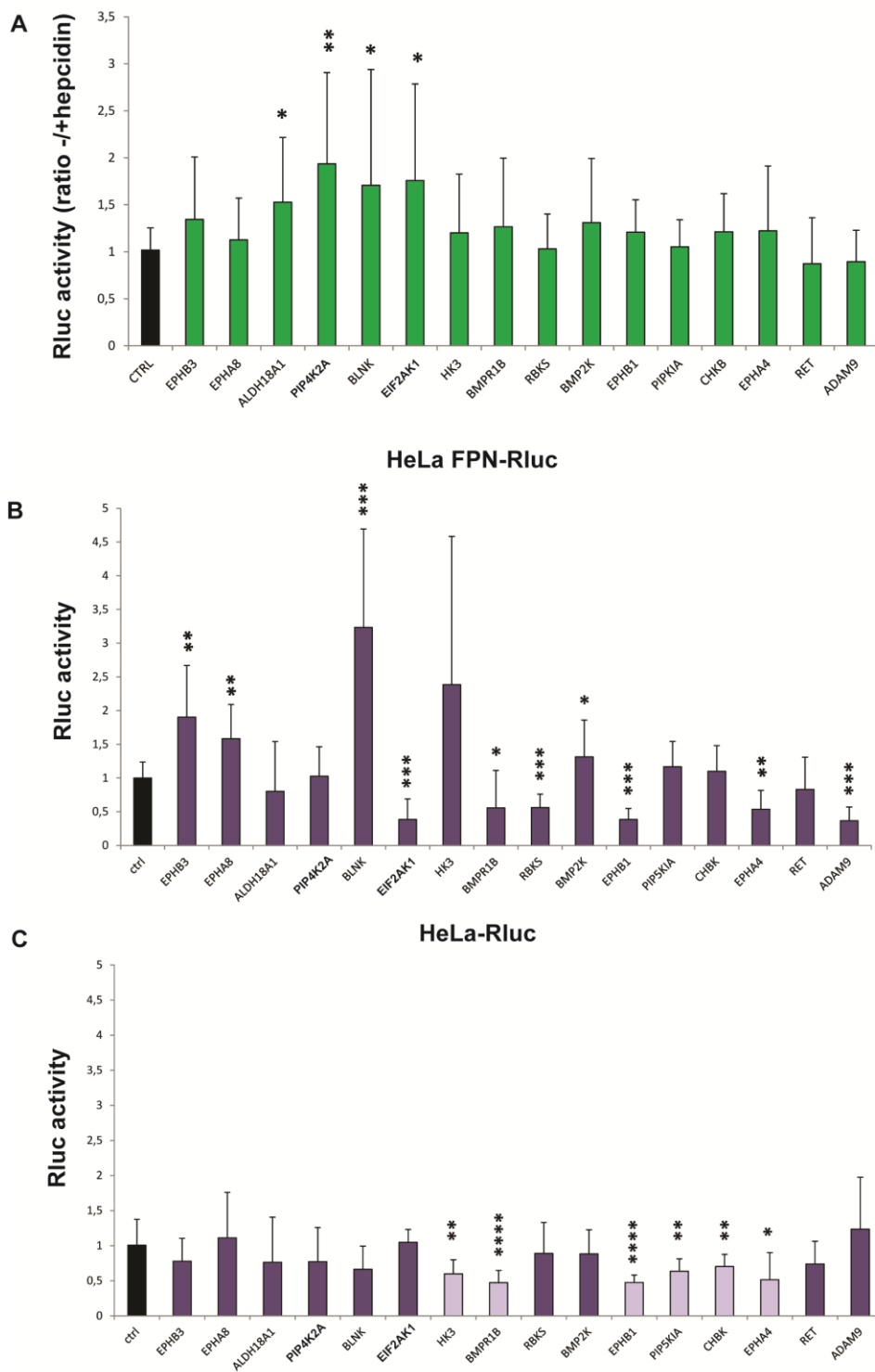


Figure 3.15 Validation of hepcidin-dependent FPN putative regulators. (A) For each experiment RNA interference of candidates was performed in duplicate. Samples were then incubated in presence or absence of hepcidin and subjected to the screening strategy described in Figure 3.5. Rluc was measured in both conditions and the ratio was calculated. (B, C) Rluc expression in absence of hepcidin treatment was measured in HeLa cells expressing FPN-Rluc (B) and in HeLa cells expressing only Rluc (C). Data

are means \pm SD from at least 3 independent experiments, * $P < 0,05$, ** $P < 0,01$, *** $P < 0,001$, **** $P < 0,0001$, Student's t test.

The validation strategy I applied yielded the following final lists of candidates:

FPN activators or stabilizers (siRNAs reducing FPN-Rluc signal) :
AZU1
EVI1
MAP3K1
TEX14
BCKDK
MAP2K7
CKMT1B
TTBK1
EIF2AK1
RBKS
ADAM9
FPN repressors (siRNAs increasing FPN-Rluc signal) :
ITPKB
TLR6
PHKA1
EPHB6
IPMK
EPHB3
EPHA8
BLNK
BMP2K
Regulators of the hepcidin-mediated FPN internalization/degradation (siRNAs accelerating hepcidin-induced FPN-Rluc reduction) :
ALDH18A1
PIP4K2A
BLNK
EIF2AK1

By inquiring the biological database and web resource STRING (*Search Tool for the Retrieval of Interacting Genes/Proteins*) I determined functional links between some candidates. For instance, association in curated database linked MAP2K7 to MAP3K1 and IPMK to ITPKB (Figure 3.16). Enrichment analysis of biological processes was limited by the use of the sole kinase library as reference dataset. However arbitrary extension with predicted functional partners derived from high-throughput experimental data, from the mining of databases and literature, and from associations based on genomic context (143), allowed identifying of some shared pathways. In particular, TLR6, ITPKB, MAP3K1, AZU1, MAP2K7, BLNK, EVI1 and ADAM9 turned out all associated with immune system processes.

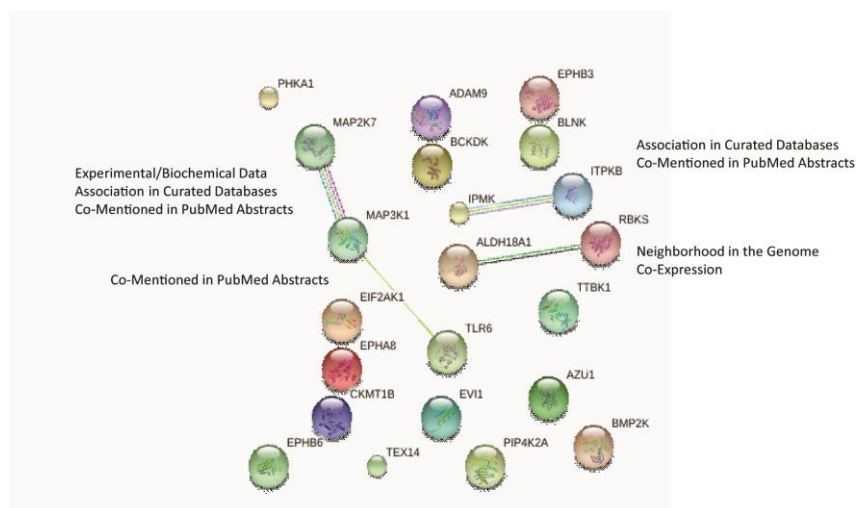


Figure 3.16 Identification of functional links between candidates by STRING analysis.

Engineered cell lines represented a powerful tool to study FPN regulation in a high throughput setting but they yet remained an artificial system. The physiological role of the candidate regulators needed to be investigated in cell types which expressed FPN at endogenous levels and which are more relevant for iron metabolism. Human macrophage cell lines met these requirements, however the lack of a working antibody against human FPN protein considerably restrained experiment feasibility. As a well-established *ex vivo* system expressing high FPN protein levels, murine bone marrow derived macrophages (BMDMs) emerged as a valid alternative. Furthermore the key

role that macrophages play in immune response made this cell type ideal to learn about the protein candidates related to immunological functions.

The whole candidate selection strategy I applied is summarized in figure 3.17.

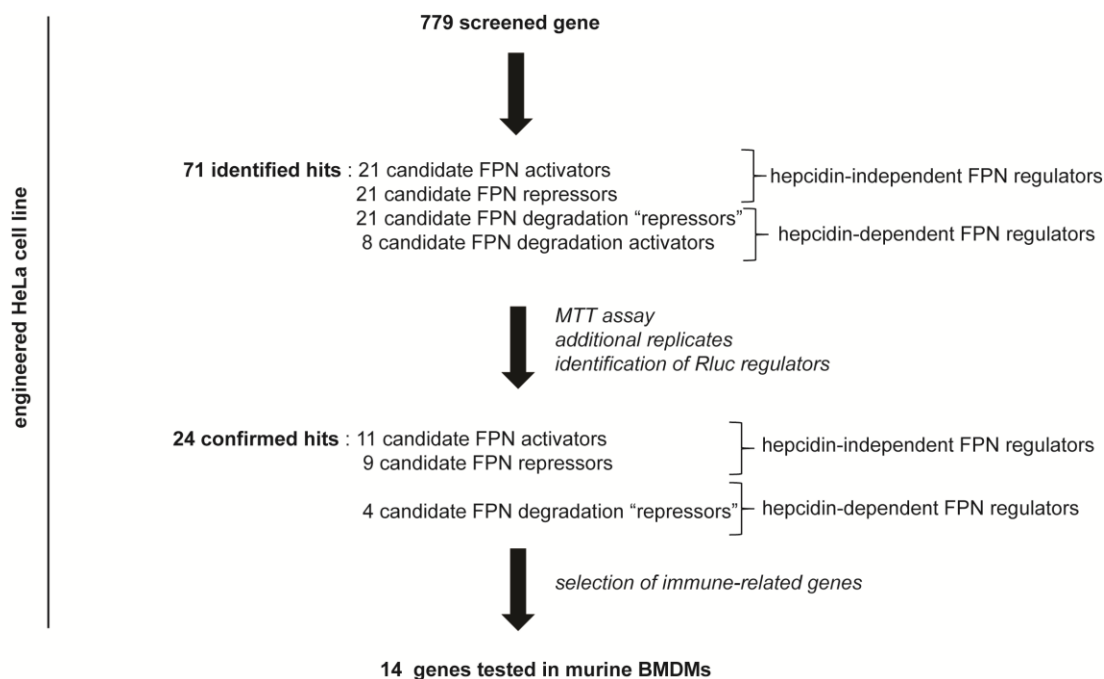


Figure 3.17 Selection process of FPN candidate regulators.

Most validated regulators of FPN expression conferred hepcidin-independent FPN protein regulation. For the validation in BMDMs I focused on 14 mouse homologs (MECOM, MAP3K1, BCKDK, MAP2K7, ADAM9, BLNK, ITPKB, PHKA1, BMP2K, TEX14, TLR6, PIP4K2A, IPMK, EPHB6), the majority associated with immune processes. I applied single siRNA sequence per gene and I then examined the FPN protein level by western blotting analysis. Unfortunately the quality of polyclonal antibodies against mouse FPN substantially dropped over this validation phase. Different batches showed variable quality, compromising the analysis between experiments, thus making quantitative analysis difficult. Nevertheless I could observe FPN protein increase following 6 transcript depletions (Figure 3.18 A) in iron-replete

BMDMs, despite a quite variable, and sometimes low, knockdown efficiency (Figure 3.18 B). The stimulation of the cells with ferric ammonium citrate (FAC) aimed at increasing the FPN expression and the antibody detection level and at overcoming the hepcidin induction observed upon some transcript interferences (Figure 3.18 C). Unlike HeLa cells, BMDMs were reported to express hepcidin, especially after inflammatory stimulation (61). Hepcidin mediates FPN protein degradation, thus the detected rise in hepcidin level could override the gene specific RNAi effects on FPN protein stability, invalidating any resulting observation. However in cells treated with iron I did not observe modified hepcidin expression profiles and I could validate the siRNA-mediated FPN protein alterations.

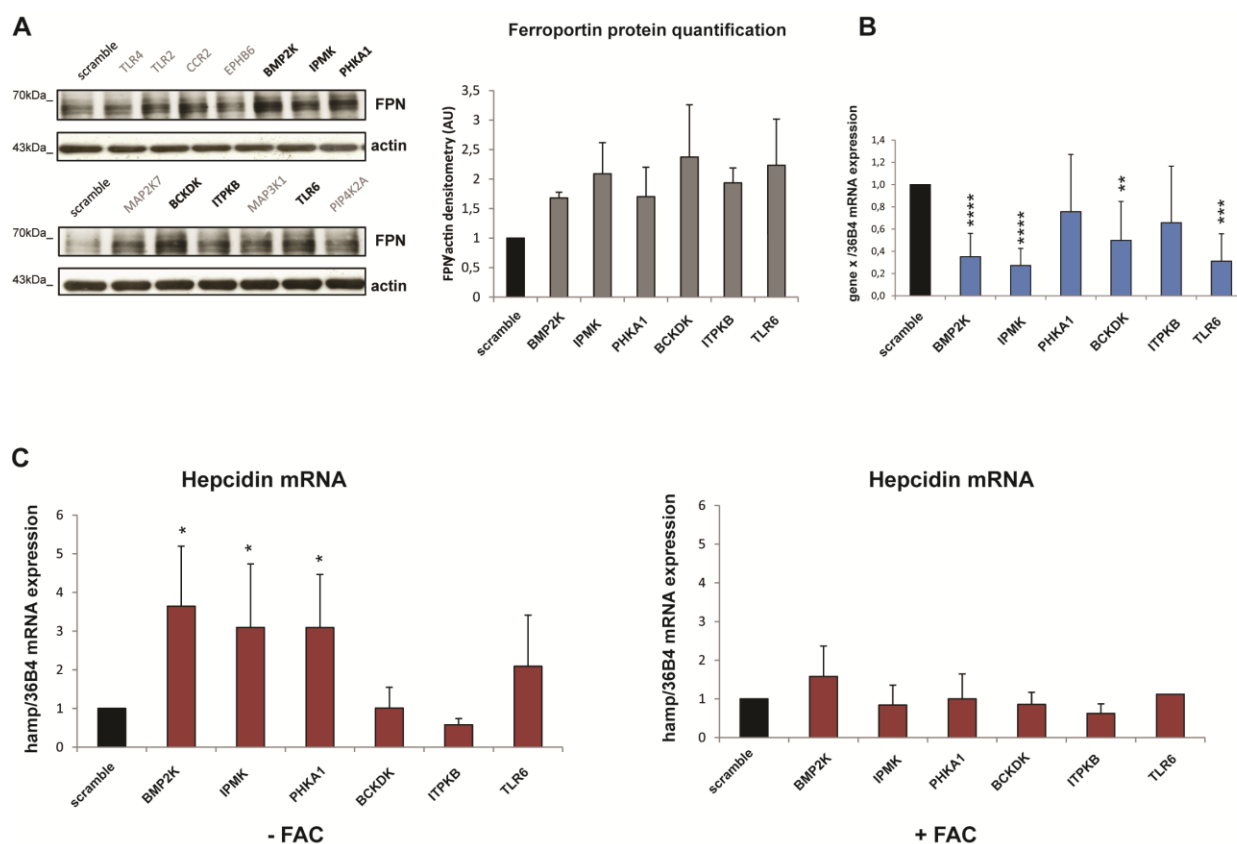


Figure 3.18 Validation of putative FPN regulators in BMDMs. (A) Representative western blot analysis and quantification of FPN protein level upon knocking down the indicated transcripts. β -actin was used as loading control. (B) The knock down efficiency of the indicated siRNAs was measured by RT-qPCR by analyzing the reduction of the relative target transcript calibrated to 36B4 mRNA level. Results are presented as a fold change \pm SD compared to samples transfected with scrambled siRNA from at least 3

independent experiments. **(C)** Hepcidin mRNA relative expression was measured in BMDMs depleted of the indicated transcripts and incubated in presence and absence of ferric ammonium citrate (FAC).

3.5 The RNAi screen identifies TLR6 as a novel regulator of ferroportin expression

For in depth functional analyses I decided to focus on a single candidate. In my view, the most interesting identified FPN regulator was Toll like receptor 6 (TLR6), whose knockdown led to increased FPN levels. Toll like receptors are key components of the innate immune system thanks to their ability to recognize a variety of pathogen-associated molecular pattern (PAMPs) such as bacterial cell-component like LPS, lipopeptides and double strands RNA of viruses. They are mainly expressed on antigen-presenting cells, such as macrophages or dendritic cells where their signalling activates innate immunity. Thirteen TLRs (named simply TLR1 to TLR13) have been identified in humans and they are believed to function as dimers, most as homodimers. The increased FPN protein stability in the absence of TLR6 was further proven in bone marrow derived macrophages (BMDMs) obtained from TLR6-deficient mice (Figure 3.19 A) clearly showing higher FPN levels. This effect occurred despite unchanged FPN and hepcidin mRNA levels (Figure 3.19 B, C), conclusively demonstrating that the lack of TLR6 affected FPN protein stability in a hepcidin-independent manner.

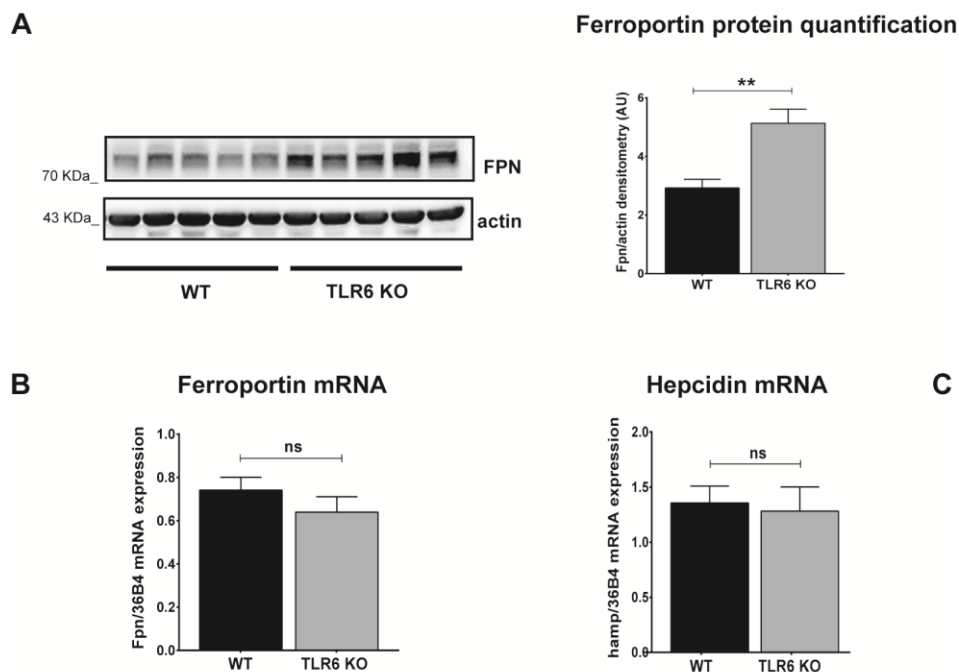


Figure 3.19 Identification of TLR6 as novel regulator of ferroportin protein expression. (A) Western-blot analysis of endogenous FPN expression in BMDMs from wild type (WT) and TLR6-deficient mice (TLR6 KO); β -actin was used as loading control. (B, C) FPN and hepcidin mRNA levels were determined by qRT-PCR and calibrated to 36B4 mRNA levels. Data are means \pm SEM, BMDMs were derived from 5 mice per group, $**P < 0,01$, Student's *t* test.

3.6 TLR2/6 stimulation reduces ferroportin expression in BMDMs

The connection between iron and innate immunity is supported by several lines of evidence. Iron plays a central role in host-pathogen interaction (144). As most pathogens require iron for proliferation and full virulence, the innate immune system fights infections by sequestering iron in macrophages of the reticuloendothelial system. The resulting hypoferremia represents a major host defense strategy (145). As member of Toll-like receptor family, TLR6 is an inflammatory sensor which recognizes specific ligands via heterodimerization with TLR2 on the cell surface (146). I next wondered how its stimulation modulated FPN and iron regulation.

I therefore took advantage of a synthetic lipoprotein ligand derived from *Mycoplasma salivarium* : FSL1 which was known to be recognized by TLR2/6 (147, 148) and to activate inflammatory response (147, 149). By treating BMDMs with different FSL1

concentrations, I observed a robust decrease in FPN mRNA levels at three different time points. This response was mediated by TLR6 because it was prevented (at short time point) or significantly blunted in TLR6-deficient BMDMs (Figure 3.20 A) as additionally confirmed by FPN protein analysis (Figure 3.20 B).

The incomplete resistance to FSL1 in absence of TLR6 suggested the importance of TLR2 signaling for FPN expression and also indicated the existence of an additional route for this inflammatory signaling to control FPN levels. To test this hypothesis I analyzed FSL1-mediated FPN regulation in the absence of TLR2, the functional partner of TLR6. Its depletion completely abolished the FPN response (Figure 3.20 C) at all time points and even at high dose of FSL1, pointing at a central role of TLR2. In addition to TLR6, TLR2 was known to heterodimerizes also with TLR1, however I verified that TLR1-deficient BMDMs retained the responsiveness to FSL1 (Figure 3.21). Thus, taking together these results revealed that the FSL1-mediated regulation of FPN could be mediated by TLR2/6 hetero- and TLR2 homodimers.

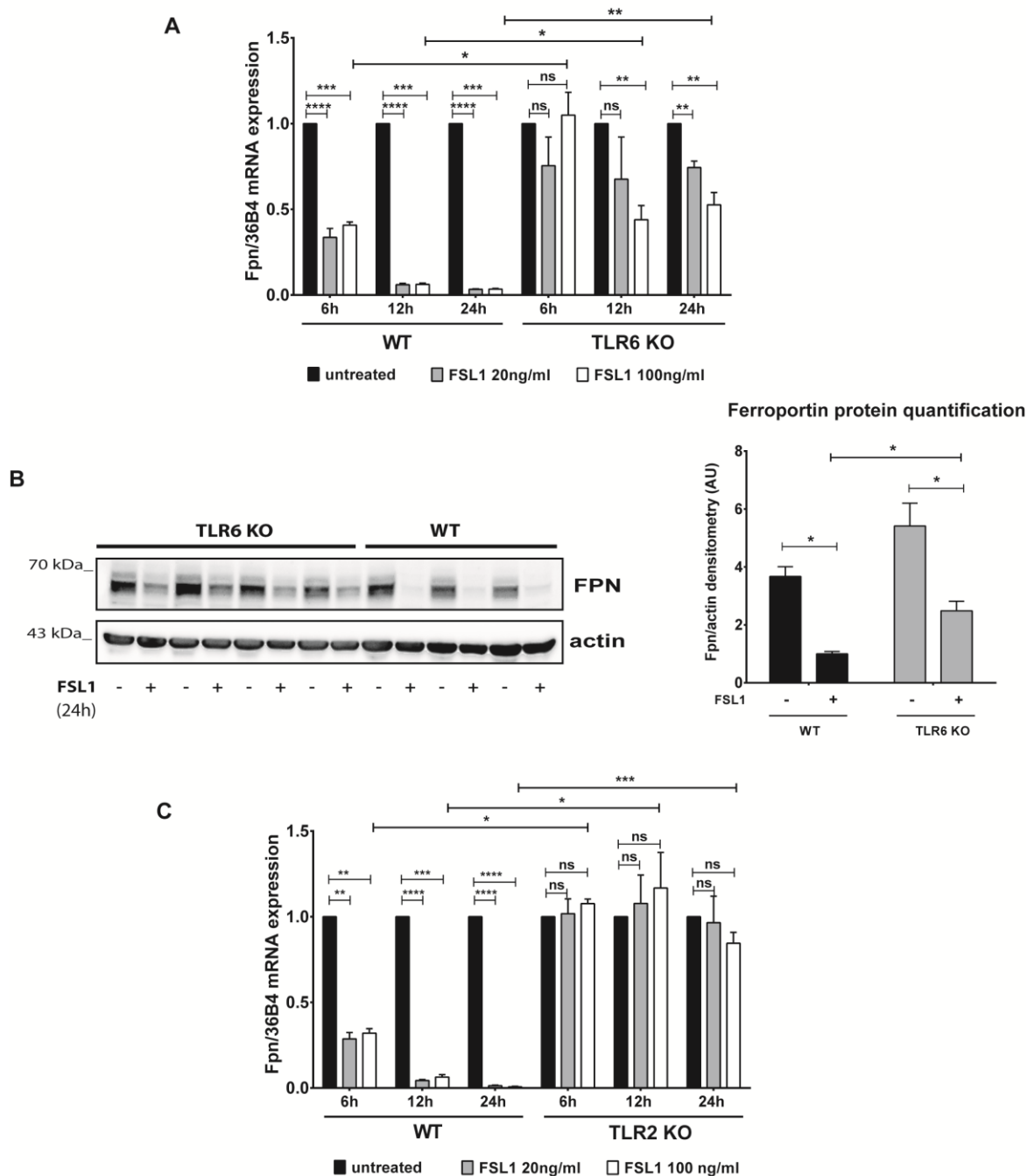


Figure 3.20 TLR2/6 stimulation by FSL1 reduces ferroportin expression in BMDMs. (A) qRT-PCR analysis of FPN in BMDMs from WT and TLR6-deficient mice stimulated with FSL1(20ng/ml and 100ng/ml) for the indicated time. Results are presented as a fold change \pm SEM compared to untreated cells. (B) Western-blot analysis and quantification of FPN expression in BMDMs from WT and TLR6-deficient mice treated with 100ng/ml FSL1 for 24h. β -actin detection ascertains equal sample loading. (C) qRT-PCR analysis of FPN in BMDMs from WT and TLR2-deficient mice treated with FSL1 (20ng/ml and 100ng/ml) for 6, 12 and 24h. All data are reported as means \pm SEM, BMDMs were derived from at least 4 mice per group, * $P < 0,05$, ** $P < 0,01$, *** $P < 0,001$, Student's t test.

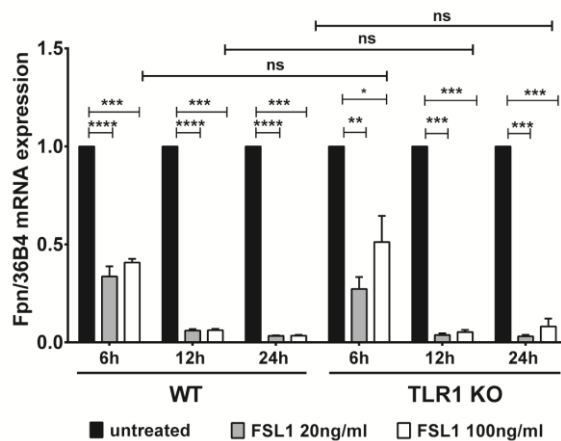


Figure 3.21 TLR1-deficient BMDMs retain responsiveness to FSL1. qRT-PCR analysis of FPN in BMDMs from WT and TLR1-deficient mice stimulated with FSL1(20ng/ml and 100ng/ml) for the indicated time. Results are presented as a fold change \pm SEM compared to untreated cells. All data are reported as means \pm SEM, BMDMs were derived from at least 3 mice per group, * $P < 0,05$, ** $P < 0,01$, *** $P < 0,001$, Student's t test.

3.7 TLR2/6 and TLR4 ligand-specific stimulations similarly reduce ferroportin expression but differentially regulate hepcidin expression

The suppression of FPN during inflammation was already reported in response to TLR4 stimulation by LPS treatment (57, 90) and associated with a robust hepcidin production in neutrophils and macrophages (61). I compared FSL1 (TLR2/6) and LPS (TLR4) stimulation on BMDMs and observed that while they both triggered the expected FPN mRNA reduction, only LPS induced hepcidin mRNA (Figure 3.22).

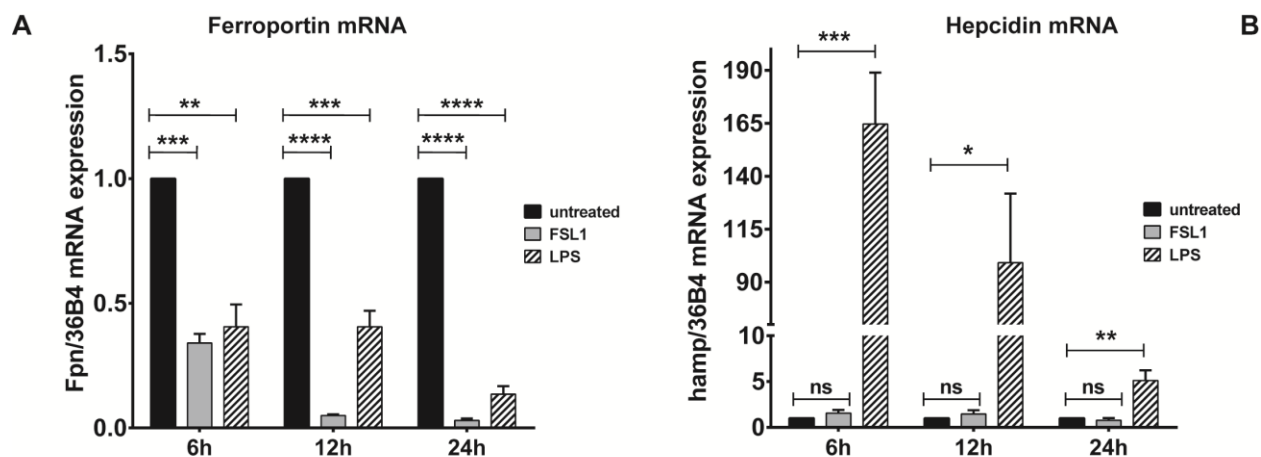


Figure 3.22 FSL1-mediated TLR2/6 ligation reduces FPN expression in BMDMs without activating hepcidin mRNA expression. Ferroportin (A) and hepcidin (B) mRNA expression in BMDMs after FSL1 and LPS (100ng/ml) stimulation. mRNA were normalized to 36B4 mRNA levels. All data are reported as means \pm SEM, BMDMs were derived from at least 4 mice per group, * $P < 0,05$, ** $P < 0,01$, *** $P < 0,001$, **** $P < 0,0001$ Student's *t* test.

To verify that both treatments induced an inflammatory response I then analyzed the IL1 β , IL6 and TNF α mRNAs which all displayed increased expression, albeit quantitatively more moderately in FSL1-treated BMDMs (Figure 3.23). This finding suggested that increased expression of these cytokines per se was not sufficient for hepcidin activation.

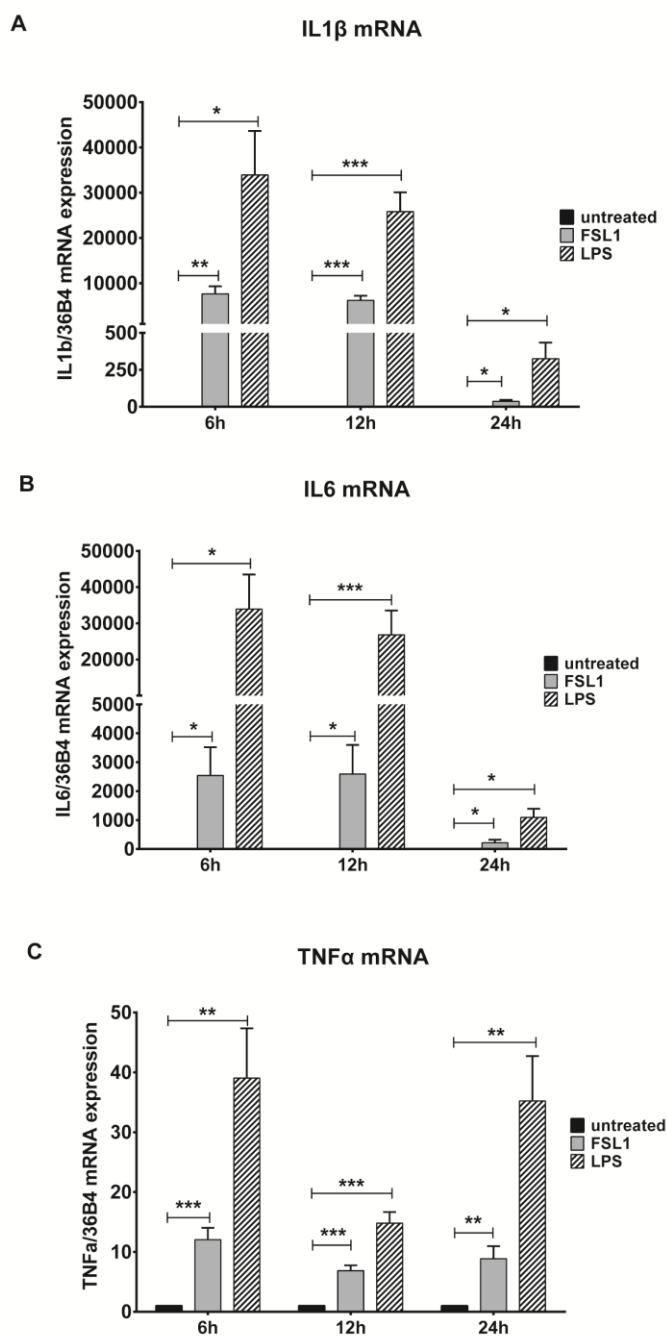


Figure 3.23 FSL1 and LPS stimulation induce cytokines response. (A) IL1 β , (B) IL6, (C) TNF α mRNA expression was assessed by qRT-PCR and calibrated to 36B4 mRNA levels in BMDMs derived from wild type mice and treated with FSL1 and LPS (100 ng/ml) for the indicated time. Data are means \pm SEM, BMDMs were derived from at least 4 mice per group, * $P < 0,05$, ** $P < 0,01$, *** $P < 0,001$, Student's t test.

I also extended the analysis to other bacterial lipopeptides, reported to activate TLR2-dependent signaling: PAM3CSK4 and PamOct2C-(VPG)4VPGKG (148, 150). Interestingly FPN mRNA levels showed quantitatively similar decrease following all ligand stimulations (Figure 3.24 A), while persistent and considerable hepcidin induction was mediated only by LPS (Figure 3.24 D), further confirming the importance and the conservation of the FPN transcriptional response in the inflammatory context irrespective of hepcidin. TLR6 and TLR2-deficient BMDMs recapitulated and reinforced this result (Figure 3.24 E, F) suggesting almost null contribution of TLR2 challenge to hepcidin production in macrophage. In addition, the lack of TLR6 resulted in partial but enduring resistance only to FSL1 to trigger FPN suppression, while TLR2-deficient macrophages resulted unresponsive to all ligands, but LPS (Figure 3.24 B, C) confirming the independence of LPS signaling on TLR2.

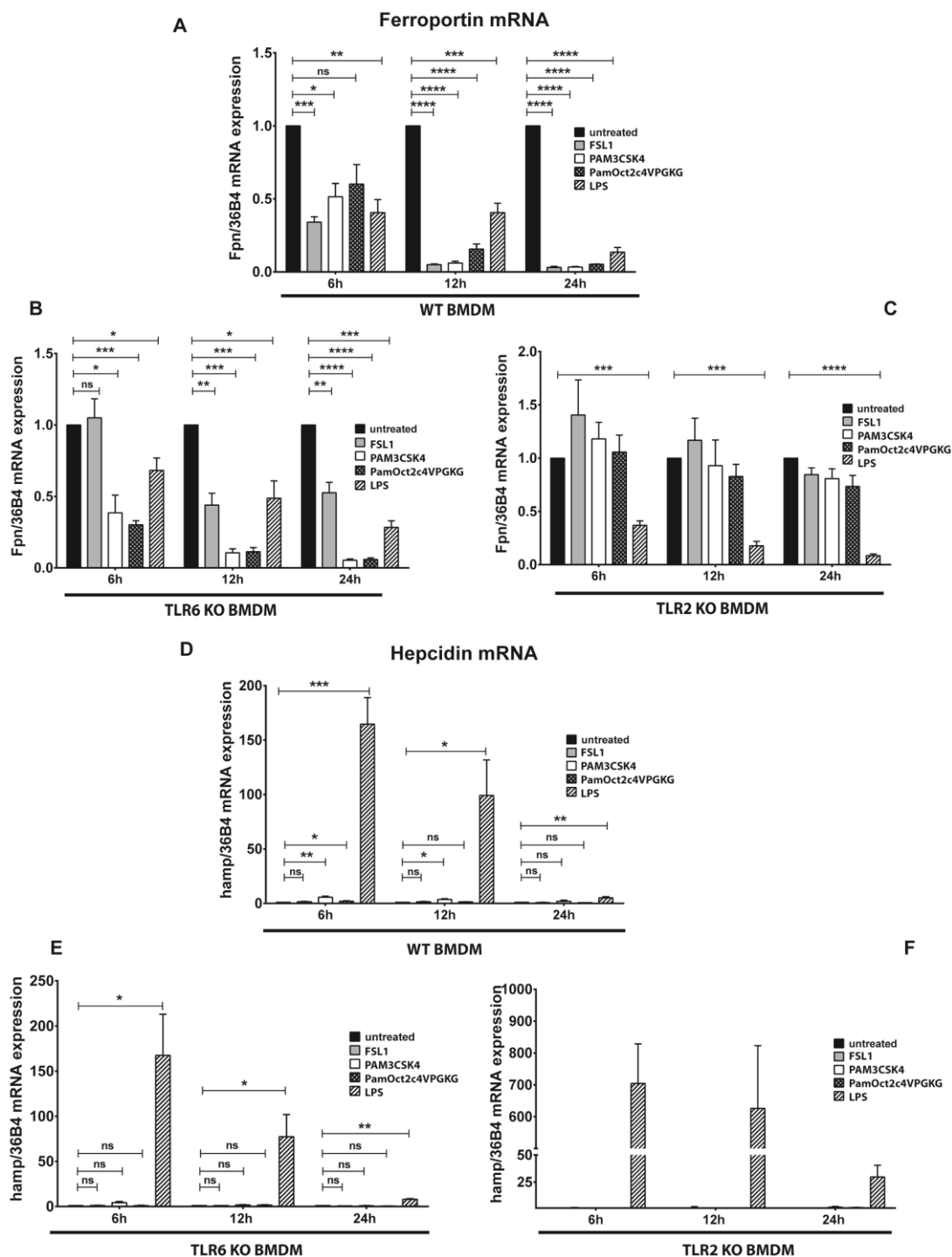


Figure 3.24 Ferroportin and hepcidin regulation by TLR2 and TLR4-specific ligands in BMDMs. (A, B, C) Ferroportin mRNA expression was determined by qRT-PCR in wild type (WT) (A) TLR2-deficient (B) and TLR6-deficient (C) BMDMs stimulated with 100ng/ml TLR2-specific ligands (FSL1, PAM3CSK4, PamOct2C-(VPG)4VPGKG) and TLR4-specific ligand (LPS) for the indicated time. (D, E, F) Hepcidin mRNA expression was analyzed in the same samples. The mRNA quantification was calibrated to 36B4 mRNA levels. All data are reported as means \pm SEM, BMDMs were derived from at least 4 mice per group, * $P < 0,05$, ** $P < 0,01$, *** $P < 0,001$, **** $P < 0,0001$, Student's t test.

3.8 FSL1 and LPS injection induce hypoferremia in mice

A common consensus in the field posits that hypoferremia during acute inflammation is caused by increased hepcidin expression. All the lines of evidence supporting so far the essential role to hepcidin in this process are mainly based on LPS injection in mice. Very different LPS concentration have been reported from 100 $\mu\text{g}/\text{mouse}$ (90) to 5 $\mu\text{g}/\text{mouse}$ (70) all showing at different time points the link between hepcidin induction and serum iron level reduction.

I decided to compare LPS and FSL1 *in vivo* response by injecting 11-weeks old mice with very low dose (25 ng/g bodyweight, corresponding to less than 1 μg per mouse) which I found sufficient to elicit hypoferremia already after 3 hours. Serum iron concentration and transferrin saturation were substantially lower compared to saline injection after both treatments (Figure 3.25 A, B).

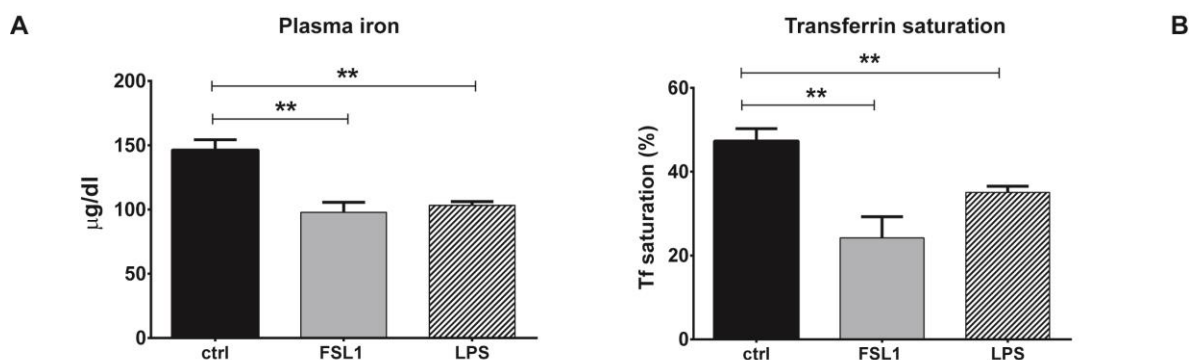


Figure 3.25 FSL1 and LPS injection induce hypoferremia in mice. Plasma iron levels and transferrin saturation were analyzed in wild type (WT) mice at 3h after saline (ctrl), FSL1, LPS injection. 25 ng of ligand per g bodyweight were used Data are means \pm SEM. Results are representative of three independent experiments. $**P < 0,01$, Student's *t* test. $n = 6$ mice per group.

3.9 Hepcidin induction is not required to set acute hypoferremia in mice

I next examined liver mRNA expression of FPN and hepcidin in response to FSL1 and LPS injections. Strikingly similar and robust FPN mRNA reduction was observed in both conditions while hepcidin up regulation resulted only in LPS injected mice (Figure 3.26

A, B). I also analyzed the expression of some inflammatory cytokines, such as TNF α and IL6, which were induced only in LPS treated samples. In particular IL6, the well-characterized inflammatory activator of hepcidin, was not significantly increased by FSL1 injection (Figure 3.26 C, D). Despite these differences, hepatic iron measurement revealed similar levels of iron retention (Figure 3.26 E) and FPN protein quantification displayed significant reduction in both conditions (Figure 3.26 F).

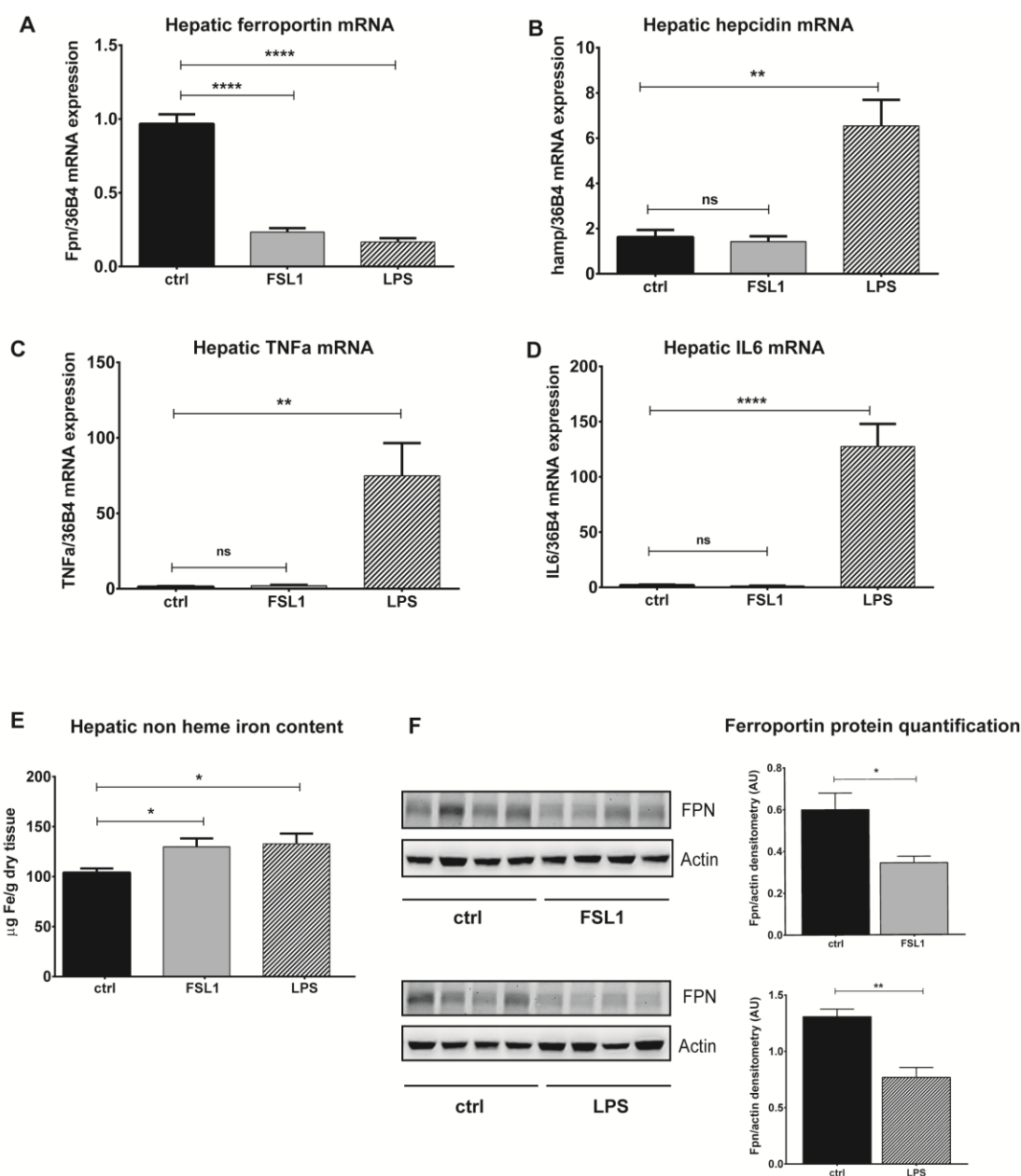


Figure 3.26 Hepatic hepcidin induction is not required to set acute hypoferremia in mice. (A, B, C, D) Hepatic FPN, hepcidin, TNF α and IL6 mRNA expression were determined by qRT-PCR and calibrated to 36B4 mRNA levels. **E** The hepatic non-heme iron content was quantified as indicated. **F** Western-blot analysis and quantification of FPN expression in the liver of the injected mice. β -actin was used as loading control. Data are means \pm SEM. Results are representative of three independent experiments. * $P < 0,05$, ** $P < 0,01$, *** $P < 0,001$, Student's t test. $n = 6$ mice per group.

Parallel analysis of the spleen showed FPN decrease at mRNA (Figure 3.27 A) and protein level even in this tissue (Figure 3.27 C, D). In particular, the FPN protein reduction resulted even more pronounced in magnitude in isolated splenic macrophages (Figure 3.27 E) which were expected to be recruited in the tissue during inflammation. Hepcidin induction in the spleen has been already reported (61, 151) in consequence of pathogen and LPS challenge. Consistently, I observed an increasing tendency in LPS injected mice, although hepcidin is generally low expressed in this tissue. As predicted from the experiments in BMDMs, splenic hepcidin mRNA expression was unchanged following FSL1 injection (Figure 3.27 B). Consistent with the findings in the liver, non heme iron content and Perl's Prussian staining demonstrated iron accumulation in the spleen with a similar pattern upon the two ligand injections (Figure 3.27 F).

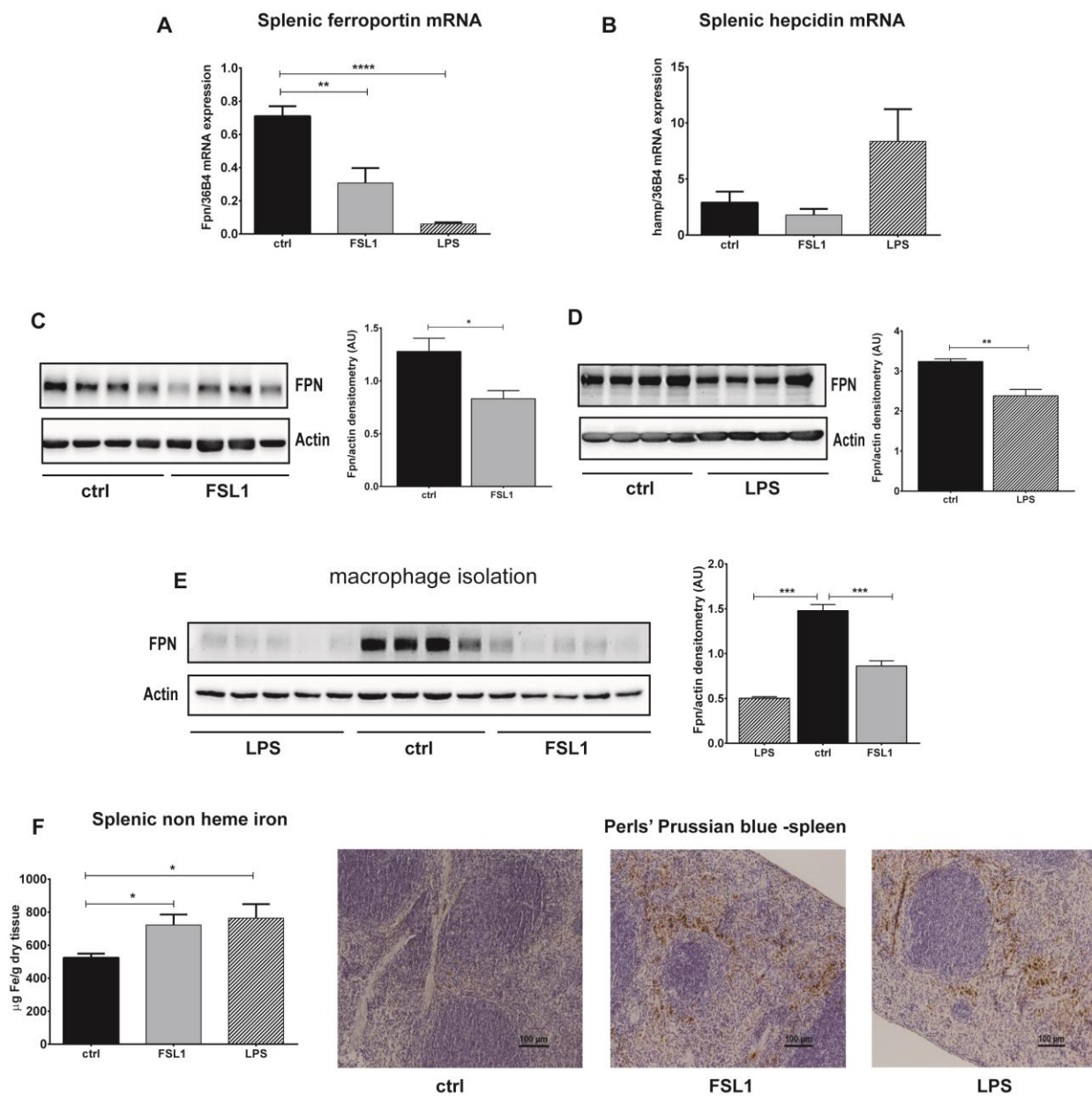


Figure 3.27 Splenic ferroportin down regulation in the hypoferremic response does not require hepcidin contribution. (A, B) FPN and hepcidin, expression was assessed by qRT-PCR in WT mice at 3h after saline (ctrl), FSL1, LPS injection. (C, D) Western-blot analysis and quantification of FPN expression in the whole spleen and E in the splenic macrophages isolated from the injected mice. β -actin was used as loading control. (F) The splenic non-heme iron content was determined in the same groups of mice. DAB-enhanced Perls' iron staining shows iron retention in the spleen of FSL1 and LPS injected mice as compared to ctrl. Data are means \pm SEM. * $P < 0,05$, ** $P < 0,01$, *** $P < 0,001$, Student's *t* test. $n = 6$ mice per group.

Inflammatory cytokines were induced by both treatments, even though to a different extent. In particular TNF α and IL6 mRNA expression levels are here showed (Figure 3.28 A, B). On the other hand I could not observe any significant changes in hepatic or splenic Tfr1 mRNA levels (Figure 3.28 C, D) whose decrease in response to IRPs inactivation when iron levels are high (93) is likely to require more time.

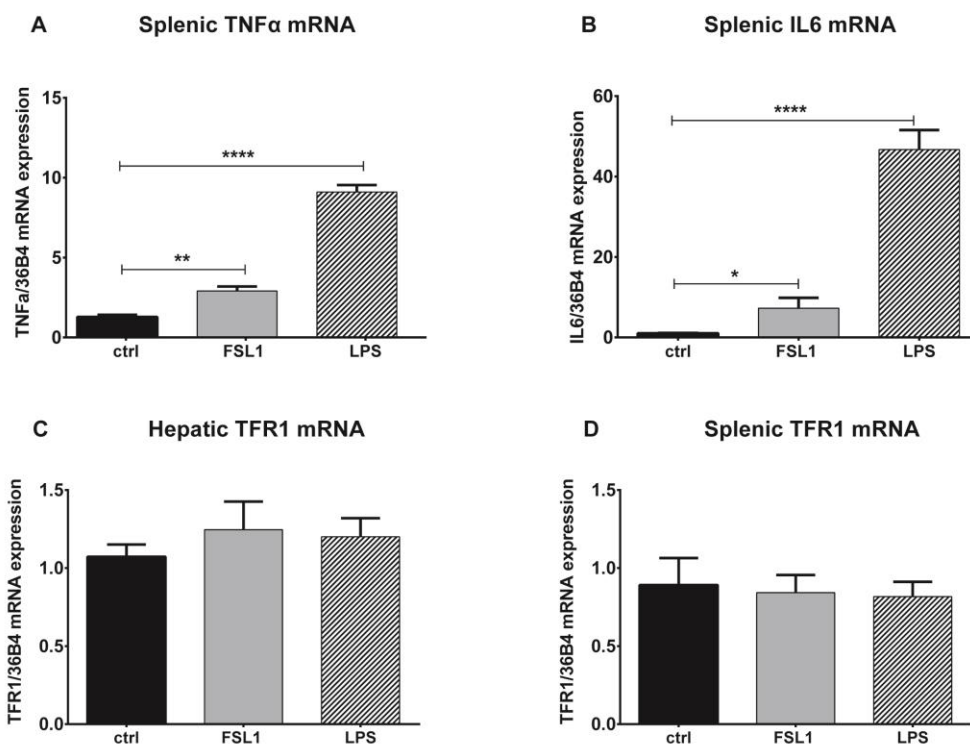


Figure 3.28 TNF α , IL6, TFR1 mRNA expression in the spleen of mice injected with FSL1 and LPS. Splenic mRNA level of TNF α and IL6 (A, B) and hepatic and splenic TFR1 mRNA levels (C, D) were measured by qRT-PCR and calibrated to 36B4 mRNA levels in wild type mice after 3hs injection with saline (ctrl), FSL1, LPS. Data are means \pm SEM. * $P < 0,05$, ** $P < 0,01$, *** $P < 0,0001$, Student's t test. $n = 6$ mice per group.

The crucial role of hepcidin in setting hypoferremia during acute inflammation has been recently questioned by LPS injection in hepcidin knockout mice. Regardless the lack of hepcidin these mice were shown to have reduced serum iron level upon the treatment, suggesting the possibility that hypoferremia during acute inflammation involves

hepcidin-independent routes. The LPS-induced hypoferremia was attributed to diminished dietary iron absorption due to decreased duodenal FPN and DMT1 mRNA expression (152). Following this lead I examined the duodenal expression of these iron transporters but I found that the duodenal mRNA expression of FPN and DMT1 was unchanged in FSL1-injected mice and I observed a trend towards decreased FPN and DMT1 mRNA levels upon LPS injection (Figure 3.29 A, B). Furthermore Perl's Prussian blue staining showed no altered iron distribution, confirming that iron acquisition was not impaired in the two inflammatory conditions (Figure 3.29 C)

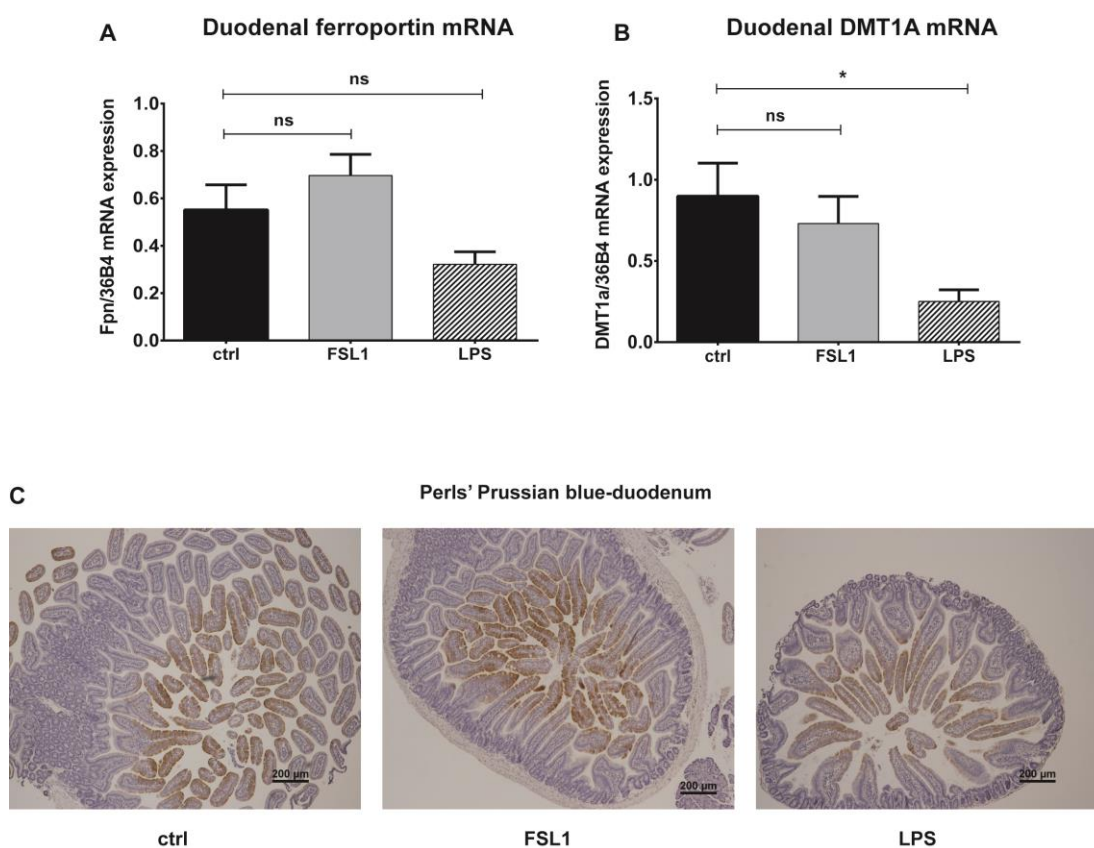


Figure 3.29 Iron absorption is not altered upon FSL1 and LPS injection. (A, B) Ferroportin and divalent metal transporter 1 (DMT1) mRNA expression were assessed in the duodenum of wild type mice at 3h after saline (ctrl), FSL1, LPS injection. Data are means \pm SEM. * $P < 0.05$, Student's *t* test, $n = 6$. (C) DAB-enhanced Perls' iron staining reveals no impaired iron distribution in the duodenum of inflamed mice compared to wild type.

Recent lines of evidence have also pointed out a novel role of HFE in the inflammation-induced hypoferrremia. In particular LPS injection was shown to lead to a rapid HFE protein reduction in the spleen which, according to the authors, explained iron retention and consequently, plasma iron decrease (153). I therefore analyzed HFE mRNA levels in the spleen and in the liver of mice injected with FSL1 and LPS and I observed that they decreased in the spleen upon both treatments (Figure 3.30 B) while they appeared to be differentially regulated in the liver (Figure 3.30 A), showing opposite trend in consequence of LPS injection. However I could not apply protein analysis in these tissues, as the antibody anti-HFE used in the mentioned report did not show a proper protein recognition and no other functional antibodies were commercially available at the moment.

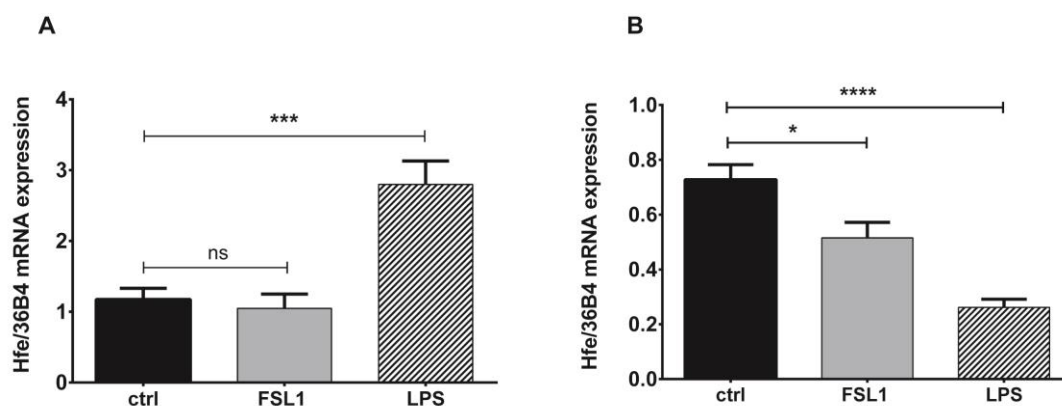


Figure 3.30 HFE mRNA regulation in liver and spleen of mice injected with FSL1 and LPS. HFE mRNA level were analyzed by RT-qPCR in the liver (A) and in the spleen (B) of wild type mice injected with FSL1 and LPS (25 ng/g) for 3h. The data are normalized on 36B4 mRNA levels and are represented as means \pm SEM. * $P < 0,05$, *** $P < 0,001$, **** $P < 0,0001$ Student's *t* test, $n=6$.

To confirm directly that FSL1-induced hypoferrremia and FPN regulation are independent of hepcidin-FPN interaction *in vivo*, I ultimately took advantage of a recently published mouse model available in the lab containing a C326S mutation in endogenous ferroportin which causes full resistance to hepcidin binding and response *in vivo* (190). Preliminary experiments showed that BMDMs derived from these mice responded to FSL1 and LPS as BMDMs derived from wild type mice, down regulating FPN mRNA and protein levels (Figure 3.31 A, E) and inducing cytokine expression, such as TNF α and IL6 (Figure 3.31 C,D). As for wild type BMDMs, hepcidin resulted

strongly up regulated only upon LPS stimulation (Figure 3.31 B). *In vivo* experiments further corroborated these findings and demonstrated that despite high iron levels that accumulate in these mice, FSL1 efficiently reduced serum iron levels 3 hours after injection (Figure 3.32 A). Most importantly FPN mRNA and protein levels were significantly reduced in the liver and in the spleen (Figure 3.32 B, C) in the absence of a significant hepcidin contribution.

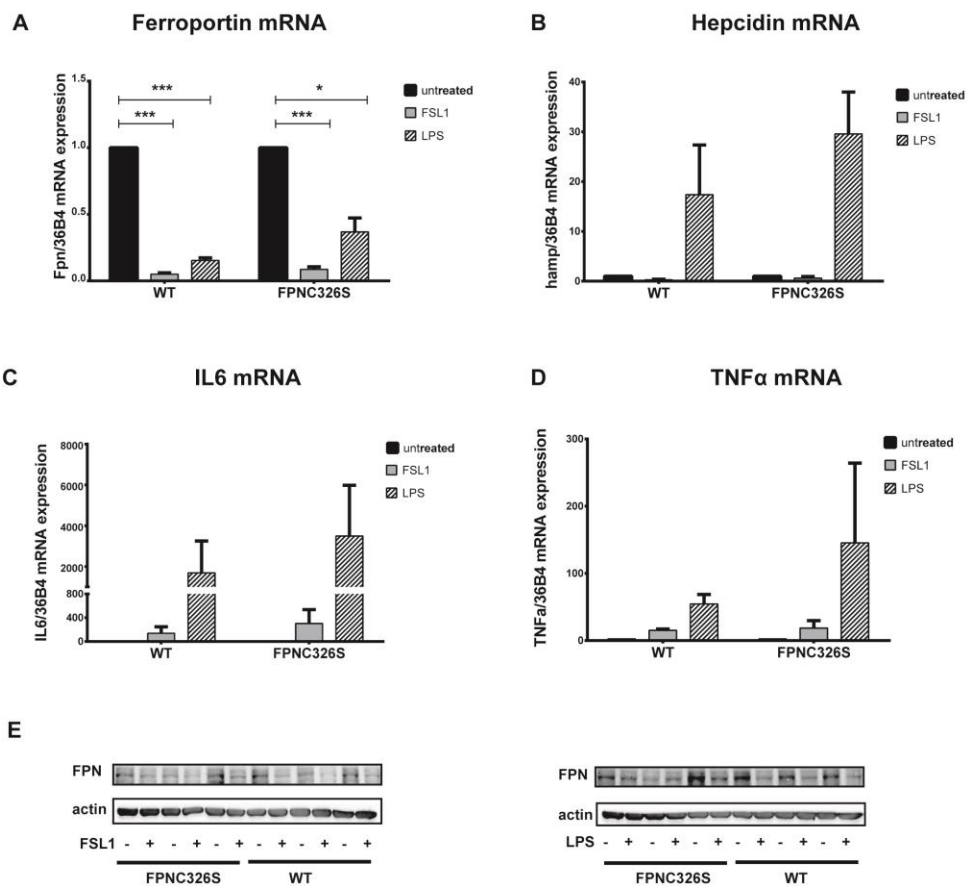


Figure 3.31 BMDMs derived from FPN^{C326S} knock-in mice down regulate FPN in response to FSL1 and LPS. (A, B, C, D) Bone marrow derived macrophages were derived from wild type mice (WT) and from FPN^{C326S} knock-in mice (FPNC326S) and stimulated with FSL1 and LPS (100ng/ml) for 24 hours. Ferroportin (A), hepcidin (B), TNFα (C) and IL6 (D) mRNA levels were analyzed by RT-qPCR and normalized to 36B4 mRNA levels. (E) FPN protein levels were analyzed by Western-blot in BMDMs untreated or treated with FSL1 and LPS as indicated. β-actin was used as loading control. BMDMs were derived from 3 mice per group. Data are means ± SEM. * $P < 0,05$, ** $P < 0,001$, Student's t test.

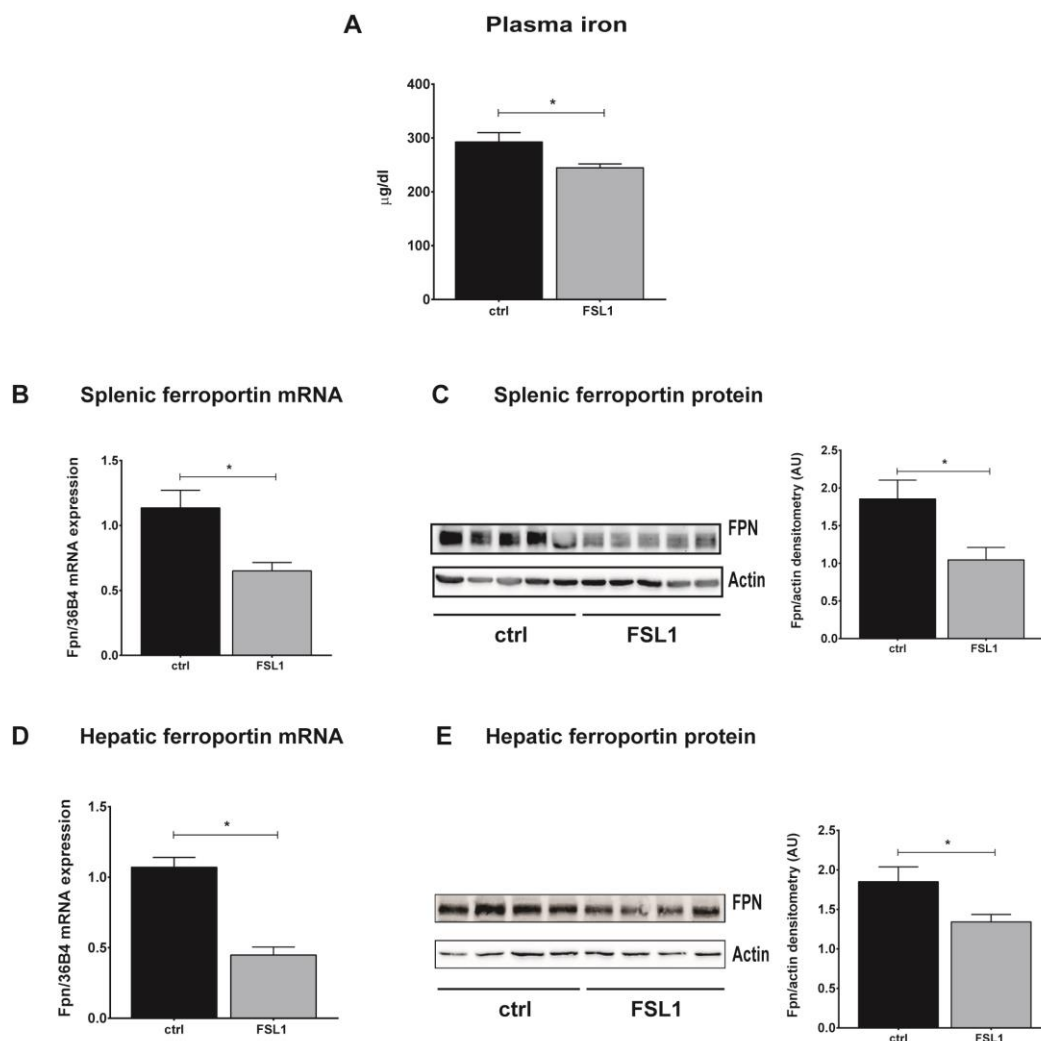


Figure 3.32 FSL1 injection in FPN^{C326S} knock-in mice induces hypoferremia. (A) Plasma iron level was measured in FPN^{C326S} knock-in mice injected with FSL1 (100 ng/g bodyweight) per 3h. Splenic (B, C) and hepatic (D, E) ferroportin mRNA and protein levels were analyzed by qRT-PCR and Western-blot in the same groups of mice. β -actin was used as loading control. Data are means \pm SEM. * $P < 0,05$, ** $P < 0,01$, *** $P < 0,001$, Student's t test. $n = 6$ mice per group.

3.10 Investigating the TLR2/6 mediated ferroportin transcriptional regulation

FPN mRNA reduction induced by Toll like receptor ligation appeared to be essential to set the hypoferremia during acute inflammation. However little is known about the molecular basis of this process. In the attempt to investigate this aspect diverse approaches were applied.

3.10.1 Testing cytokine stimulation

Controversial results were reported on the direct and indirect role of inflammatory cytokines to modulate FPN levels. In particular, the importance of TNF α for FPN regulation has been highly debated (90, 91). To better understand its role I treated BMDMs with different concentration of recombinant IL1 β , IL6 and TNF α and I analyzed FPN mRNA level at three different time points. As shown in figure 3.33 only TNF α induced strong FPN down regulation even after short incubation time and at low dose. This result may suggest a role of TNF α in reducing FPN expression. In support of this I also observed that in TLR6- deficient BMDMs TNF α was not induced 6h after FSL1 treatment, the same time point at which I observed no change in FPN mRNA level (Figure 3.33 D). The same did not apply to IL1 β and IL6 (Figure 3.33 E).

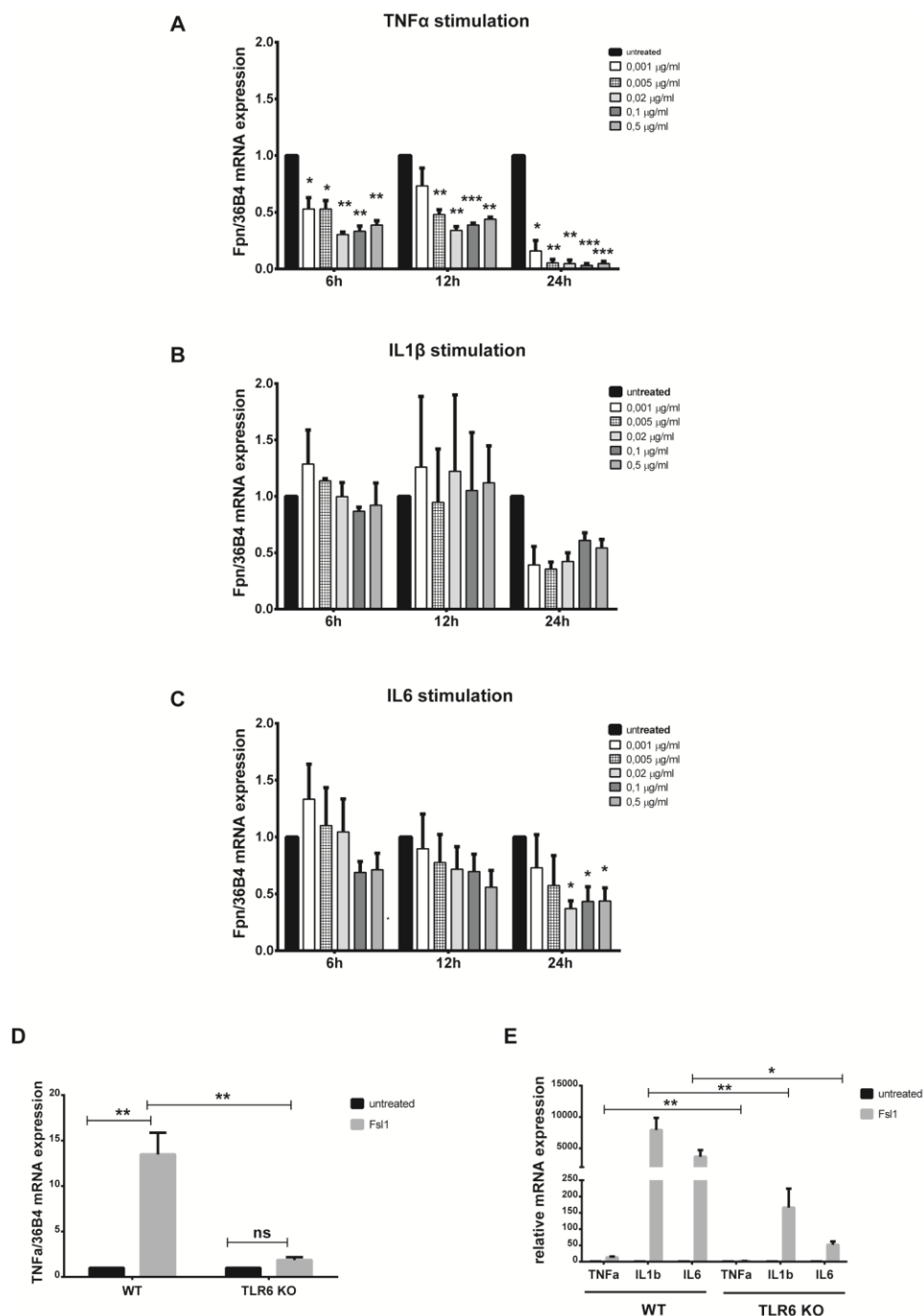


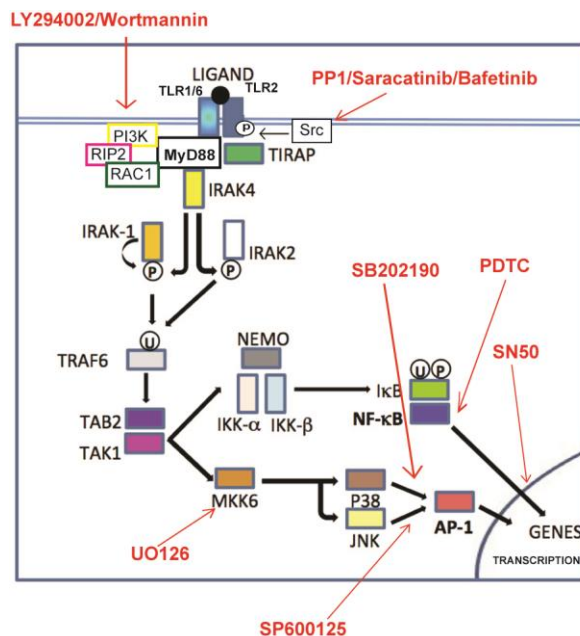
Figure 3.33 TNF α stimulation induces FPN mRNA reduction in BMDMs. BMDMs were stimulated with TNF α (A), IL1 β (B) and IL6 (C) at the indicated concentrations. FPN mRNA levels were analyzed after 6h, 12h and 24h by RT-qPCR and calibrated to 36B4. TNF α (D) and, in addition, IL1 β and IL6 (E) mRNA expression was measured in BMDMs derived from wild type (WT) and TLR6-deficient mice (TLR6 KO) after 6h of FSL1 treatment. Data are means \pm SEM, BMDMs were derived from at least 4 mice per group, * $P < 0,05$, ** $P < 0,01$, *** $P < 0,001$, **** $P < 0,0001$ Student's t test.

3.10.2 Testing specific inhibitors of TLRs pathway

To investigate the molecular pathways triggering FPN suppression as a consequence of inflammatory stimuli I applied specific inhibitors for signaling molecules and kinases that could be involved in the process. Following ligand recognition, TLR2 heterodimers were known to initiate a MyD88-dependent pathway which ultimately induced nuclear translocation of nuclear factor- κ B (NF κ B) to modulate gene transcription. In addition MAP kinases were reported to mediate JNK and p38 activation which triggered the induction of the transcription factor activation protein 1 (AP-1) to control gene transcription of cytokines and other molecules (154, 155). Further studies in human macrophage cell lines also demonstrated, by using specific inhibitors, that phosphatidylinositol-3 kinase (PI3K) and AKT played a role in the TLR-mediated induction of cytokines (149, 156, 157) and that tyrosine phosphorylation by Src kinases was required for TLRs activation (157-159). To better dissect the molecular mechanism leading to TLR-mediated FPN regulation I tested several inhibitors which specifically targeted key elements of the TLR signaling pathway (Table 3.1 and figure 3.34) on BMDMs challenged with FSL1.

Inhibitor	Target
LY294002/ Wortmannin	PI3K kinase inhibitors
PP1/Saracatinib/Bafetinib	c-Src inhibitors Abl/Lyn inhibitor
SB202190 /SP600125	P38-MAPK and JNK inhibitor
UO126	MEK1/2 inhibitors
PDTC/SN50	NF κ B activation/ translocation inhibitors

Table 3.1 Inhibitors of TLR signaling pathway tested on BMDMs.



Adapted from Oliveira-Nascimento et al., *Frontiers in Immunology*, 2012

Figure 3.34 Inhibition of key components of the TLR2 signaling. After ligand recognition, TLR2 heterodimerizes with TLR1 or TLR6. Activation of the signal requires the phosphorylation of TLR2 cytosolic domain by Src. TIR domain of TIRAP binds the TIR domain of TLR2 and recruits the adaptor protein MyD88. IRAKs are then recruited and IRAK 4 phosphorylates (P) IRAK1, which then mediates auto-phosphorylation to activate TRAF6. Since IRAK1 is rapidly degraded, IRAK2 also activates TRAF 6 in latter responses. Ubiquitinated (U) TRAF6 triggers the activation sequence TAB2 – TAK1 – IKK complex which ultimately leads to IκB phosphorylation and ubiquitination by the IKK complex. IκB degradation then releases NF-κB to translocate to the nucleus and activate gene transcription. In parallel, TAK1 also activates MKK6 for subsequent JNK and p38-mediated AP-1 activation that triggers gene transcription of cytokines and accessory molecules. MyD88, myeloid differentiation primary-response gene 88; TIRAP, TIR adaptor protein; IRAK, interleukin-1 receptor associated kinase; TRAF, TNF receptor associated factor; TAK, transforming growth factor beta-activated kinase 1; TAB, TAK1-binding protein; MKK/JNK/P38, MAP kinases, NEMO/IKKs, kinase complex; NF-κB, nuclear factor-κB; IκB, kinase complex; AP, activator protein; PI3K, phosphatidylinositol-3 kinase, RIP2, receptor interacting protein 2; RAC1, ras-related C3 botulinum toxin substrate 1. Inhibitors and their targets are indicated.

Interestingly I observed that the inhibition of the PI3K (by LY294002 and Wortmannin) and the Src kinases (by PP1 and Saracatinib) led to FPN mRNA increase irrespectively of any additional treatment (Figure 3.35 A, B). As a positive control I analyzed the decreased phosphorylation of AKT for PI3K inhibitors and Tyr416 which is the auto-phosphorylated on active Src. In particular LY294002 appeared to induce strong FPN protein up regulation after 24h treatment (Figure 3.35 C), although the phosphorylation of its target (AKT) recovered already within few hours from the treatment. On the other hand, the inhibition mediated by the other PI3K inhibitor Wortmannin was visible even

after 24h (Figure 3.35 D), but FPN protein levels displayed no increase. This suggested that LY294002 altered FPN expression in a PI3K-independent manner.

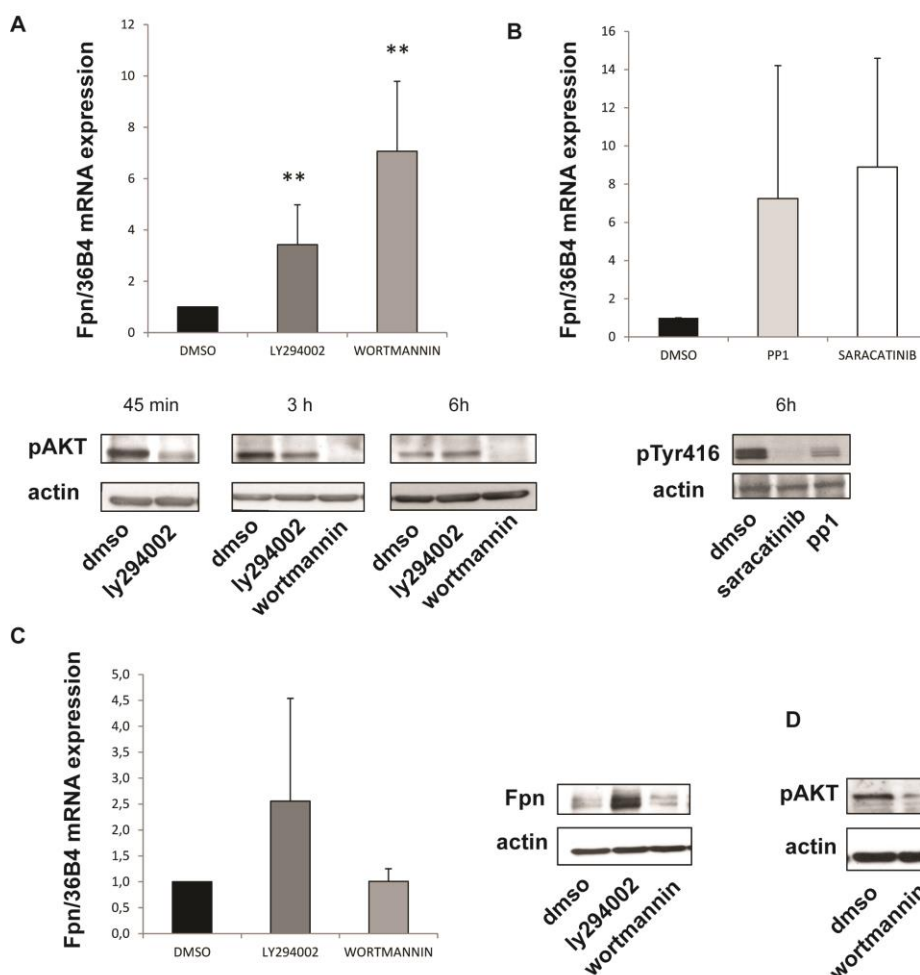


Figure 3.35 PI3K and Src kinase inhibitors increase FPN expression in BMDMs. (A, B) FPN mRNA level were analyzed after 6h treatment with the indicated inhibitors. Western blot analysis ascertains specific target inhibition of AKT phosphorylation for PI3K inhibitors (A) and Tyr416 phosphorylation for Src kinase inhibitors (B). (C) FPN mRNA and protein level were evaluated after 24h treatment with the indicated PI3K inhibitors. (D) Inhibition of AKT phosphorylation results stable till 24h Wortmannin treatment. β -actin was used as loading control. Data are means \pm SD from 3 independent experiments, ** $P < 0,01$, Student's t test.

None of the inhibitors I tested completely prevented the FSL1-mediated FPN reduction. However while FSL1 treatment completely overrode the effect of Src inhibitors on FPN mRNA levels (which return comparable to the levels of untreated sample) (Figure 3.36 C, D) PI3K inhibition, and in particular LY294002 pre-treatment, yet displayed higher FPN expression (Figure 3.36 A, B).

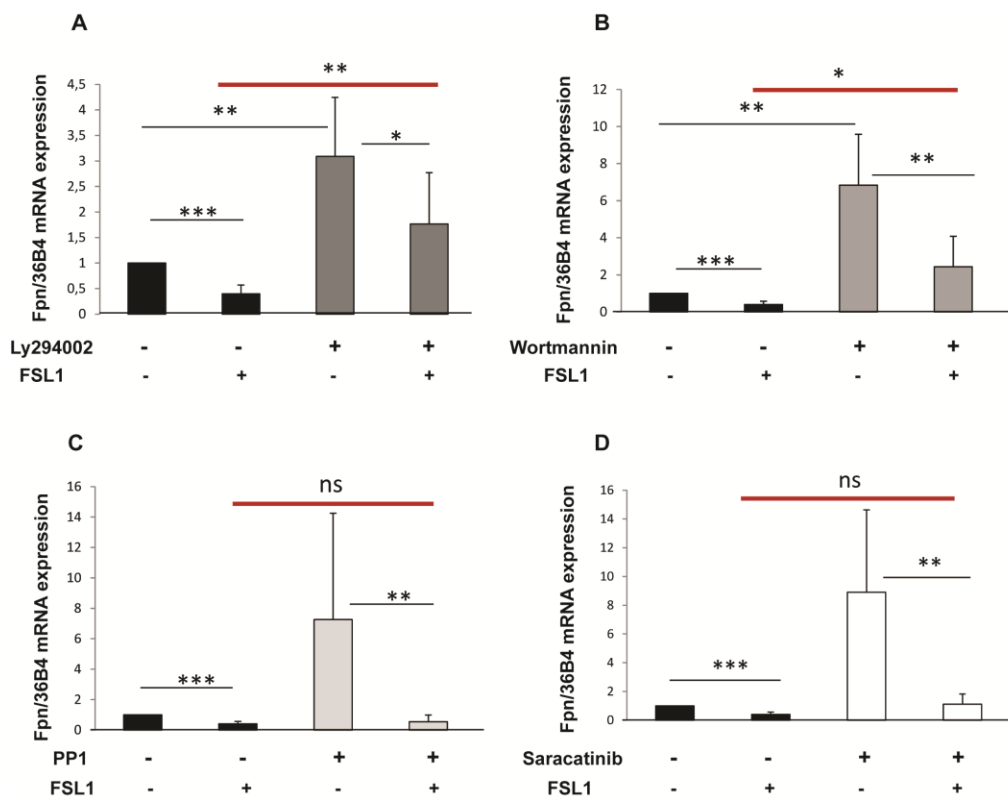


Figure 3.36 PI3K inhibitors reduce the FPN decrease induced by FSL1. BMDMs were incubated with PI3K inhibitors (LY294002 and Wortmannin) (**A, B**) or Src kinase inhibitors (PP1 and Saracatinib) (**C, D**) for 30 minutes before the addition of FSL1 (100ng/ml). After 6h FPN mRNA levels were analyzed by RT-qPCR and calibrated to 36B4 mRNA levels. Data are means \pm SD from 3 independent experiments, * $P < 0,05$, ** $P < 0,01$, *** $P < 0,001$, Student's t test.

4. DISCUSSION AND PERSPECTIVES

4.1 Unresolved and controversial aspects of ferroportin regulation

The maintenance of systemic iron homeostasis plays a pivotal role in human health. Iron overload and deficiency diseases belong to the most common pathologies across the globe. Systemic iron homeostasis evolved to maintain a plasma iron concentration that ensures sufficient iron supplies to organs while preventing iron overload. This regulatory mechanism is executed through the interaction between the hepatic hormone hepcidin and the sole known iron exporter ferroportin (FPN). FPN is predominantly expressed in tissues that supply iron to plasma, such as hepatocytes, duodenal enterocytes, macrophages and placental trophoblasts. Hepcidin binds to FPN and induces its internalization and degradation, reducing cellular iron export and thereby regulating mobilization of iron from hepatic stores, dietary iron absorption, iron release from macrophages and iron transfer across the placenta. Misregulation of the hepcidin/FPN system causes diseases of iron overload (e.g. hereditary hemochromatosis) and iron deficiency (e.g. the anaemia of chronic inflammation), two of the most frequent disorders worldwide.

FPN was identified as the receptor for hepcidin in 2004. An engineered HEK293 cell line expressing the FPN-GFP fusion protein was shown to bind hepcidin and mediate FPN degradation in lysosomes (28). Following mechanistic studies in the same cellular system then claimed that phosphorylation and ubiquitination were crucial modifications to induce the internalization and degradation of FPN (97). In particular mutations at specific tyrosine residues (302, 303) in FPN and the treatment with Src kinase inhibitor PP2 were reported to prevent the hepcidin-mediate phosphorylation of FPN at the plasma membrane. Furthermore by using JAK2-deficient cells and siRNA approaches De Domenico et al. proposed that JAK2 was the kinase responsible for FPN phosphorylation and that the dimerization of FPN monomers was required for JAK2 activation (98). However several papers from these authors were retracted (188, 189) and a more recent report has demonstrated that neither JAK2 nor phosphorylation of the tyrosine residues was necessary for the post translational control of FPN (99). In particular FPN mutants for several tyrosine residues were proven to retain

responsiveness to hepcidin and FPN internalization was shown to be preserved in JAK2 null cells as well as in cells treated with Pan-Jak and JAK2-selective inhibitors. In addition, hepcidin treatment did not result in the activation of JAK2-STAT signaling and *in vivo* JAK2 inhibition did not prevent the reduction of serum iron levels normally observed by hepcidin administration. While these lines of evidence have conclusively disproven the role of JAK2 and phosphorylation for FPN regulation, ubiquitination has been further shown to be the relevant modification required for FPN endocytosis (100). Hepcidin addition induced FPN ubiquitination within 5 minutes in HEK293 engineered cell lines as well as in primary bone marrow derived macrophages. Consistently, mutations of lysine residues in the third intracellular loop of FPN impaired its hepcidin-mediated endocytosis and, consequently the ability of cells to retain iron. This finding also seemed to explain the mild iron overload observed in a patient carrying a mutation in heterozygosity at the lysine residue 240 of FPN which was expected to cause at least partial resistance to hepcidin *in vivo*.

RNA interference approaches in a HEK293 cell line expressing a FPN-GFP fusion protein suggested that a clathrin-dependent process controls FPN internalization. In particular depletion of epsin, a protein required for clathrin-mediated endocytosis, was reported to inhibit the FPN degradation following hepcidin addition (97). Different conclusions were drawn by Auriac et al. in murine macrophages by using drug inhibitor strategies (101). In particular, FPN expression was demonstrated to localize in specific detergent-resistant membrane compartments containing raft markers, such as caveolin and flotillin. The integrity of the raft was required for the hepcidin control of FPN, as the lipid raft breakdown caused by two drugs (filipin and methyl- β -cyclodextrin) through the sequestration of cholesterol, affected the endocytosis and degradation of FPN in BMDMs and macrophage cell lines. On the other hand the inhibition of clathrin-dependent endocytosis by another drug (chlorpromazine) did not cause any alteration in the hepcidin-mediated FPN regulation, suggesting that clathrin-independent mechanisms mediated FPN internalization in macrophages. Such a discrepancy has suggested the existence of new and yet not defined cellular pathways controlling the hepcidin-dependent FPN endocytosis, although different cell types and different experimental procedures were used in the described works.

A second route of FPN internalization independent of hepcidin has also been characterized in a HEK293 engineered cell line in response to cytosolic iron depletion or activity reduction of the multicopper oxidase ceruloplasmin (141). Under these conditions the ubiquitination of FPN by the E3 ubiquitin ligase Nedd4-2 and its accessory protein Ndfip-1, was shown to induce FPN internalization from the plasma membrane to protect cells from iron depletion and apoptosis. This hepcidin-independent degradation pathway was proposed to be an ancestral conserved mechanism that has preceded the hepcidin-dependent FPN endocytosis as supported by additional data in the invertebrate *Caenorhabditis elegans*. In this organism FPN protein lacks the critical cysteine residues required for hepcidin binding, however iron deprivation induced its internalization despite the absence of hepcidin contribution. Although the authors continue endorsing the validity and the conclusions of the study, this publication has been retracted because of a number of errors declared in the figures (188).

4.2 Rationale of the study

High throughput RNA interference has been used over the last years as a powerful technology to reduce expression levels of specific genes and learn about their potential functions in a defined biological process. Thus, the goal of my PhD project was to identify genes that control or modify the hepcidin-dependent FPN internalization by applying an RNAi screen. The importance of FPN phosphorylation upon hepcidin binding appeared to be well established at the beginning of my PhD. However the discovery of new molecular details in primary cells already began to challenge the model proposed for FPN internalization and degradation (Figure 1.5). At this stage the role of kinases and related signalling molecules was expected to be essential for the post transcriptional regulation of FPN stability and, therefore it was of priority interest to apply an RNAi screen focused on kinases.

4.3 A focused RNAi screen identifies hepcidin-independent ferroportin regulators

HeLa cells were already reported to support hepcidin-mediated FPN internalization from expressed reporter genes (28) and robust protocols of reverse transfection of cells on siRNA arrays for these cells were available (137, 139). For these reasons the screening was applied to a stable and inducible HeLa cell line expressing a hFPN-Rluc fusion protein. The quantification of the Rluc reporter activity in the assay provided a fast, quantitative simple and sensitive read-out of FPN expression and regulation. However it precluded the visualization and the quantitative analysis of intermediate FPN internalization steps or cell viability alterations which, in principle, could have been monitored by a cell-imaging based approach. For the screen I used a pool of 4 siRNA sequences per gene. This approach in principle promises a greater phenotypic penetrance, while raising the risk of possible off-target effects. One way to enhance confidence in the screening results was the identification of possible siRNA-mediated side effects regulating the reporter gene only rather than FPN. I therefore took advantage of a HeLa cell line with stable and inducible expression of the Rluc protein that was generated in an identical manner and subjected to the same screening strategy. By this approach I excluded those siRNAs which altered Rluc expression *per se* from the follow-up analysis.

Unexpectedly, the screening yielded many candidates which potentially controlled FPN protein stability in a hepcidin-independent manner and identified only few genes involved in the hepcidin-induced FPN internalization pathway (Figure 3.17). Importantly, the depletion of JAK2 kinase did not result in significant alteration of the FPN-Rluc regulation after hepcidin treatment, excluding it from the hit list and further questioning its role in the FPN internalization process. This finding is consistent with the evidence accumulated during the last years (previously discussed) that disproved the importance of phosphorylation for the hepcidin-mediated FPN regulation. The usage of a focused library, mainly containing kinases, limited functional association analysis among the candidates and precluded the identification of shared pathways. However, 14 potential FPN regulators were associated with immune processes. The relationship between iron and immunity plays a critical role during pathogen infection (see paragraph 4.4) and this made these candidates interesting for further analysis.

Engineered cell lines have been extensively used to investigate molecular mechanisms underlying hepcidin-mediated FPN regulation. Although they represent a powerful tool to dissect molecular signalling by applying high throughput techniques, they do not fully recapitulate the physiological regulation of FPN which plays its essential role in specialized cell types, such as macrophages or enterocytes.

In this project results obtained in HeLa cells needed to be validated in a more physiological system. Technical limitation was the lack of an effective antibody which recognizes the human FPN protein. Human and mouse FPN share 95% of homology and the mechanisms mediating FPN regulation are expected to be highly conserved between these two species. Macrophages express high levels of FPN and constitute the primary site of body iron turnover, playing a major role in ensuring adequate plasma iron levels. In addition, for their functions as scavengers, antigen presenting cells and secretory cells, they are vital to the regulation of immune responses and the development of inflammation. For these reasons I chose to further validate the role of the identified putative FPN regulators in murine bone marrow-derived macrophages, focusing on the genes related to immune processes. The mRNA expression of some mouse homologs of putative FPN regulators (TEX14, BLNK, MECOM, ADAM9, EPHB6) was very low or undetectable in BMDMs, preventing their characterization. For others (BMP2K, IPMK, PHKA1, ITPKB, TLR6) I could confirm the screening results by observing an increase in FPN protein levels despite the limited quality of the anti-FPN antibody used for Western-blot detection. Among them, ITPKB (inositol-trisphosphate 3-kinase B) and IPMK (inositol polyphosphate multikinase) are known to be involved in the inositol phosphate metabolism. These kinases both mediate the phosphorylation of the second messenger inositol 1,4,5-trisphosphate to Ins(1,3,4,5)P₄ which is important for cellular signaling and, in particular, in the control of Ca²⁺ release from intracellular stores (160-162). Studies in humans demonstrated that Ca²⁺ supplementation can have short-term inhibitory effects on iron absorption (163-166). In addition Ca²⁺ treatment of human intestinal Caco-2 cells was reported to decrease FPN abundance at the basolateral membrane and increase cellular iron retention within 1.5 hour, although this effect was of short duration and adaptation occurred with time (167). Taking together these data may suggest that the depletion of inositol phosphate kinases could alter FPN

expression levels because of changes in intracellular Ca^{2+} concentration. However this hypothesis was not investigated further in this work and remains to be tested by additional experiments.

For its well-established role in pathogen recognition and innate immunity activation I rather decided to focus on TLR6 for further functional analysis.

4.3.1 TLR6 is a novel regulator of ferroportin protein expression

Toll like receptors (TLRs) 1, 3, 4 and 6 were present in the siRNA library used for the screening. Among them only TLR6 was identified and validated as a putative ferroportin repressor. Its key role in the innate immune system and the tight relationship between iron and host defense, made it the most interesting candidate to better characterize in macrophages. The availability of BMDMs deficient for TLR6 allowed me to confirm the finding from HeLa cells overcoming all the technical limitations that I faced analyzing the effects of transient transcript depletions (page 75-76). Furthermore the increase of FPN protein levels independent of alterations in ferroportin and hepcidin mRNA levels corroborated that the lack of TLR6 affected FPN protein stability irrespectively of hepcidin contribution (Figure 3.19).

The responsible mechanism was not addressed in this work, however it is possible to imagine that under basal conditions TLR6 reduces or maintains low FPN protein levels indirectly, perhaps modulating the protein turnover. TLRs mostly play a role under inflammatory conditions which are known to modulate iron homeostasis. Therefore I chose to explore FPN regulation following TLR6 ligation and activation, mimicking a pathogen-induced inflammatory response.

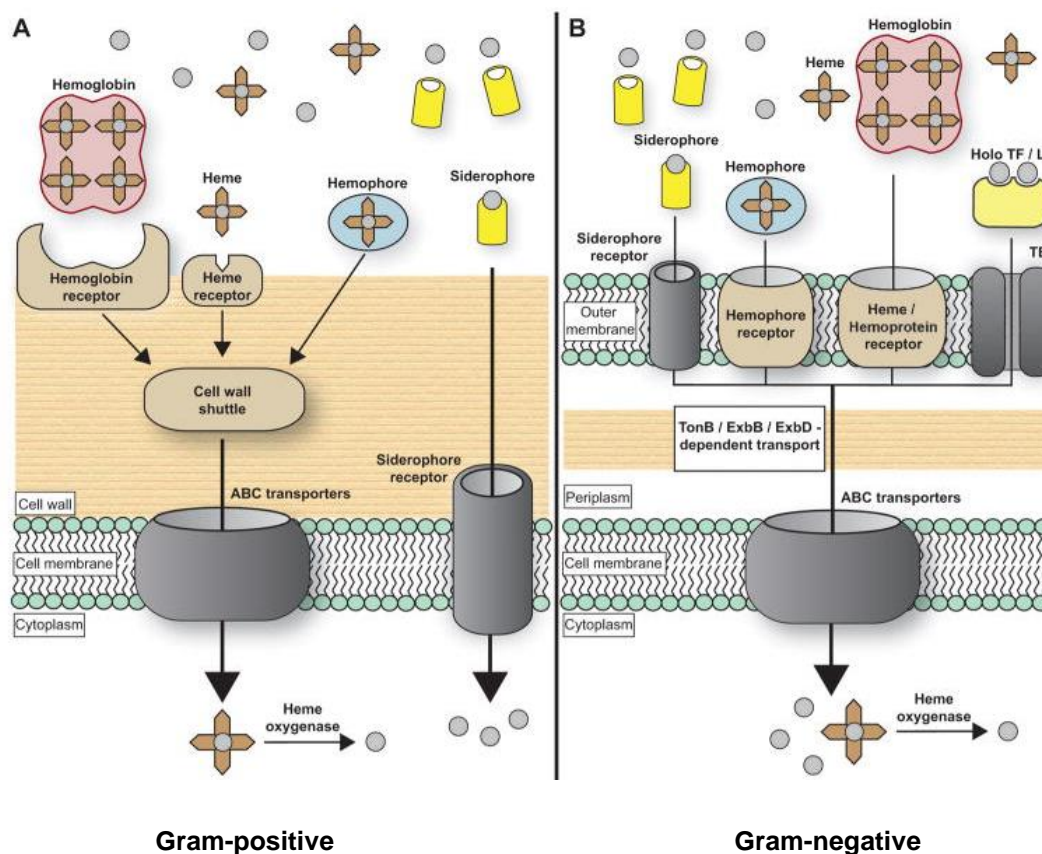
4.4 Battle for iron

Iron is a central player for host-pathogen interactions. It is an essential nutrient for both humans and pathogens and it is required to allow for microbial proliferation and to achieve full virulence. Given its relevance for microbe survival, an important response of the innate immune system has evolved to limit iron availability to invading pathogens.

The fact that pathogens developed a number of mechanisms to acquire host iron and the attempt of the host to withhold iron as defence, has generated an ever-evolving battleground for this metal. Bacterial pathogens employ several systems to satisfy iron requirements (Figure 4.1). Among them, siderophores are small iron chelating compounds secreted by microorganism under conditions of low-iron availability, which bind to soluble Fe^{3+} with high affinity (168). A special example is represented by mycobactins, the lipophilic siderophores of mycobacteria which chelate intracellular iron in macrophages. Mycobactins accumulate in macrophage lipid droplets that can diffuse out of phagosome to capture cytoplasmic iron (169). Many pathogens, including fungi, have also developed the ability to acquire iron from heme via direct heme uptake (most Gram-positive bacteria) or hemophore-dependent mechanisms (e.g. *B.anthraxis*) which allow for the extraction of heme groups from host hemoprotein, such as hemoglobin (170). Alternatively, microorganisms like *Neisseria gonorrhoeae* under iron-limiting conditions can express transferrin or lactoferrin binding proteins on the membrane to directly internalize transferrin- or lactoferrin-bound iron (171).

During infection the innate immune system counteracts pathogen iron uptake by limiting local and systemic iron availability. Local iron sequestration at infectious foci is mainly achieved by lactoferrin and siderocalin production. Lactoferrin is a host glycoprotein with antimicrobial activity contained in mucosal secretions and in secondary granules of neutrophils and, like transferrin, has the capacity to bind free iron with high affinity (172). Siderocalins, also known as neutrophil gelatinase-associated lipocalins, are produced by neutrophils during acute infection and neutralize pathogen iron intake by sequestering the siderophores released from pathogens (173). Systemically, the inflammatory response triggered by the innate immune system alters the expression of several iron-related genes, resulting in the sequestration of iron in macrophages of the reticuloendothelial system and in reduced serum iron levels. The hypoferrremia induced during infection is a major host defence strategy and it was first observed in the forties following *Staphylococcus aureus* inoculation and turpentine injection (174). It seems well established that the crucial effector of this response is hepcidin whose release from the liver is known to be induced by inflammatory stimuli (paragraph 1.5.4). Hepcidin induction provokes FPN protein decrease and, consequently, tissue iron retention thus

explaining the drop in serum iron levels. However, in addition to the FPN post-translation regulation mediated by hepcidin, infectious agents were also reported to reduce FPN mRNA levels (57, 90), suggesting that different mechanisms can modulate FPN levels during infection.



Adapted from Cassat and Skaar, *Cell Host Microbe*, 2013

Figure 4.1 Pathogen iron uptake strategies. (A) Gram-positive microorganisms can acquire iron from heme through heme and hemoprotein receptors or through the release of hemophores. Heme is then transported into the cytoplasm by ABC-type transporters and degraded by heme oxygenase to extract iron. Alternatively, under low-iron conditions pathogens secrete siderophores which capture extracellular iron and then re-enter the cell through specific transporters. (B) In addition to these iron acquisition systems, some Gram-negative microorganisms also express transferrin or lactoferrin binding proteins (TBP/LBP) to acquire transferrin(TF)- or lactoferrin(LF)- bound iron. The transport of heme, siderophore-iron or transferrin-iron complexes across the Gram-negative outer membrane requires energy generated from the TonB/ExbB/ExbD system.

4.5 Ferroportin mRNA down regulation is a conserved response to pathogen infection

FPN is one of the iron-related genes whose expression is altered in consequence of immune system activation, for instance during pathogen invasion. Its reduction is one of the defense mechanisms evolved to diminish iron supply to pathogens. Yang et al., in 2002 and Liu et al., in 2005 demonstrated that LPS stimulation of splenocytes induced TLR4-dependent reduction of FPN mRNA and protein, in a hepcidin-independent and dependent manner, respectively. My data showed that TLR6 ligation with FSL1 decreased FPN levels in bone marrow derived macrophages (Figure 3.20, A, B). However, in this case, even the protein reduction occurred independently of hepcidin as I did not observe an increase in hepcidin expression following FSL1 stimulation (Figure 3.22 B). FPN mRNA expression responded with a quantitatively similar decrease to other bacterial lipopeptides (PAM3CSK4 and PamOct2C-(VPG)4VPGKG) (Figure 3.24) known to activate TLR2 which is the functional partner of TLR6 (148, 150). These results, in addition to the reported FPN decrease in consequence of other bacterial, fungi and virus components (153, 175), together indicated that this is an important and conserved transcriptional response in the inflammatory context. However under defined conditions the control of FPN and hepcidin expression can be uncoupled as the decrease of FPN levels downstream of TLR2/6 signaling was independent of hepcidin activation. This conclusion is in contradiction to the data published by Layoun et al. in 2012 by using the RAW264.7 cell line and peritoneal macrophages challenged with several bacterial cell wall constituents (176). However in my hands, RAW264.7 cells did neither show FPN mRNA down regulation nor hepcidin mRNA induction following FSL1 treatment, despite increased cytokine expression. The reason of such discrepancy remains unclear, nevertheless my data suggest that this cell line may not represent a proper system for the study of the inflammatory-mediated FPN regulation.

4.5.1 TLR2/6 heterodimers and/or TLR2 homodimers mediate ferroportin response to FSL1

The specific activation of TLR6 can be achieved by ligation with *Mycoplasma fermentas* derived lipopeptides other than FSL1, like the macrophage-activating lipopeptide 2 (MALP-2). TLR6-depleted peritoneal macrophages were reported to be unresponsive to

MALP-2 (177). To test the specificity of FSL1 for TLR6 and the dependency of FPN response on it, I analyzed the FPN mRNA regulation in TLR6-deficient BMDMs. According to the identity of framework structure between FSL1 and MALP-2 I expected FSL1-mediated FPN down regulation not to occur in absence of TLR6. Conversely I showed that the FPN mRNA down regulation was partially dependent on TLR6, because it was prevented only at 6h time point and significantly blunted at later time points (Figure 3.20 A, B). Rather, TLR2 played a further role in this regulation, as in TLR2-deficient BMDMs the FSL1-mediated control of FPN was completely abolished (Figure 3.20 C). TLR2 is known to form heterodimers with TLR6 and TLR1 (146). The existence of these different heterodimers expand the ligand spectrum enabling the innate immune system to recognize different lipopeptide but it does not seem to lead to differential signaling (148). It is assumed that diacylated lipopeptide, such as FSL1 or MALP-2, signal through TLR2-TLR6 heteromers, whereas triacylated lipopeptide, such as PAM3CSK4, induce signaling through TLR2-TLR1 heteromers (178). However investigations with new synthetic lipopeptide derivates have shown that this distinction is not clear-cut and some lipopeptide are recognized by TLR2 in a TLR1- and TLR6-independent manner, indicating that TLR2 might be able to signal as homomers (150, 179). I demonstrated that TLR1 was not involved in the FSL-1 controlled FPN response, as TLR1-deficient BMDMs retained their responsiveness to FSL1 (Figure 3.21). Thus, taken together my results revealed that FSL1-mediated FPN regulation can be mediated by TLR2/6 heterodimers and/or TLR2 homodimers. Such redundancy may enable the immune system to trigger a more immediate and robust response to rapidly reduce iron supply to pathogens.

While FSL1-triggered FPN suppression depended on TLR2 and TLR6, the FPN response mediated by PAM3CSK4 and PamOct2C-(VPG)4VPGKG only depended on TLR2 signaling (Figure 3.24 A, B, C). Conversely, as expected (61), LPS stimulation reduced FPN and induced hepcidin mRNA expression throughout the time-course that I applied by mechanisms that were independent on TLR2 and TLR6 (Figure 3.24 D, E, F).

In this work FPN mRNA reduction resulted a conserved response to TLR2 (FSL1, PAM3CSK4, PamOct2C-(VPG)4VPGKG) and TLR4 (LPS) ligation while hepcidin mRNA expression appeared to be mainly mediated by TLR4 activation (61). This may suggest that FPN transcriptional reduction represents the key mechanism shared between all TLRs to restrict iron export and that hepcidin induction in macrophages is a secondary event maybe triggered by specific pathogens.

4.6 The importance of hepcidin induction in macrophages

In addition to hepcidin production in the liver, several infectious agents were also reported to induce hepcidin synthesis in neutrophils and macrophages. The first evidence of hepcidin induction in macrophages was reported in 2005 in RAW 264.7 murine cell line, mouse peritoneal splenocytes and in the mouse spleen following LPS stimulation and injection (57). Its importance in the host response to bacterial pathogens and its dependency on TLR4 was characterized by Peyssonnaud et al. one year later (61) by exposing macrophages and neutrophils to either Gram-positive bacteria or Gram-negative bacteria. *In vivo* data also demonstrated that systemic infection with the Gram-negative bacterium *P. aeruginosa* or the Gram-positive bacterium GAS activated hepcidin expression in the liver and in the spleen of mice, ultimately causing serum iron level decrease. Mutations in the lipopolysaccharide response locus of TLR4 prevented hypoferremic response, iron retention in the spleen and splenic hepcidin induction, but it did not affect the hepatic production of hepcidin, suggesting that, at least in this infection model, the autocrine production of hepcidin played an important role to reduce FPN levels in the spleen and this was required to reduce serum iron levels. On the contrary, my data indicated that the lack of hepcidin induction either in the spleen (Figure 3.27B) or in the liver (Figure 3.26B) did not affect the hypoferremic response (Figure 3.25) and did not prevent splenic iron retention (Figure 3.27F) suggesting that other hepcidin-independent mechanisms were crucial to mediate these effects during the acute phase of inflammation. In BMDMs increased hepcidin mRNA levels were observed only after LPS treatment, while incubation of cells with FSL1 did not induce such response. Similar results were also obtained with other bacterial lipopeptides that activate TLR2-dependent signaling (PAM3CSK4 and PamOct2C-(VPG)4VPGKG) suggesting a

negligible contribution of TLR2 signaling to hepcidin production in macrophages (Figure 3.24). Further investigations would be required to clarify the importance of hepcidin release from macrophages which may assist the systemic immune response in localized infection microenvironments where immune cells are recruited and prompt to restrict iron to invading pathogens. However my results suggest that hepcidin production is not the only critical line of defense and that, at least in certain inflammatory conditions, the hepcidin-independent FPN down regulation represents a more relevant and conserved response to restrain iron access.

4.7 Cytokine contribution to the inflammation-mediated regulation of ferroportin and hepcidin

4.7.1 The controversial role of TNF α in ferroportin down regulation

The role of cytokines, and in particular, of TNF α in controlling FPN regulation is controversial. In support of TNF α -independent FPN down regulation Yang et al. in 2002 demonstrated that TNF α injection of mice and TNF α treatment of mouse splenocytes did not lead to mRNA reduction of FPN. In addition, mice lacking TNF α receptor developed hypoferrremia following LPS injection and down regulated FPN in the spleen to a similar extent as wild type mice (90). Similar results were also obtained in IL6, IL1 and NFkB1 KO mice indicating that FPN regulation did not require these mediators (57). Conversely, two papers in the late eighties reported hypoferrremic response in mice in consequence of recombinant TNF α injection (180) (181), already suggesting that alterations in the ability of macrophages to handle iron was responsible for reduced serum iron as recently demonstrated by Schubert et al. in a model of acute inflammation (91). My results showed that FSL1 and LPS stimulation while reducing FPN mRNA levels, induced TNF α (and other cytokine) mRNA expression in BMDMs (Figure 3.23 C) and in the spleens of injected mice (Figure 3.28 A). On the other hand BMDM treatment with murine recombinant TNF α induced FPN down regulation throughout a time course even with a low dose of the cytokine (Figure 3.33 A). The same was not observed after IL6 and IL1 β addition (Figure 3.33 B, C) suggesting that TNF α may play a role in the FPN transcriptional regulation under inflammatory conditions. Some lines of evidence

were also indirectly provided by the TLR6-deficient BMDM response to FSL1, as at 6h time point the lack of FPN down regulation was accompanied by the lack of TNF α (and not IL6 or IL1 β) up regulation (Figure 3.33 D, E). Although promising, these results did not address the contribution of TNF α for the systemic FPN regulation which remains to be ascertained.

4.7.2 The importance of IL6 and other cytokines for hepcidin induction and hypoferremia

It seems well established that hepatic hepcidin induction during inflammation is mediated by IL6 as described in 1.5.4. However the importance of this cytokine for the hepcidin regulation in macrophages and for the inflammation-mediated hypoferremic response remains controversial.

In macrophages hepcidin regulation appears to be different between human and mouse cells. In particular it was shown that IL6-deficient splenocytes retained the ability to increase hepcidin mRNA levels following LPS stimulation (57) while treatment with IL6, IL1 β and TNF α did not induce hepcidin expression (57, 151). By using different TLR ligands, Koenig et al. also proved that hepcidin induction in BMDMs occurred either in presence or in absence of the translation inhibitor cycloheximide, further suggesting that the new synthesis of cytokines was not required to mediate hepcidin response. Significant differences were found in studies of human monocytes which were reported to increase hepcidin mRNA levels upon LPS, IL6 or IFN α treatment (182, 183). Likewise, in human peripheral blood mononuclear cells (PBMC) IL6 and TGF β 1 were shown to induce hepcidin up regulation as well as flagellin (TLR5 agonist) and FSL1 (66). Consistent with data reported in mice I showed that FSL1 and LPS both activated IL1 β , IL6 and TNF α mRNA expression throughout a time course, albeit quantitatively less in FSL1 treated BMDMs (Figure 3.23). However hepcidin expression was upregulated only upon LPS stimulation (Figure 3.22B), indicating that increased expression of these cytokines was not sufficient for hepcidin activation in these cells.

In hepatocytes the importance of IL6 for hepcidin induction was mainly supported by the observation that hepcidin response, triggered by FSL1, LPS and other bacterial

lipopeptides, was strongly reduced in the absence of this cytokine. (58). Additional studies in mice also indicated that IL6 was necessary and sufficient to set hypoferrremia in a model of acute inflammation using turpentine (55).

On the contrary, Liu et al. showed that in IL6 knockout mice, serum iron level decreased after LPS injection following normal down regulation of splenic and hepatic FPN protein (57) suggesting that hepcidin production and hypoferrremia were independent of IL6. Furthermore IL6-independent hepcidin induction was reported in primary hepatocytes as result of IL1 α / β treatment (65). Indirect lines of evidence also derived from LPS injection in HFE knockout mice which were demonstrated to develop an impaired hepcidin response despite a preserved IL6 expression induction (70). My *in vivo* data did not directly address the role of IL6 for hepcidin induction. However I observed that FSL1 injection in mice triggered a mild, but significant IL6 mRNA up regulation only in the spleen (Figure 3.28 B) while, in the liver, the absence of hepcidin induction associated with the lack of IL6 mRNA increase (Figure 3.26 B, D). This may suggest either that the levels of circulating IL6, produced by the spleen, were not sufficient to induce hepatic hepcidin induction or that the autocrine liver production of IL6 actually accounts for hepatic hepcidin stimulation (as the cytokine production observed in the spleen appeared not to be sufficient to determine such response). Both these hypotheses would require additional investigations.

4.8 The “critical” role of hepcidin in inducing hypoferrremia during acute inflammation

It is widely thought that the hypoferrremia associated with acute and chronic inflammatory conditions is determined by the induction of hepcidin expression which reduces FPN protein amount, diminishing cellular iron export and serum iron levels. Injection of a wide range of LPS doses has been reported to induce hepatic hepcidin expression and hypoferrremia in mice (70, 90) and humans (56) corroborating the link between them. However two recent publications have added new insights into the inflammation-mediated hypoferrremia challenging the belief that hepcidin plays a crucial role.

By injecting LPS in hepcidin knock-out mice Deschemin and Vaulont (152) showed that plasma iron levels significantly decreased irrespective of hepcidin absence. Gene and protein expression analyses in the duodenum and in the spleen revealed that FPN mRNA levels were strongly reduced in both tissues, while protein levels only decreased in the duodenum. In addition, the membrane iron transporter DMT1 and the oxidoreductase Dcytb expression were down regulated in the duodenum following LPS treatment in hepcidin KO mice as well as in wild type mice leading the authors to the conclusion that the observed hypoferrremia was the result of compromised iron absorption.

Other lines of evidence questioning the crucial role of hepcidin in the hypoferrremic response were presented by Layoun et al. (153) who showed that TLR3 activation induced acute hypoferrremia in absence of hepcidin induction. Interestingly, in the same work the analysis of serum iron levels and hepcidin induction after LPS injection throughout a time course, indicated that hypoferrremia already occurred after 1.5h injection, a time point in which hepcidin levels were not yet significantly increased. Despite a rapidly LPS-induced hypoferrremia, splenic FPN protein appeared to be significantly reduced only after 12h from LPS injection, while HFE protein levels showed a faster reduction in the spleen. Given the competition between HFE protein and transferrin for the same binding site on TfR1, the authors speculated that the suppression of HFE may enhance the transferrin-mediated iron uptake in macrophages thus contributing to lower circulating iron amount. Through this conclusion they assigned a prominent and novel role to HFE in mediating the hypoferrremic response independent of hepcidin.

Challenging the prevailing notions and the latest findings, my data showed that hypoferrremia can be effected in a hepcidin-independent way and that it is mainly caused by rapid FPN down regulation. In particular, mice injected with FSL1 and LPS both reduced FPN mRNA and protein levels in the liver (Figure 3.26 F) and in the spleen (Figure 3.27 C, D) although only LPS-treated mice induced hepcidin mRNA expression (Figure 3.26 B). Hypoferrremia appeared to be a rapid response triggered by both stimuli, as plasma iron and transferrin saturation decreased already after 3h

injection (Figure 3.25) and hepatic (Figure 3.26 E) and splenic (Figure 3.27 F) iron content increased, indicating iron retention in both tissues. The FPN protein reduction observed in the spleen was even more pronounced in magnitude in isolated splenic macrophages (Figure 3.27 E), explaining perhaps the difficulty of other authors to observe such response. On the other hand, inconsistently with the data presented in hepcidin knockout mice, the duodenal analysis I applied did not reveal alterations in the iron absorption routes, as, especially in FSL1 injected mice, neither FPN nor DMT1a mRNA levels were decreased (Figure 3.29). Following the finding reported about the role of HFE in inflammatory hypoferremia, I also analyzed HFE expression after FSL1 and LPS injection. Reduction in HFE mRNA levels was observed in the spleen of FSL1 and LPS injected mice, while the liver of LPS injected mice displayed an opposite trend (Figure 3.30). However the antibody anti-HFE used in the work of Layoun et al. did not meet necessary specificity criteria in my hands, thus preventing additional HFE protein analysis in the spleen.

The direct proof that FSL1-induced hypoferremia and FPN regulation are independent of the hepcidin-FPN interaction *in vivo* was demonstrated in the C326S knock-in mouse strain in which the hepcidin/FPN regulatory circuitry was disrupted (190). As anticipated in paragraph 1.8.1 this model of *non classical ferroportin disease* is characterized by progressive iron accumulation in many organs and high circulating iron levels due to the resistance of FPN to hepcidin binding. The control mediated by hepcidin on FPN is completely lost, making these mice a good system to verify the inflammation-mediated FPN response irrespective of hepcidin contribution. BMDMs derived from these mice treated with FSL1 or LPS induced cytokine expression and regulated FPN expression similarly to BMDMs derived from wild type mice (Figure 3.31), already suggesting that inflammatory stimuli rather than hepcidin activity were mainly responsible for the strong FPN down regulation at mRNA and protein levels. Importantly I demonstrated that despite the systemic iron overload developed by these mice, FSL1 significantly reduced plasma iron levels within 3 hours and that FPN mRNA and protein levels were decreased in the liver as well as in the spleen (Figure 3.32).

These results demonstrate that hypoferremia can be effected in a hepcidin-independent way and assign a crucial role to the hepcidin-independent FPN down regulation in

inducing hypoferremia during infection. Hepcidin induction may complement this pathway in the generation of hypoferremia and its major contribution may be expressed in chronic inflammatory conditions to assist and prolong the hypoferremic response.

Taken together, beside the well-established hepcidin-dependent hypoferremia (induced for example by LPS), a complementary hepcidin-independent route can be derived from the present study, as represented in the following working model (Figure 4.2):

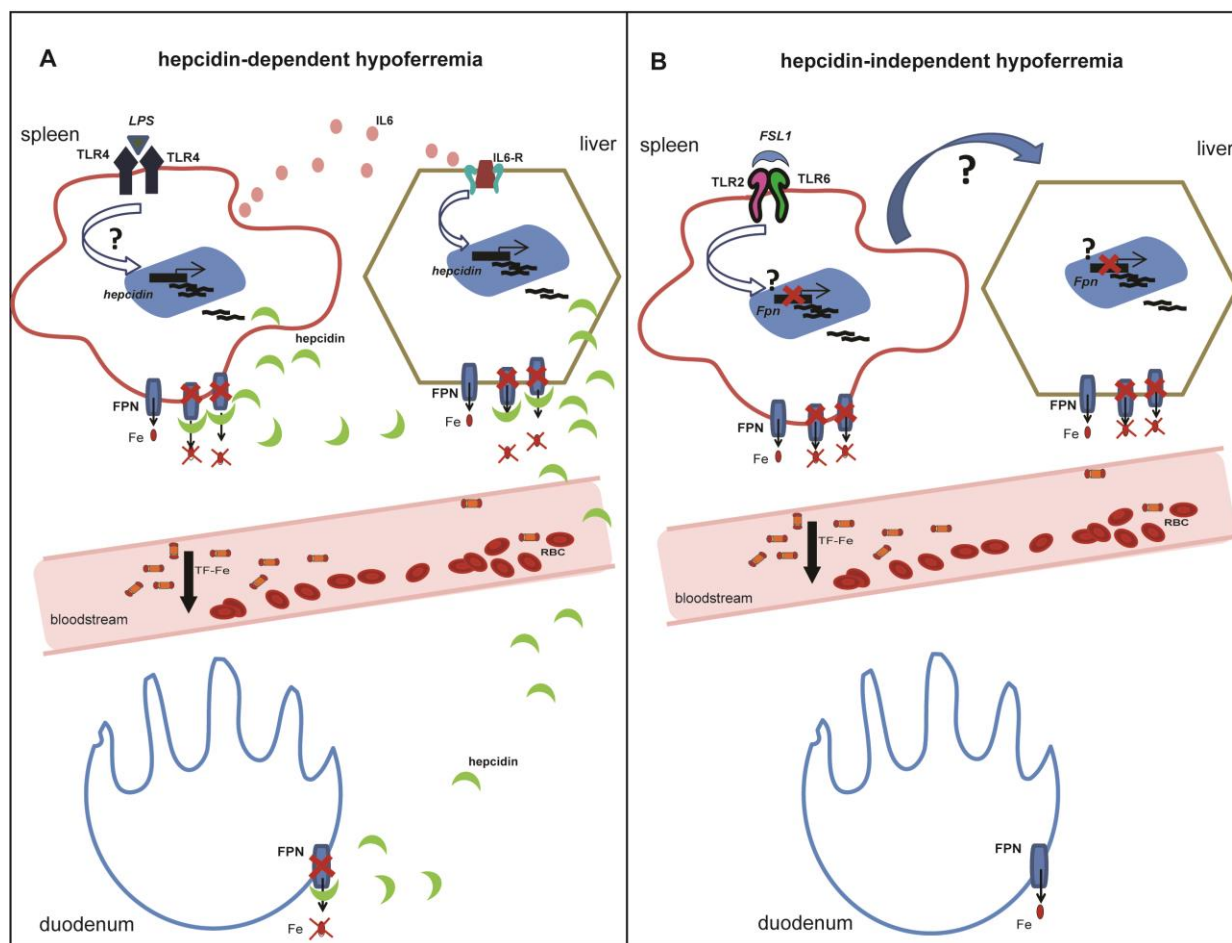


Figure 4.2 Working model. (A) According to the current model, TLR4 ligation by LPS induces hepcidin release from macrophages via undefined pathways. Hepcidin in turn reduces FPN protein level in an autocrine manner. In addition, the release of the inflammatory cytokine IL6 stimulates the hepatic hepcidin production which decreases FPN protein amounts in the liver, in the spleen and in the duodenum, therefore inhibiting hepatocyte and macrophage iron release and intestinal iron absorption, leading to diminished serum iron levels and transferrin saturation (Tf-Fe). **(B)** The ligation of TLR2/6 by FSL1 can mediate a hepcidin-independent hypoferremia by inducing FPN mRNA and protein down

regulation in the liver and in the spleen, while FPN expression in the duodenum is unchanged. The expression of TLRs on hepatocytes is unclear, leading to the hypothesis that FPN down regulation in this cell type is mediated via cytokines or other factors released from the proximate macrophages present in the tissue.

4.9 Dissecting the TLR-mediated ferroportin regulation: an “inhibitor approach”

Given its importance, understanding the molecular mechanism of the FPN transcription regulation during inflammation remains a critical point for the development of therapies against anemias caused by infectious and inflammatory diseases.

One way to identify important players of TLR-mediated FPN regulation was to test FSL1-induced FPN response after the inhibition of important components of the TLR signaling. In 2001 Re and Strominger demonstrated that TLR2 and TLR4 signaling were not equivalent and led to differential cytokine and chemokine expression (156). Nevertheless their ligation both induced a comparable activation of NFkB and MAPK kinases. By using specific inhibitors (Wortmannin and LY294002) these and other authors (157) showed in human macrophage cell lines that phosphatidylinositol 3-kinase (PI3K) was recruited to TLR2 cytosolic domain and that this was required for TLR2-mediated signaling to NFkB. In addition, the activation of the TLR pathways upon ligation was also demonstrated to be dependent on tyrosine phosphorylation, as protein kinase inhibitors and in particular Src kinase inhibitors suppressed TLR2 and TLR4 phosphorylation and prevented their signaling (157, 158). In particular, Lyn is a member of Src kinase family and its deficiency was proven to up regulate cytokine production by BMDMs following FSL1 and LPS treatment. The same effect was also observed with PI3K inhibition by Wortmannin, while an opposite effect was mediated by SHIP1, the protein which hydrolyzes the phospholipid second messenger produced by PI3K catalysis (159). Together these lines of evidence suggested that SHIP1 and Lyn/PI3K regulated TLR2 and TLR4-induced cytokine production in a positive and negative manner, respectively and assigned a crucial role to Src kinase and PI3K in mediating the TLRs signaling pathway. Further studies in human macrophage cell lines also indicated that other signaling molecules were involved in cytokine expression in response to FSL1. Consistently, several inhibitors targeting protein kinase C, PI3K-AKT and mitogen-activated protein kinases resulted in significantly attenuated FSL1-mediate

cytokine response, indicating that multiple and different classes of molecule controlled this signaling (149). For this reason I analyzed the FSL1-mediated FPN mRNA response following the inhibition of several classes of molecules listed in Table 3.1 and mostly representing kinases. The pre-incubation with none of these inhibitors totally prevented the FPN mRNA down regulation, although an attenuated response could be observed with the PI3K inhibitor LY294002 (Figure 3.36 A). Interestingly the same blunted effect was not observed with the other PI3K inhibitor Wortmannin (Figure 3.36 B) suggesting that LY294002 may have a specific effect independent of PI3K inhibition. This hypothesis was also supported by the analysis of these inhibitor effects on FPN expression in absence of inflammatory stimuli. Both inhibitors induced an increase in FPN mRNA levels (Figure 3.35 A). However despite a very transient inhibition of the PI3K pathway (monitored by the phosphorylation status of AKT protein) only the prolonged treatment with LY294002 induced a strong up regulation of FPN protein level (Figure 3.35 C). This suggested that FPN expression was altered through PI3K-independent mechanisms and appeared to be consistent with several publications reporting diverse effects mediated by LY294002 independent of the PI3K-AKT pathway (184-187).

FPN mRNA amount was also increased by Src kinase inhibition (Figure 3.35 B). Nevertheless FSL1 treatment completely overcame such effect down regulating FPN expression at the same extent of untreated cells (Figure 3.36 C, D). The regulation of FPN mediated by PI3K and Src inhibitors would require further investigations however the inhibitor approach I applied was not successful to identify critical elements required for FPN response during inflammation. A different approach, like the study of the FPN promoter may represent a potential alternative to determine transcription factors and promoter binding sites responsible for the FPN mRNA down regulation which I demonstrated to be a crucial component of the immune system response during inflammation.

4.10 Concluding remarks

The present study aimed at identifying novel regulators of FPN-mediated iron export, and, in particular, new molecular mechanisms that controlled FPN internalization and degradation. The results obtained from the kinome RNAi screen that I applied and from its validation indicated that phosphorylation is not a key modification required for the hepcidin-mediated FPN response as believed few years ago. In particular the role of JAK2 kinase was not confirmed by the screening analysis consistent with data reported in recent publications.

Few putative regulators of the hepcidin-dependent FPN degradation process were identified by the screen. Interestingly, most validated regulators of FPN expression conferred hepcidin-independent FPN protein regulation. Some of the putative FPN repressors were related to immune processes further corroborating the relationship between iron homeostasis and the immune response.

Specifically, TLR6 was identified as a novel FPN repressor in an engineered HeLa cell line and in bone marrow derived macrophages (BMDMs). Its stimulation by FSL1 in BMDMs and in mice revealed a hepcidin-independent FPN down regulation sufficient to induce inflammatory hypoferremia. This challenges the prevailing notion of the crucial role of hepcidin in setting the hypoferremic response and uncovers a rapid and potent inflammatory response pathway.

This work ultimately highlights the importance of the hepcidin-independent FPN transcriptional response during inflammation. The identification of molecular players and transcriptional factors responsible for this process would bear direct consequences for the development of targeted therapies against anemias caused by infectious and inflammatory diseases.

REFERENCES

1. M. Ilbert, V. Bonnefoy, Insight into the evolution of the iron oxidation pathways. *Biochimica et biophysica acta* **1827**, 161 (Feb, 2013).
2. P. Ponka, Cell biology of heme. *The American journal of the medical sciences* **318**, 241 (Oct, 1999).
3. A. Sheftel, O. Stehling, R. Lill, Iron-sulfur proteins in health and disease. *Trends in endocrinology and metabolism: TEM* **21**, 302 (May, 2010).
4. C. C. Winterbourn, Toxicity of iron and hydrogen peroxide: the Fenton reaction. *Toxicology letters* **82-83**, 969 (Dec, 1995).
5. J. M. Gutteridge, B. Halliwell, Free radicals and antioxidants in the year 2000. A historical look to the future. *Annals of the New York Academy of Sciences* **899**, 136 (2000).
6. Y. Cheng, O. Zak, P. Aisen, S. C. Harrison, T. Walz, Structure of the human transferrin receptor-transferrin complex. *Cell* **116**, 565 (Feb 20, 2004).
7. R. S. Ohgami *et al.*, Identification of a ferrireductase required for efficient transferrin-dependent iron uptake in erythroid cells. *Nature genetics* **37**, 1264 (Nov, 2005).
8. R. S. Ohgami, D. R. Campagna, A. McDonald, M. D. Fleming, The Steap proteins are metalloreductases. *Blood* **108**, 1388 (Aug 15, 2006).
9. H. Gunshin *et al.*, Cloning and characterization of a mammalian proton-coupled metal-ion transporter. *Nature* **388**, 482 (Jul 31, 1997).
10. M. Kristiansen *et al.*, Identification of the haemoglobin scavenger receptor. *Nature* **409**, 198 (Jan 11, 2001).
11. M. Shayeghi *et al.*, Identification of an intestinal heme transporter. *Cell* **122**, 789 (Sep 9, 2005).
12. A. Rajagopal *et al.*, Haem homeostasis is regulated by the conserved and concerted functions of HRG-1 proteins. *Nature* **453**, 1127 (Jun 19, 2008).
13. P. M. Harrison, F. A. Fischbach, T. G. Hoy, G. H. Haggis, Ferric oxyhydroxide core of ferritin. *Nature* **216**, 1188 (Dec 23, 1967).
14. S. Abboud, D. J. Haile, A novel mammalian iron-regulated protein involved in intracellular iron metabolism. *The Journal of biological chemistry* **275**, 19906 (Jun 30, 2000).
15. A. Donovan *et al.*, Positional cloning of zebrafish ferroportin1 identifies a conserved vertebrate iron exporter. *Nature* **403**, 776 (Feb 17, 2000).
16. A. T. McKie *et al.*, A novel duodenal iron-regulated transporter, IREG1, implicated in the basolateral transfer of iron to the circulation. *Molecular cell* **5**, 299 (Feb, 2000).
17. Z. L. Harris, A. P. Durley, T. K. Man, J. D. Gitlin, Targeted gene disruption reveals an essential role for ceruloplasmin in cellular iron efflux. *Proceedings of the National Academy of Sciences of the United States of America* **96**, 10812 (Sep 14, 1999).
18. C. P. Anderson, M. Shen, R. S. Eisenstein, E. A. Leibold, Mammalian iron metabolism and its control by iron regulatory proteins. *Biochimica et biophysica acta* **1823**, 1468 (Sep, 2012).
19. M. Muckenthaler, N. K. Gray, M. W. Hentze, IRP-1 binding to ferritin mRNA prevents the recruitment of the small ribosomal subunit by the cap-binding complex eIF4F. *Molecular cell* **2**, 383 (Sep, 1998).
20. J. Wang, K. Pantopoulos, Regulation of cellular iron metabolism. *The Biochemical journal* **434**, 365 (Feb 24, 2011).

21. B. Galy, D. Ferring-Appel, S. Kaden, H. J. Grone, M. W. Hentze, Iron regulatory proteins are essential for intestinal function and control key iron absorption molecules in the duodenum. *Cell metabolism* **7**, 79 (Jan, 2008).
22. S. R. Smith, M. C. Ghosh, H. Ollivierre-Wilson, W. Hang Tong, T. A. Rouault, Complete loss of iron regulatory proteins 1 and 2 prevents viability of murine zygotes beyond the blastocyst stage of embryonic development. *Blood cells, molecules & diseases* **36**, 283 (Mar-Apr, 2006).
23. B. Galy *et al.*, Altered body iron distribution and microcytosis in mice deficient in iron regulatory protein 2 (IRP2). *Blood* **106**, 2580 (Oct 1, 2005).
24. D. Casarrubea *et al.*, Abnormal body iron distribution and erythropoiesis in a novel mouse model with inducible gain of iron regulatory protein (IRP)-1 function. *Journal of molecular medicine* **91**, 871 (Jul, 2013).
25. M. Sanchez, B. Galy, M. W. Hentze, M. U. Muckenthaler, Identification of target mRNAs of regulatory RNA-binding proteins using mRNP immunopurification and microarrays. *Nat Protoc* **2**, 2033 (2007).
26. T. Ganz, Heparin, a key regulator of iron metabolism and mediator of anemia of inflammation. *Blood* **102**, 783 (Aug 1, 2003).
27. M. W. Hentze, M. U. Muckenthaler, B. Galy, C. Camaschella, Two to tango: regulation of Mammalian iron metabolism. *Cell* **142**, 24 (Jul 9, 2010).
28. E. Nemeth *et al.*, Heparin regulates cellular iron efflux by binding to ferroportin and inducing its internalization. *Science* **306**, 2090 (Dec 17, 2004).
29. A. Krause *et al.*, LEAP-1, a novel highly disulfide-bonded human peptide, exhibits antimicrobial activity. *FEBS Lett* **480**, 147 (Sep 1, 2000).
30. C. H. Park, E. V. Valore, A. J. Waring, T. Ganz, Heparin, a urinary antimicrobial peptide synthesized in the liver. *The Journal of biological chemistry* **276**, 7806 (Mar 16, 2001).
31. C. Pigeon *et al.*, A new mouse liver-specific gene, encoding a protein homologous to human antimicrobial peptide heparin, is overexpressed during iron overload. *The Journal of biological chemistry* **276**, 7811 (Mar 16, 2001).
32. B. Andriopoulos, Jr. *et al.*, BMP6 is a key endogenous regulator of heparin expression and iron metabolism. *Nature genetics* **41**, 482 (Apr, 2009).
33. D. Meynard *et al.*, Lack of the bone morphogenetic protein BMP6 induces massive iron overload. *Nature genetics* **41**, 478 (Apr, 2009).
34. L. Kautz *et al.*, Iron regulates phosphorylation of Smad1/5/8 and gene expression of Bmp6, Smad7, Id1, and Atoh8 in the mouse liver. *Blood* **112**, 1503 (Aug 15, 2008).
35. J. L. Babitt *et al.*, Bone morphogenetic protein signaling by hemojuvelin regulates heparin expression. *Nature genetics* **38**, 531 (May, 2006).
36. L. Silvestri *et al.*, The serine protease matriptase-2 (TMPRSS6) inhibits heparin activation by cleaving membrane hemojuvelin. *Cell metabolism* **8**, 502 (Dec, 2008).
37. M. Vujic Spasic *et al.*, Smad6 and Smad7 are co-regulated with heparin in mouse models of iron overload. *Biochimica et biophysica acta* **1832**, 76 (Jan, 2013).
38. K. Mleczo-Sanecka *et al.*, SMAD7 controls iron metabolism as a potent inhibitor of heparin expression. *Blood* **115**, 2657 (Apr 1, 2010).
39. E. Corradini *et al.*, Iron regulation of heparin despite attenuated Smad1,5,8 signaling in mice without transferrin receptor 2 or Hfe. *Gastroenterology* **141**, 1907 (Nov, 2011).
40. T. Goswami, N. C. Andrews, Hereditary hemochromatosis protein, HFE, interaction with transferrin receptor 2 suggests a molecular mechanism for mammalian iron sensing. *The Journal of biological chemistry* **281**, 28494 (Sep 29, 2006).

41. P. J. Schmidt, P. T. Toran, A. M. Giannetti, P. J. Bjorkman, N. C. Andrews, The transferrin receptor modulates Hfe-dependent regulation of hepcidin expression. *Cell metabolism* **7**, 205 (Mar, 2008).
42. A. Piperno *et al.*, Modulation of hepcidin production during hypoxia-induced erythropoiesis in humans in vivo: data from the HIGHCARE project. *Blood* **117**, 2953 (Mar 10, 2011).
43. N. P. Talbot *et al.*, Regulation of hepcidin expression at high altitude. *Blood* **119**, 857 (Jan 19, 2012).
44. C. Peyssonnaud *et al.*, Regulation of iron homeostasis by the hypoxia-inducible transcription factors (HIFs). *The Journal of clinical investigation* **117**, 1926 (Jul, 2007).
45. G. G. Braliou *et al.*, 2-Oxoglutarate-dependent oxygenases control hepcidin gene expression. *J Hepatol* **48**, 801 (May, 2008).
46. Q. Liu, O. Davidoff, K. Niss, V. H. Haase, Hypoxia-inducible factor regulates hepcidin via erythropoietin-induced erythropoiesis. *The Journal of clinical investigation* **122**, 4635 (Dec 3, 2012).
47. E. Maurer, M. Gutschow, M. Stirnberg, Matriptase-2 (TMPRSS6) is directly up-regulated by hypoxia inducible factor-1: identification of a hypoxia-responsive element in the TMPRSS6 promoter region. *Biological chemistry* **393**, 535 (May, 2012).
48. M. Pak, M. A. Lopez, V. Gabayan, T. Ganz, S. Rivera, Suppression of hepcidin during anemia requires erythropoietic activity. *Blood* **108**, 3730 (Dec 1, 2006).
49. J. P. Pinto *et al.*, Erythropoietin mediates hepcidin expression in hepatocytes through EPOR signaling and regulation of C/EBPalpha. *Blood* **111**, 5727 (Jun 15, 2008).
50. M. Vokurka, J. Krijt, K. Sulc, E. Necas, Hepcidin mRNA levels in mouse liver respond to inhibition of erythropoiesis. *Physiological research / Academia Scientiarum Bohemoslovaca* **55**, 667 (2006).
51. T. Tanno *et al.*, Identification of TWSG1 as a second novel erythroid regulator of hepcidin expression in murine and human cells. *Blood*, (May 4, 2009).
52. T. Tanno *et al.*, High levels of GDF15 in thalassemia suppress expression of the iron regulatory protein hepcidin. *Nature medicine* **13**, 1096 (Sep, 2007).
53. L. Kautz *et al.*, Identification of erythroferrone as an erythroid regulator of iron metabolism. *Nature genetics*, (Jun 1, 2014).
54. E. Nemeth *et al.*, Hepcidin, a putative mediator of anemia of inflammation, is a type II acute-phase protein. *Blood* **101**, 2461 (Apr 1, 2003).
55. E. Nemeth *et al.*, IL-6 mediates hypoferrremia of inflammation by inducing the synthesis of the iron regulatory hormone hepcidin. *The Journal of clinical investigation* **113**, 1271 (May, 2004).
56. E. Kemna, P. Pickkers, E. Nemeth, H. van der Hoeven, D. Swinkels, Time-course analysis of hepcidin, serum iron, and plasma cytokine levels in humans injected with LPS. *Blood* **106**, 1864 (Sep 1, 2005).
57. X. B. Liu, N. B. Nguyen, K. D. Marquess, F. Yang, D. J. Haile, Regulation of hepcidin and ferroportin expression by lipopolysaccharide in splenic macrophages. *Blood cells, molecules & diseases* **35**, 47 (Jul-Aug, 2005).
58. R. Rodriguez *et al.*, Hepcidin induction by pathogens and pathogen-derived molecules is strongly dependent on interleukin-6. *Infection and immunity* **82**, 745 (Feb, 2014).
59. S. Liu *et al.*, Role of toll-like receptors in changes in gene expression and NF-kappa B activation in mouse hepatocytes stimulated with lipopolysaccharide. *Infection and immunity* **70**, 3433 (Jul, 2002).
60. M. Nishimura, S. Naito, Tissue-specific mRNA expression profiles of human toll-like receptors and related genes. *Biological & pharmaceutical bulletin* **28**, 886 (May, 2005).
61. C. Peyssonnaud *et al.*, TLR4-dependent hepcidin expression by myeloid cells in response to bacterial pathogens. *Blood* **107**, 3727 (May 1, 2006).

62. A. Pietrangelo *et al.*, STAT3 is required for IL-6-gp130-dependent activation of hepcidin in vivo. *Gastroenterology* **132**, 294 (Jan, 2007).
63. M. V. Verga Falzacappa *et al.*, STAT3 mediates hepatic hepcidin expression and its inflammatory stimulation. *Blood* **109**, 353 (Jan 1, 2007).
64. D. M. Wrighting, N. C. Andrews, Interleukin-6 induces hepcidin expression through STAT3. *Blood* **108**, 3204 (Nov 1, 2006).
65. P. Lee, H. Peng, T. Gelbart, L. Wang, E. Beutler, Regulation of hepcidin transcription by interleukin-1 and interleukin-6. *Proceedings of the National Academy of Sciences of the United States of America* **102**, 1906 (Feb 8, 2005).
66. A. E. Armitage *et al.*, Hepcidin regulation by innate immune and infectious stimuli. *Blood* **118**, 4129 (Oct 13, 2011).
67. R. H. Wang *et al.*, A role of SMAD4 in iron metabolism through the positive regulation of hepcidin expression. *Cell metabolism* **2**, 399 (Dec, 2005).
68. P. B. Yu *et al.*, Dorsomorphin inhibits BMP signals required for embryogenesis and iron metabolism. *Nat Chem Biol* **4**, 33 (Jan, 2008).
69. C. Besson-Fournier *et al.*, Induction of activin B by inflammatory stimuli up-regulates expression of the iron-regulatory peptide hepcidin through Smad1/5/8 signaling. *Blood* **120**, 431 (Jul 12, 2012).
70. C. N. Roy *et al.*, An Hfe-dependent pathway mediates hyposideremia in response to lipopolysaccharide-induced inflammation in mice. *Nature genetics* **36**, 481 (May, 2004).
71. D. F. Wallace, C. J. McDonald, L. Ostini, V. N. Subramaniam, Blunted hepcidin response to inflammation in the absence of Hfe and transferrin receptor 2. *Blood*, (Jan 18, 2011).
72. M. V. Verga Falzacappa, G. Casanovas, M. W. Hentze, M. U. Muckenthaler, A bone morphogenetic protein (BMP)-responsive element in the hepcidin promoter controls HFE2-mediated hepatic hepcidin expression and its response to IL-6 in cultured cells. *J Mol Med* **86**, 531 (May, 2008).
73. A. Donovan *et al.*, The iron exporter ferroportin/Slc40a1 is essential for iron homeostasis. *Cell metabolism* **1**, 191 (Mar, 2005).
74. X. B. Liu, F. Yang, D. J. Haile, Functional consequences of ferroportin 1 mutations. *Blood cells, molecules & diseases* **35**, 33 (Jul-Aug, 2005).
75. A. E. Rice, M. J. Mendez, C. A. Hokanson, D. C. Rees, P. J. Bjorkman, Investigation of the biophysical and cell biological properties of ferroportin, a multipass integral membrane protein iron exporter. *J Mol Biol* **386**, 717 (Feb 27, 2009).
76. H. Drakesmith *et al.*, Resistance to hepcidin is conferred by hemochromatosis-associated mutations of ferroportin. *Blood* **106**, 1092 (Aug 1, 2005).
77. L. M. Schimanski *et al.*, Ferroportin: lack of evidence for multimers. *Blood cells, molecules & diseases* **40**, 360 (May-Jun, 2008).
78. I. De Domenico *et al.*, The molecular basis of ferroportin-linked hemochromatosis. *Proceedings of the National Academy of Sciences of the United States of America* **102**, 8955 (Jun 21, 2005).
79. J. A. McGregor *et al.*, Impaired iron transport activity of ferroportin 1 in hereditary iron overload. *The Journal of membrane biology* **206**, 3 (Jul, 2005).
80. Z. Yin *et al.*, Ferroportin is a manganese-responsive protein that decreases manganese cytotoxicity and accumulation. *Journal of neurochemistry* **112**, 1190 (Mar, 2010).
81. M. B. Troadec, D. M. Ward, E. Lo, J. Kaplan, I. De Domenico, Induction of FPN1 transcription by MTF-1 reveals a role for ferroportin in transition metal efflux. *Blood* **116**, 4657 (Nov 25, 2010).
82. M. D. Knutson, M. R. Vafa, D. J. Haile, M. Wessling-Resnick, Iron loading and erythrophagocytosis increase ferroportin 1 (FPN1) expression in J774 macrophages. *Blood* **102**, 4191 (Dec 1, 2003).

83. C. Delaby *et al.*, A physiological model to study iron recycling in macrophages. *Exp Cell Res* **310**, 43 (Oct 15, 2005).
84. C. Delaby, N. Pilard, H. Puy, F. Canonne-Hergaux, Sequential regulation of ferroportin expression after erythrophagocytosis in murine macrophages: early mRNA induction by haem, followed by iron-dependent protein expression. *The Biochemical journal* **411**, 123 (Apr 1, 2008).
85. S. Marro *et al.*, Heme controls ferroportin1 (FPN1) transcription involving Bach1, Nrf2 and a MARE/ARE sequence motif at position -7007 of the FPN1 promoter. *Haematologica* **95**, 1261 (Aug, 2010).
86. M. Mastrogiannaki *et al.*, HIF-2alpha, but not HIF-1alpha, promotes iron absorption in mice. *The Journal of clinical investigation* **119**, 1159 (May, 2009).
87. M. Taylor *et al.*, Hypoxia-inducible factor-2alpha mediates the adaptive increase of intestinal ferroportin during iron deficiency in mice. *Gastroenterology* **140**, 2044 (Jun, 2011).
88. F. Aydemir, S. Jenkitkasemwong, S. Gulec, M. D. Knutson, Iron loading increases ferroportin heterogeneous nuclear RNA and mRNA levels in murine J774 macrophages. *The Journal of nutrition* **139**, 434 (Mar, 2009).
89. J. Chung, D. J. Haile, M. Wessling-Resnick, Copper-induced ferroportin-1 expression in J774 macrophages is associated with increased iron efflux. *Proceedings of the National Academy of Sciences of the United States of America* **101**, 2700 (Mar 2, 2004).
90. F. Yang *et al.*, Regulation of reticuloendothelial iron transporter MTP1 (Slc11a3) by inflammation. *The Journal of biological chemistry* **277**, 39786 (Oct 18, 2002).
91. T. E. Schubert *et al.*, Hypoferraemia during the early inflammatory response is dependent on tumour necrosis factor activity in a murine model of protracted peritonitis. *Molecular medicine reports* **6**, 838 (Oct, 2012).
92. P. N. Paradkar *et al.*, Iron depletion limits intracellular bacterial growth in macrophages. *Blood* **112**, 866 (Aug 1, 2008).
93. M. U. Muckenthaler, B. Galy, M. W. Hentze, Systemic iron homeostasis and the iron-responsive element/iron-regulatory protein (IRE/IRP) regulatory network. *Annu Rev Nutr* **28**, 197 (2008).
94. D. L. Zhang, R. M. Hughes, H. Ollivierre-Wilson, M. C. Ghosh, T. A. Rouault, A ferroportin transcript that lacks an iron-responsive element enables duodenal and erythroid precursor cells to evade translational repression. *Cell metabolism* **9**, 461 (May, 2009).
95. I. De Domenico *et al.*, Hecpidin mediates transcriptional changes that modulate acute cytokine-induced inflammatory responses in mice. *The Journal of clinical investigation* **120**, 2395 (Jul, 2010).
96. G. Ramey *et al.*, Hecpidin targets ferroportin for degradation in hepatocytes. *Haematologica* **95**, 501 (Mar, 2010).
97. I. De Domenico *et al.*, The molecular mechanism of hecpidin-mediated ferroportin down-regulation. *Mol Biol Cell* **18**, 2569 (Jul, 2007).
98. I. De Domenico, E. Lo, D. M. Ward, J. Kaplan, Hecpidin-induced internalization of ferroportin requires binding and cooperative interaction with Jak2. *Proceedings of the National Academy of Sciences of the United States of America* **106**, 3800 (Mar 10, 2009).
99. S. L. Ross *et al.*, Molecular mechanism of hecpidin-mediated ferroportin internalization requires ferroportin lysines, not tyrosines or JAK-STAT. *Cell metabolism* **15**, 905 (Jun 6, 2012).
100. B. Qiao *et al.*, Hecpidin-induced endocytosis of ferroportin is dependent on ferroportin ubiquitination. *Cell metabolism* **15**, 918 (Jun 6, 2012).
101. A. Auriac, A. Willemetz, F. Canonne-Hergaux, Lipid raft-dependent endocytosis: a new route for hecpidin-mediated regulation of ferroportin in macrophages. *Haematologica* **95**, 1269 (Aug, 2010).

102. M. Davis, S. Clarke, Influence of microRNA on the maintenance of human iron metabolism. *Nutrients* **5**, 2611 (Jul, 2013).
103. A. E. Williams, Functional aspects of animal microRNAs. *Cellular and molecular life sciences : CMLS* **65**, 545 (Feb, 2008).
104. C. Sangokoya, J. F. Doss, J. T. Chi, Iron-responsive miR-485-3p regulates cellular iron homeostasis by targeting ferroportin. *PLoS genetics* **9**, e1003408 (Apr, 2013).
105. M. Castoldi *et al.*, The liver-specific microRNA miR-122 controls systemic iron homeostasis in mice. *The Journal of clinical investigation* **121**, 1386 (Apr, 2011).
106. S. M. McDonnell, D. L. Witte, M. E. Cogswell, R. McIntyre, Strategies to increase detection of hemochromatosis. *Annals of internal medicine* **129**, 987 (Dec 1, 1998).
107. Q. Yang, S. M. McDonnell, M. J. Khoury, J. Cono, R. G. Parrish, Hemochromatosis-associated mortality in the United States from 1979 to 1992: an analysis of Multiple-Cause Mortality Data. *Annals of internal medicine* **129**, 946 (Dec 1, 1998).
108. J. N. Feder *et al.*, A novel MHC class I-like gene is mutated in patients with hereditary haemochromatosis. *Nature genetics* **13**, 399 (Aug, 1996).
109. M. Muckenthaler *et al.*, Regulatory defects in liver and intestine implicate abnormal hepcidin and Cybrd1 expression in mouse hemochromatosis. *Nature genetics* **34**, 102 (May, 2003).
110. K. R. Bridle *et al.*, Disrupted hepcidin regulation in HFE-associated haemochromatosis and the liver as a regulator of body iron homeostasis. *Lancet* **361**, 669 (Feb 22, 2003).
111. G. Papanikolaou *et al.*, Mutations in HFE2 cause iron overload in chromosome 1q-linked juvenile hemochromatosis. *Nature genetics* **36**, 77 (Jan, 2004).
112. F. W. Huang, J. L. Pinkus, G. S. Pinkus, M. D. Fleming, N. C. Andrews, A mouse model of juvenile hemochromatosis. *J Clin Invest* **115**, 2187 (Aug, 2005).
113. H. Nick *et al.*, Deferasirox reduces iron overload in a murine model of juvenile hemochromatosis. *Exp Biol Med (Maywood)* **234**, 492 (May, 2009).
114. A. Roetto *et al.*, Mutant antimicrobial peptide hepcidin is associated with severe juvenile hemochromatosis. *Nature genetics* **33**, 21 (Jan, 2003).
115. E. Nemeth, A. Roetto, G. Garozzo, T. Ganz, C. Camaschella, Hepcidin is decreased in TFR2 hemochromatosis. *Blood* **105**, 1803 (Feb 15, 2005).
116. A. Pietrangelo, The ferroportin disease. *Blood cells, molecules & diseases* **32**, 131 (Jan-Feb, 2004).
117. A. Pietrangelo *et al.*, Hereditary hemochromatosis in adults without pathogenic mutations in the hemochromatosis gene. *The New England journal of medicine* **341**, 725 (Sep 2, 1999).
118. I. E. Zohn *et al.*, The flatiron mutation in mouse ferroportin acts as a dominant negative to cause ferroportin disease. *Blood* **109**, 4174 (May 15, 2007).
119. A. Fernandes *et al.*, The molecular basis of hepcidin-resistant hereditary hemochromatosis. *Blood* **114**, 437 (Jul 9, 2009).
120. I. De Domenico *et al.*, The hepcidin-binding site on ferroportin is evolutionarily conserved. *Cell metabolism* **8**, 146 (Aug, 2008).
121. R. L. Sham, P. D. Phatak, E. Nemeth, T. Ganz, Hereditary hemochromatosis due to resistance to hepcidin: high hepcidin concentrations in a family with C326S ferroportin mutation. *Blood* **114**, 493 (Jul 9, 2009).
122. A. Kattamis *et al.*, The effects of erythropoietic activity and iron burden on hepcidin expression in patients with thalassemia major. *Haematologica* **91**, 809 (Jun, 2006).
123. G. Papanikolaou *et al.*, Hepcidin in iron overload disorders. *Blood* **105**, 4103 (May 15, 2005).
124. R. Origa *et al.*, Liver iron concentrations and urinary hepcidin in beta-thalassemia. *Haematologica* **92**, 583 (May, 2007).

125. S. L. Kearney *et al.*, Urinary hepcidin in congenital chronic anemias. *Pediatric blood & cancer* **48**, 57 (Jan, 2007).
126. G. Garcia-Manero, Update on treatments for patients with myelodysplastic syndrome. *Clinical advances in hematology & oncology : H&O* **8**, 407 (Jun, 2010).
127. K. E. Finberg *et al.*, Mutations in Tmprss6 cause iron-refractory iron deficiency anemia (IRIDA). *Nature genetics* **40**, 569 (May, 2008).
128. G. Weiss, L. T. Goodnough, Anemia of chronic disease. *The New England journal of medicine* **352**, 1011 (Mar 10, 2005).
129. I. Theurl *et al.*, Regulation of iron homeostasis in anemia of chronic disease and iron deficiency anemia: diagnostic and therapeutic implications. *Blood* **113**, 5277 (May 21, 2009).
130. C. N. Roy *et al.*, Hepcidin antimicrobial peptide transgenic mice exhibit features of the anemia of inflammation. *Blood* **109**, 4038 (May 1, 2007).
131. G. Nicolas *et al.*, Severe iron deficiency anemia in transgenic mice expressing liver hepcidin. *Proceedings of the National Academy of Sciences of the United States of America* **99**, 4596 (Apr 2, 2002).
132. S. Rivera *et al.*, Hepcidin excess induces the sequestration of iron and exacerbates tumor-associated anemia. *Blood* **105**, 1797 (Feb 15, 2005).
133. C. L. Bennett *et al.*, Venous thromboembolism and mortality associated with recombinant erythropoietin and darbepoetin administration for the treatment of cancer-associated anemia. *JAMA* **299**, 914 (Feb 27, 2008).
134. J. Bohlius *et al.*, Recombinant human erythropoiesis-stimulating agents and mortality in patients with cancer: a meta-analysis of randomised trials. *Lancet* **373**, 1532 (May 2, 2009).
135. G. D. Cuny *et al.*, Structure-activity relationship study of bone morphogenetic protein (BMP) signaling inhibitors. *Bioorganic & medicinal chemistry letters* **18**, 4388 (Aug 1, 2008).
136. C. C. Sun, V. Vaja, J. L. Babbitt, H. Y. Lin, Targeting the hepcidin-ferroportin axis to develop new treatment strategies for anemia of chronic disease and anemia of inflammation. *American journal of hematology* **87**, 392 (Apr, 2012).
137. H. Erfle *et al.*, Reverse transfection on cell arrays for high content screening microscopy. *Nat Protoc* **2**, 392 (2007).
138. S. Terjung *et al.*, High-throughput microscopy using live mammalian cells. *Cold Spring Harbor protocols* **2010**, pdb top84 (Jul, 2010).
139. F. Bartz *et al.*, Identification of cholesterol-regulating genes by targeted RNAi screening. *Cell metabolism* **10**, 63 (Jul, 2009).
140. F. Wang *et al.*, Genetic variation in Mon1a affects protein trafficking and modifies macrophage iron loading in mice. *Nature genetics* **39**, 1025 (Aug, 2007).
141. I. De Domenico *et al.*, The role of ubiquitination in hepcidin-independent and hepcidin-dependent degradation of ferroportin. *Cell metabolism* **14**, 635 (Nov 2, 2011).
142. M. Boutros, L. P. Bras, W. Huber, Analysis of cell-based RNAi screens. *Genome biology* **7**, R66 (2006).
143. C. von Mering *et al.*, STRING: known and predicted protein-protein associations, integrated and transferred across organisms. *Nucleic acids research* **33**, D433 (Jan 1, 2005).
144. R. J. Ward *et al.*, Iron and the immune system. *Journal of neural transmission* **118**, 315 (Mar, 2011).
145. G. Weiss, Iron metabolism in the anemia of chronic disease. *Biochimica et biophysica acta* **1790**, 682 (Jul, 2009).
146. A. Ozinsky *et al.*, The repertoire for pattern recognition of pathogens by the innate immune system is defined by cooperation between toll-like receptors. *Proceedings of the National Academy of Sciences of the United States of America* **97**, 13766 (Dec 5, 2000).

147. T. Okusawa *et al.*, Relationship between structures and biological activities of mycoplasmal diacylated lipopeptides and their recognition by toll-like receptors 2 and 6. *Infection and immunity* **72**, 1657 (Mar, 2004).
148. K. Farhat *et al.*, Heterodimerization of TLR2 with TLR1 or TLR6 expands the ligand spectrum but does not lead to differential signaling. *Journal of leukocyte biology* **83**, 692 (Mar, 2008).
149. K. Won *et al.*, Multiple Signaling Molecules are Involved in Expression of CCL2 and IL-1beta in Response to FSL-1, a Toll-Like Receptor 6 Agonist, in Macrophages. *The Korean journal of physiology & pharmacology : official journal of the Korean Physiological Society and the Korean Society of Pharmacology* **16**, 447 (Dec, 2012).
150. U. Buwitt-Beckmann *et al.*, TLR1- and TLR6-independent recognition of bacterial lipopeptides. *The Journal of biological chemistry* **281**, 9049 (Apr 7, 2006).
151. F. B. Sow *et al.*, Expression and localization of hepcidin in macrophages: a role in host defense against tuberculosis. *Journal of leukocyte biology* **82**, 934 (Oct, 2007).
152. J. C. Deschemin, S. Vaulont, Role of hepcidin in the setting of hypoferraemia during acute inflammation. *PLoS one* **8**, e61050 (2013).
153. A. Layoun, H. Huang, A. Calve, M. M. Santos, Toll-like receptor signal adaptor protein MyD88 is required for sustained endotoxin-induced acute hypoferric response in mice. *The American journal of pathology* **180**, 2340 (Jun, 2012).
154. L. Oliveira-Nascimento, P. Massari, L. M. Wetzler, The Role of TLR2 in Infection and Immunity. *Frontiers in immunology* **3**, 79 (2012).
155. T. M. Watters, E. F. Kenny, L. A. O'Neill, Structure, function and regulation of the Toll/IL-1 receptor adaptor proteins. *Immunology and cell biology* **85**, 411 (Aug-Sep, 2007).
156. F. Re, J. L. Strominger, Toll-like receptor 2 (TLR2) and TLR4 differentially activate human dendritic cells. *The Journal of biological chemistry* **276**, 37692 (Oct 5, 2001).
157. L. Arbibe *et al.*, Toll-like receptor 2-mediated NF-kappa B activation requires a Rac1-dependent pathway. *Nature immunology* **1**, 533 (Dec, 2000).
158. A. E. Medvedev *et al.*, Role of TLR4 tyrosine phosphorylation in signal transduction and endotoxin tolerance. *The Journal of biological chemistry* **282**, 16042 (Jun 1, 2007).
159. S. Keck, M. Freudenberg, M. Huber, Activation of murine macrophages via TLR2 and TLR4 is negatively regulated by a Lyn/PI3K module and promoted by SHIP1. *Journal of immunology* **184**, 5809 (May 15, 2010).
160. D. M. Zhu, E. Tekle, C. Y. Huang, P. B. Chock, Inositol tetrakisphosphate as a frequency regulator in calcium oscillations in HeLa cells. *The Journal of biological chemistry* **275**, 6063 (Mar 3, 2000).
161. T. H. Millard, P. J. Cullen, G. Banting, Effects of elevated expression of inositol 1,4,5-trisphosphate 3-kinase B on Ca²⁺ homeostasis in HeLa cells. *The Biochemical journal* **352 Pt 3**, 709 (Dec 15, 2000).
162. M. M. Nalaskowski, G. W. Mayr, The families of kinases removing the Ca²⁺ releasing second messenger Ins(1,4,5)P₃. *Current molecular medicine* **4**, 277 (May, 2004).
163. A. Bendich, Calcium supplementation and iron status of females. *Nutrition* **17**, 46 (Jan, 2001).
164. A. Gleerup, L. Rossander-Hulten, L. Hallberg, Duration of the inhibitory effect of calcium on non-haem iron absorption in man. *European journal of clinical nutrition* **47**, 875 (Dec, 1993).
165. L. Yan *et al.*, The effect of long-term calcium supplementation on indices of iron, zinc and magnesium status in lactating Gambian women. *The British journal of nutrition* **76**, 821 (Dec, 1996).
166. H. J. Kalkwarf, S. D. Harrast, Effects of calcium supplementation and lactation on iron status. *The American journal of clinical nutrition* **67**, 1244 (Jun, 1998).
167. B. Lonnerdal, Calcium and iron absorption--mechanisms and public health relevance. *International journal for vitamin and nutrition research. Internationale Zeitschrift fur Vitamin-*

- und Ernährungsforschung. Journal international de vitaminologie et de nutrition* **80**, 293 (Oct, 2010).
168. R. C. Hider, X. Kong, Chemistry and biology of siderophores. *Natural product reports* **27**, 637 (May, 2010).
169. M. Luo, E. A. Fadeev, J. T. Groves, Mycobactin-mediated iron acquisition within macrophages. *Nat Chem Biol* **1**, 149 (Aug, 2005).
170. L. L. Anzaldi, E. P. Skaar, Overcoming the heme paradox: heme toxicity and tolerance in bacterial pathogens. *Infection and immunity* **78**, 4977 (Dec, 2010).
171. C. N. Cornelissen *et al.*, The transferrin receptor expressed by gonococcal strain FA1090 is required for the experimental infection of human male volunteers. *Mol Microbiol* **27**, 611 (Feb, 1998).
172. S. Baveye, E. Ellass, J. Mazurier, G. Spik, D. Legrand, Lactoferrin: a multifunctional glycoprotein involved in the modulation of the inflammatory process. *Clinical chemistry and laboratory medicine : CCLM / FESCC* **37**, 281 (Mar, 1999).
173. C. Correnti, R. K. Strong, Mammalian siderophores, siderophore-binding lipocalins, and the labile iron pool. *The Journal of biological chemistry* **287**, 13524 (Apr 20, 2012).
174. G. E. Cartwright, M. A. Lauretsen, *et al.*, The anemia associated with chronic infection. *Science* **103**, 72 (Jan 18, 1946).
175. R. Ben-Othman *et al.*, Leishmania-mediated inhibition of iron export promotes parasite replication in macrophages. *PLoS pathogens* **10**, e1003901 (Jan, 2014).
176. A. Layoun, M. M. Santos, Bacterial cell wall constituents induce hepcidin expression in macrophages through MyD88 signaling. *Inflammation* **35**, 1500 (Aug, 2012).
177. O. Takeuchi *et al.*, Discrimination of bacterial lipoproteins by Toll-like receptor 6. *International immunology* **13**, 933 (Jul, 2001).
178. S. Akira, Mammalian Toll-like receptors. *Current opinion in immunology* **15**, 5 (Feb, 2003).
179. U. Buwitt-Beckmann *et al.*, Toll-like receptor 6-independent signaling by diacylated lipopeptides. *European journal of immunology* **35**, 282 (Jan, 2005).
180. T. Tanaka, E. Araki, K. Nitta, M. Tateno, Recombinant human tumor necrosis factor depresses serum iron in mice. *Journal of biological response modifiers* **6**, 484 (Oct, 1987).
181. X. Alvarez-Hernandez, J. Liceaga, I. C. McKay, J. H. Brock, Induction of hypoferremia and modulation of macrophage iron metabolism by tumor necrosis factor. *Laboratory investigation; a journal of technical methods and pathology* **61**, 319 (Sep, 1989).
182. I. Theurl *et al.*, Autocrine formation of hepcidin induces iron retention in human monocytes. *Blood* **111**, 2392 (Feb 15, 2008).
183. X. Zhang, B. H. Rovin, Hepcidin expression by human monocytes in response to adhesion and pro-inflammatory cytokines. *Biochimica et biophysica acta* **1800**, 1262 (Dec, 2010).
184. E. K. Choi *et al.*, LY294002 inhibits monocyte chemoattractant protein-1 expression through a phosphatidylinositol 3-kinase-independent mechanism. *FEBS Lett* **559**, 141 (Feb 13, 2004).
185. Y. H. Kim, K. H. Choi, J. W. Park, T. K. Kwon, LY294002 inhibits LPS-induced NO production through a inhibition of NF-kappaB activation: independent mechanism of phosphatidylinositol 3-kinase. *Immunology letters* **99**, 45 (Jun 15, 2005).
186. T. W. Poh, S. Pervaiz, LY294002 and LY303511 sensitize tumor cells to drug-induced apoptosis via intracellular hydrogen peroxide production independent of the phosphoinositide 3-kinase-Akt pathway. *Cancer research* **65**, 6264 (Jul 15, 2005).
187. K. Yamaguchi *et al.*, Activating transcription factor 3 and early growth response 1 are the novel targets of LY294002 in a phosphatidylinositol 3-kinase-independent pathway. *Cancer research* **66**, 2376 (Feb 15, 2006).

188. I. De Domenico *et al.*, Retracted: the role of ubiquitination in hepcidin-independent and hepcidin-dependent degradation of ferroportin. *Cell Metabolism* **15**, 927 (June 6, 2012).
189. I. De Domenico *et al.*, Retraction notice to: The hepcidin binding site of ferroportin is evolutionarily conserved. *Cell Metabolism* **18**, 146 (August 6, 2008).
190. S. Altamura *et al.*, Resistance of ferroportin to hepcidin binding causes exocrine pancreatic failure and fatal iron overload. *Cell Metabolism*, in press.

ACKNOWLEDGEMENTS

My thanks go to my supervisors: Martina Muckenthaler and Matthias Hentze for giving me the possibility to perform my PhD project in an interesting and inspiring scientific environment. These four years have been a life time experience!

I also wish to thank the members of my Thesis Advisory Committee, Dr. Lars Steinmetz, Prof. Ralf Bartenschlager and Dr. Rainer Pepperkok for their valuable feedback and discussions throughout these years. I would also like to thank Prof. Friedrich Frischknecht for his agreement to join my thesis defense as examiner.

Thanks to all the people who contributed to my work, even for a short period of time, in particular to Felix Klein for helping me in the screening analysis and Prof. Artur Ulmer for kindly providing the TLRs KO mice and for all the helpful discussions/emails we exchanged.

Big thanks to Dr. Bruno Galy for being an inspiring example and for the help and ideas he gave me especially during “hard times”. I have really appreciated all the hours you spent with me trying to find solutions to my scientific problems!

I also owe my gratitude to all my colleagues for the nice time we spent together in and outside the lab and for creating a friendly and helpful working environment. It has been a pleasure to work with you all!

Thanks to Christian Hauer and Christoph Metzendorf for translating the thesis summary into German and for being always helpful.

Special “thank you” goes to Dr. Sandro Altamura for teaching me innumerable things and for being always very supportive, helpful and constructive. You have been the most patient and helpful mentor I could have ever wished and you will always be an example to follow, as person, as scientist and as mentor. I will never forget the time and the support you gave me every time I sat on the sink with all my troubles. Grazie davvero!

Special thanks also go to my former colleague and best friend Flavia, for making this time wonderful, despite all the worries and the problems I experienced. You have been a gift and the best moments of my life in Heidelberg will be always related to you and your smile. Ti voglio bene!

Also, thanks to all my friends near and far, who supported me in these years. In particular I wish to thank Andrea, Yuri, Giulia who walked this path with me from the beginning. Già lo so, mi mancherete tanto!

Infine, la mia più profonda gratitudine va alla mia famiglia per esser sempre stata “presente” in questi anni nonostante la distanza. Grazie per avermi sempre spinto e aiutato a realizzare i miei sogni, grazie per avermi dato tutti gli strumenti materiali e mentali per arrivare fin qui e grazie, più di tutto, per essere sempre l’esempio migliore a cui guardare e in cui trovare la forza per affrontare ogni ostacolo. Senza di voi non ce l’avrei mai fatta! Mi ultimo, fundamental gracias es para ti, Alfredo, la fuente de mi felicidad en cada dia. Tu has sido el regalo mas precioso que este tiempo en Heidelberg me ha regalado, tu has sido mi fuerza en este camino y tu has sido la cosa mas importante que he encontrado aquí, hasta volverte mi propia familia...Gracias porquè has hecho mi vida “brillante” y porquè sin ti nada tendría el mismo valor! Te quiero!